

**Linking Avalanche Problem Types to Modelled
Weather and Snowpack Conditions: A Pilot Study in
Glacier National Park, British Columbia**

**by
Moses J. Towell**

B.Sc. Honours in Geological Science, University of British Columbia, 2015

Project Submitted in Partial Fulfillment of the
Requirements for the Degree of
Master of Resource Management

in the
School of Resource and Environmental Management
Faculty of Environment

© Moses J. Towell
SIMON FRASER UNIVERSITY
Fall 2019

Copyright in this work rests with the author. Please ensure that any reproduction or re-use is done in accordance with the relevant national copyright legislation.

Approval

Name: Moses J Towell

Degree: Master of Resource Management

Project Number: 723

Title: Linking Avalanche Problem Types to Modelled Weather and Snowpack Conditions: A Pilot Study in Glacier National Park, British Columbia

Examining Committee: Chair: Richard Farthing-Nichol
MRM Planning Candidate

Pascal Haegeli
Senior Supervisor
Assistant Professor

Simon Horton
Supervisor
Post-Doctoral Fellow

Date Defended/Approved: December 13th, 2019

Abstract

To help amateur recreationists to make better informed decisions about when and where to travel in the backcountry, Canadian avalanche bulletins include structured information on the nature of avalanche problems of concern. Using conditional inference trees, this study explores the relationships between modelled weather and snowpack conditions and avalanche problems identified by forecasters in Glacier Nation Park, British Columbia, during the 2013 to 2018 winter seasons to better understand what makes avalanche forecasters identify individual avalanche problem types and explore possibilities for predicting avalanche problems in data-spare regions using numerical models. The results confirm the influence of the expected weather and snowpack variables and provide useful additional insight into forecaster practices when making decisions about avalanche problems. This study provides an important step for integrating avalanche problems and the Conceptual Model of Avalanche Hazard into existing weather and snowpack model chains and making avalanche bulletins in Canada more consistent.

Keywords: numeric weather prediction models; snow cover models; avalanche problem types; avalanche forecasting; SNOWPACK model; conditional inference trees;

Acknowledgements

I would first like to acknowledge that here on the lower mainland of British Columbia we are on the traditional, unceded territory of the sk̓wx̓wú7mesh (Squamish), sel̓íl̓wítulh (Tsleil-Waututh), x̓m̓əθk̓w̓əy̓əm (Musqueam) First Nations. It has been a privilege to study and live here.

I am grateful for my partnership with Dr. Pascal Haegeli and I thank him for the infinite wisdom and valuable guidance bestowed on me both about the research process and the vast field of avalanches which enabled me to complete this research project. I am also thankful to Dr. Simon Horton for his unwavering support and accountability to providing me with the knowledge and direction required to complete this work. I especially appreciate your patience and assistance with everything from the study design, the rigorous analyses and especially the interpretation of my results.

An immense thank you to my SARP colleagues and the rest of my REM colleagues for being there for discussions, challenges and most importantly, the laughs... I wish you well as you pursue new exciting adventures and continue to use your passion, drive, and commitment towards the bettering our planet.

I would also like to acknowledge Avalanche Canada, Parks Canada, the Canadian Avalanche Association, and NSERC for their financial support, valuable datasets and encouragement throughout the entire process.

A big shout-out to my parents for their pride and encouragement, to my siblings for being awesome, and to my amazing group of friends for helping me to balance life and being there to hangout when I needed it most.

Finally, I would like to extend the deepest gratitude to my wife Tara for her unconditional love and support throughout this life we have built together. This educational journey has been a long hard road that would not have been possible without your drive, determination and ability to see the ultimate goal. I must also thank my son Revy who was literally named in honour of this project and who showers me with hugs and smiles, making it all worth it. One day we will all be skiing the slopes together!

Table of Contents

Approval.....	ii
Abstract.....	iii
Acknowledgements.....	iv
Table of Contents.....	v
List of Tables.....	vii
List of Figures.....	viii
List of Acronyms.....	xi
Chapter 1. Introduction.....	1
Chapter 2. Background.....	6
2.1. Conceptual Model of Avalanche Hazard.....	6
2.2. Numerical Weather Prediction Models.....	12
2.3. SNOWPACK Model.....	13
2.4. SNOWPACK Research and Application in Canada.....	16
2.5. Modelling of Avalanche Hazard.....	16
Chapter 3. Methods.....	20
3.1. Study Area.....	20
3.2. Study Period.....	21
3.3. Dataset.....	23
3.3.1. Avalanche Bulletins from Parks Canada.....	23
3.3.2. NWP Model.....	25
3.3.3. SNOWPACK Model.....	27
3.3.4. Weather Observations.....	28
3.4. Data Preparation and Manipulation.....	28
3.4.1. Surface Avalanche Problem Types.....	29
3.4.2. Persistent Slab Avalanche Problem Types.....	31
3.5. Statistical Analysis.....	35
3.5.1. Exploratory Data Analysis.....	35
3.5.2. Model Validation.....	36
3.5.3. Conditional Inference Trees.....	36
Chapter 4. Results.....	39
4.1. Validation of Model Data.....	39
4.2. Surface Avalanche Problem Types.....	41
4.2.1. Analysis Dataset Overview.....	41
4.2.2. Wind Slab Avalanche Problems.....	48
WS Avalanche Problem Dataset and Timeseries Analysis.....	48
Representing WS avalanche problem relationships with a CIT model.....	51
4.2.3. Storm Slab Avalanche Problems.....	53
SS Avalanche Problem Dataset and Timeseries Analysis.....	53
Representing SS avalanche problem relationships with a CIT model.....	56

4.2.4.	Loose Dry Avalanche Problems.....	60
	LDRY Avalanche Problem Dataset and Timeseries Analysis.....	60
	Representing LDRY avalanche problem relationships with a CIT model	63
4.2.5.	Cornice Avalanche Problems.....	65
	CORN Avalanche Problem Dataset and Timeseries Analysis.....	65
	Representing CORN avalanche problem relationships with a CIT model	68
4.2.6.	Wet Loose Avalanche Problems.....	70
	LWET Avalanche Problem Dataset and Timeseries Analysis	70
	Representing LWET avalanche problem relationships with a CIT model.....	73
4.3.	Persistent Avalanche Problems	75
4.3.1.	Analysis Dataset Overview	75
4.3.2.	Persistent Slab/Deep Persistent Slab Avalanche Problems	82
	PS/DPS Avalanche Problem Dataset and Timeseries Analysis	82
	Representing PS/DPS avalanche problem relationships with a CIT model.....	88
Chapter 5.	Discussion	91
5.1.	Main Themes Developed from the CIT Analyses.....	91
5.1.1.	Relevant Weather and Snowpack Factors.....	91
	Surface Avalanche Problem Patterns.....	91
	Persistent Slab Avalanche Problem Patterns	94
5.1.2.	Insight into Forecaster Practices.....	96
5.1.3.	The Challenge of “Turning off” Avalanche Problems	97
5.2.	Limitations	98
Chapter 6.	Conclusions.....	100
References.....		103

List of Tables

Table 2.1	Types of avalanche problems. Edited from Statham, Haegeli, et al. (2018).	7
Table 2.2	Canadian Avalanche Association size classification (CAA, 2014).	11
Table 3.1	Station ID #s - 2013 – 2017 Seasons.....	25
Table 3.2	Station ID #s - 2018 Season	26
Table 3.3	Modelled and calculated variables for surface avalanche problem types	30
Table 3.4	Modelled and calculated variables for PS avalanche problem types	34
Table 4.1	Model validation calculations.....	39
Table 4.2	Surface avalanche problem type hazard assessment summary by elevation band and season.	42
Table 4.3	Season Summaries – WS Avalanche Problem Type – Alpine Elevation	49
Table 4.4	Season Summaries – SS Avalanche Problem Type – TL Elevation	54
Table 4.5	Season Summaries – LDRY Avalanche Problem Type – TL Elevation ..	61
Table 4.6	Season Summaries – CORN Avalanche Problem Type – ALP Elevation	66
Table 4.7	Season Summaries – LWET Avalanche Problem Type – BTL Elevation	71
Table 4.8	Persistent avalanche problem type hazard assessment summary by elevation band and season.	77
Table 4.9	Season Summaries – PS/DPS Avalanche Problem Types – Treeline Elevation.....	83
Table 4.10	Season Summaries – Tracked Interfaces and Persistent Weak Layers of concern from assessments	83

List of Figures

Figure 2.1	Workflow process of the CMAH, defining an avalanche problem by its type, likelihood and size (Statham, Haegeli, et al., 2018).	6
Figure 2.2	Likelihood of avalanches as a function of its spatial distribution and its sensitivity to triggers (Statham, Haegeli, et al., 2018).	10
Figure 2.3	Example of a daily hazard chart. The yellow square represents a SS avalanche problem while the red square represents a PS avalanche problem. The middle point represents the typical value while the outer edges represent the minimum and maximum values (Statham, Haegeli, et al., 2018).	12
Figure 2.4	Example of SNOWPACK’s timeseries evolution output for one NWP grid point over the duration of one season. Colours are representative of grain type: Precipitation Particles (PP, +), Decomposing Fragments (DF, /), Rounded Grains (RG, ●), Faceted Crystals (FC, □), Depth Hoar (DH, △), Surface Hoar (SH, ∨), Melt Forms (MF, O), Melt-Freeze Crusts (MFcr, ∞).	15
Figure 3.1	Study Area - Glacier National Park of British Columbia. Parks Canada study plots at Mt. Fidelity and Roger’s Pass are shown.	21
Figure 3.2	Sample of a daily avalanche bulletin from GNP (Parks Canada, 2019)..	24
Figure 3.3	2013-2017 NWP grid point locations.	26
Figure 3.4	2018 NWP grid point locations.	27
Figure 3.5	Sample (2016 Season @ TL) of how each tracked interface (January 4 th PWL shown) was labelled according to the text descriptions from the daily avalanche bulletins (<i>Surface</i> problem = green and yellow bands, <i>Present</i> problem = red band, <i>Absent</i> problem = grey band).	35
Figure 4.1	Scatterplots of observed versus modelled data from Mt. Fidelity study plot and matched NWP grid point. a) minimum air temperature (°C); b) maximum air temperature (°C); c) 24 hour snowfall (HN24, cm); and d) height of snowpack (cm). Colours represent separate seasons. Dashed line represents 1-to-1 trendline, and solid line is line of best fit.	40
Figure 4.2	Distribution of surface avalanche problems per elevation band for all seasons within the study period.	41
Figure 4.3	Frequency distribution of all variables in the Surface Avalanche Problems Types dataset. Zero precipitation values (hn24, hn72 & rain_sum variables) are omitted to show distributions more clearly.	45
Figure 4.4	Sample of frequency distributions of stability indexes from interface at the bottom of HST and the minimum within the HST.	46
Figure 4.5	a) Summary of total rainfall per season; Frequency distribution for all seasons of: b) average air temperatures; c) Ski penetration per season; d) HST thickness per season.	46
Figure 4.6	Wind speed distributions per season.	47
Figure 4.7	Correlation plot of all numeric weather and snowpack variables included in the Surface Avalanche Problem Type dataset.	48

Figure 4.8	Timeseries (2018 Season - Alpine) of WS avalanche problems, associated weather variables (HN72 and wind speed) and snowpack evolution. Yellow bands represent the presence of a WS avalanche problem on any given day.	50
Figure 4.9	Distribution of average air temperature and 72 h wind run when WS avalanche problems were absent or present (2015-2018 Seasons).	51
Figure 4.10	Conditional Inference Tree for WS avalanche problems (2015-2018 Seasons).	53
Figure 4.11	Timeseries (2018 Season - Treeline) of SS avalanche problems, associated weather variables (air temperatures, HN24 and rain) and snowpack evolution. Yellow bands represent the presence of a SS avalanche problem on any given day. Air temperature timeseries colours are defined as: red = maximum, black = average, blue = minimum.	55
Figure 4.12	Distribution of snowfall amounts (HN24 & HN72), HN48 layer thickness and ski penetration depth when SS avalanche problems were absent and present (2013 - 2018 Seasons).	56
Figure 4.13	Conditional Inference Tree for SS avalanche problem types	59
Figure 4.14	Timeseries (2017 Season - Treeline) of LDRY avalanche problems, associated weather variables (air temperature, HN24 and rainfall) and snowpack evolution. Yellow bands represent the presence of a LDRY avalanche problem on any given day. Air temperature timeseries colours are defined as: red = maximum, black = average, blue = minimum, & snow surface temperature = green.	62
Figure 4.15	Distribution of maximum air temperature, HST slab density and ski penetration depth when LDRY avalanche problems were absent and present (2013 - 2018 Seasons).	63
Figure 4.16	Conditional Inference Tree for LDRY avalanche problem types	65
Figure 4.17	Timeseries (2017 Season - Alpine) of CORN avalanche problems, associated weather variables (HN24, rain, and wind speed) and snowpack evolution. Yellow bands represent the presence of a CORN avalanche problem on any given day.	67
Figure 4.18	Distribution of height of snowpack, maximum wind speed, 72 h wind run and HST slab density when CORN avalanche problems were absent and present (2013 - 2018 Seasons).	68
Figure 4.19	Conditional Inference Tree for CORN avalanche problem types	70
Figure 4.20	Timeseries (2015 Season – Below Treeline) of LWET avalanche problems, associated weather variables (air temperature, HN24 = grey bars, and rainfall = black bars) and snowpack evolution. Yellow bands represent the presence of a LWET avalanche problem on any given day. Air temperature timeseries colours are defined as: red = maximum, black = average, blue = minimum.	72
Figure 4.21	Distribution of HN24, average air temperature, ski penetration depth and HST slab density when LWET avalanche problems were absent and present (2013 - 2018 Seasons).	73
Figure 4.22	Conditional Inference Tree for LWET avalanche problem types	75

Figure 4.23	Distribution of DPS and PS avalanche problems per elevation band for all seasons within the study period.	76
Figure 4.24	Frequency distribution of all variables in the Persistent Avalanche Problems Types dataset. Zero precipitation values (hn24, hn72 & rain_sum variables) are omitted to clearly show distributions	78
Figure 4.25	Correlation plot of all numeric weather and snowpack variables included in the Persistent Avalanche Problem Type dataset.....	80
Figure 4.26	Timeseries (2016 Season – Treeline) of PS/DPS avalanche problems, precipitation (HN24 = grey bars, and rainfall = black bars) and snowpack evolution (black lines = tracked layers). Yellow bands represent the presence of a PS/DPS avalanche problem on any given day.....	86
Figure 4.27	Distribution of slab thickness, average density and average hardness and weak layer age, density and hardness when PS/DPS avalanche problems were surface problems, present and absent (2013 - 2018 Seasons).	87
Figure 4.28	Tracked weak layer evolution for all tracked interfaces showing weak layer age versus slab thickness (Red = <i>Surface</i> problem; Green = <i>Present</i> PS/DPS problem; Grey = <i>Absent</i> PS/DPS problem)	87
Figure 4.29	Conditional Inference Tree for turning PS/DPS Avalanche Problem on	90

List of Acronyms

ALP	Alpine elevation band
ASARC	Applied Snow and Avalanche Research group at the University of Calgary
BC	British Columbia
BTL	Below treeline elevation band
CAA	Canadian Avalanche Association
CART	Classification and regression tree
CIT	Conditional inference tree
CMAH	Conceptual model of avalanche hazard
CORN	Cornice avalanche problem
DF	Decomposing fragments
DH	Depth hoar
DPS	Deep persistent slab avalanche problem
FC	Faceted grains
FCxr	Rounded facet particles
GEM	Global Environmental Multiscale weather model
GEM-LAM	GEM limited area model (same as HRDPS)
GEM15	GEM regional deterministic prediction system (same as RDPS)
GNP	Glacier National Park, B.C.
HRDPS	High Resolution Deterministic Prediction System
HST	Height of storm snow
LDRY	Dry loose avalanche problem
LWET	Wet loose avalanche problem
MF	Melt forms
MFcr	Melt-freeze crust
NWP	Numerical weather prediction
PP	Precipitation particles
PS	Persistent slab avalanche problem
RDPS	Regional Deterministic Prediction System
RG	Rounded grains
RMSE	Root mean squared error
SARP	Simon Fraser Avalanche Research Program
SFU	Simon Fraser University
SH	Surface hoar
SS	Storm slab avalanche problem
SSI	Structural stability index
SVM	Support vector machines
TL	Treeline elevation band
WS	Wind slab avalanche problem

Chapter 1. Introduction

Every winter, snow avalanches pose a serious threat to human life and are responsible for large amounts of economic loss in mountainous regions around the world. In Canada, there has been an average of 11 avalanche fatalities per year over the last decade, and the vast majority of these victims are amateur recreationists making their own decisions about when and where to expose themselves to avalanche hazard (Avalanche Canada, 2019). In addition, avalanches can destroy resources (e.g., timber), damage critical infrastructure (e.g., transmission lines) and affect traffic flow across mountain passes. In Canada, the economic loss due to avalanches affecting transportation routes has been estimated to be greater than \$125M per year. These costs can be broken down into three major sources: 1) delays to vital transportation routes estimated at \$7.5M, 2) losses for downstream operations estimated to be more than \$100M, and 3) costs of avalanche control and defense structures estimated at \$18M (Sinickas, Jamieson, & Maes, 2016).

The risk from avalanches to an object of value or a person emerges from a combination of a) the severity of the avalanche hazard at the time, b) the exposure of the objective or person to that hazard, and c) the vulnerability of the object or person, which describes its susceptibility to getting damaged, injured or killed should an avalanche occur (CAA, 2016; Statham, 2008). The goal of avalanche risk mitigation is to reduce the risk from avalanches to an acceptable level given the operational objective by modifying one or several of these components (CAA, 2016). Avalanche hazard can be mitigated by artificially releasing avalanches using explosives, installing snow fences to prevent potential avalanches from releasing, and a variety of other methods. The exposure to avalanche hazard can be reduced by avoiding avalanche prone areas when conditions are hazardous and/or building defense structures such as avalanche sheds that allow avalanches to cross over roads or railway lines without affecting traffic. The vulnerability of a person to avalanches can be reduced by using safety equipment (e.g., avalanche transceiver, avalanche airbag), and buildings and infrastructure can be structurally reinforced to strengthen their ability to withstand avalanches. Depending on the avalanche safety context, avalanche risk is managed through long-term planning which focuses on site selection and engineering solutions (e.g., land use planning,

transportation infrastructure), short-term operational programs that include avalanche forecasting program (e.g. ski areas, backcountry recreation), or a combination of the two approaches (Haegeli, 2018).

When travelling in the backcountry, the possible approaches for mitigating the risk from avalanche are somewhat limited as it is not possible to modify the hazard conditions over large areas. Hence, the avalanche risk in the backcountry is primarily managed by continuously monitoring the hazard conditions and choosing terrain that is considered appropriate under the given conditions. To do this effectively, a functional understanding of the underlying processes of avalanche formation, how they contribute to the likelihood and the destructive size of expected avalanche, and how far potential avalanches might be running is critical (Statham, 2008).

To allow amateur recreationists—backcountry skiers, mountain snowmobile riders, snowshoers, alpinists and ice-climbers—to make informed decisions about when and where to travel in the backcountry, avalanche warning services have been established in many western countries with mountainous areas. During the wintertime, these warning services regularly publish avalanche conditions reports that include information on the short term likelihood and severity of avalanches, and succinctly communicate any relevant mitigation measures to help backcountry recreationists reduce the associated risk (McClung & Schaerer, 2006; Statham, 2008). In western Canada, Avalanche Canada, Parks Canada and Alberta Parks publish daily avalanche bulletins for 18 different forecast regions that cover popular backcountry recreation areas in the Coast Mountains, the Columbia Mountains, and the Rocky Mountains. Information included in Canadian avalanche bulletin is presented according to an information pyramid, which starts with a general overview of the severity of the conditions before progressively providing more details about the nature of the avalanche hazard conditions. Canadian avalanche bulletins use the North American Avalanche Danger Scale (Statham et al., 2010b), a five-level ordinal scale with keywords and signal colors to provide a concise overview of the conditions at the top of the information pyramid. At the second level of the pyramid, the nature of avalanche problems is described in detail according to the Conceptual Model of Avalanche Hazard (CMAH; Statham, Haegeli, et al., 2018). This information allows recreationists with a higher level of understanding to make better informed choices about when and where to travel in the backcountry. At the bottom of the information pyramid are even more detailed descriptions of the conditions

that include a summary of the original weather, snowpack and avalanche conditions that were the foundation for the hazard assessment.

Assessing avalanche hazard is an iterative process that uses weather, snowpack, and avalanche observational data to develop a comprehensive picture of the existing avalanche conditions primarily relying on inductive reasoning and human judgment (LaChappelle, 1980). Avalanche forecasters use field observations to help develop this picture, and methods for collecting data include: a) digging snow pits to observe snowpack structure such as weak layers and their associated depths, b) performing snow stability tests to measure the strength of snow layers, and c) analyzing recent and current meteorological observations to understand how the weather patterns could affect the existing snowpack instabilities (Haegeli, Atkins, & Klassen, 2010; LaChappelle, 1965; McClung & Schaerer, 2006). For most forecast regions, the original weather data, snowpack information, avalanche observations and local hazard assessments that are used to produce the public avalanche bulletin either come from independent professional avalanche safety operations (e.g., commercial backcountry recreation, transportation or worksite avalanche safety programs) or dedicated field teams whose mandate it is to collect observations for the public avalanche forecasters. However, there are forecast regions (e.g., North Rockies) that do not have a steady stream of observations from professional avalanche safety operations and are too remote to have permanent dedicated field teams. At the same time, there are substantial numbers of backcountry recreationists in these areas who need an avalanche forecast for their trip planning.

To address the issue of data-spare forecast regions, avalanche researchers in Canada have combined physical snowpack models with numerical weather prediction models to simulate the evolution of the seasonal snowpack in regions that would otherwise not have any observations. Current Canadian numeric weather prediction (NWP) models can forecast the weather over grids with 2.5 km horizontal spacing (Milbrandt et al., 2016). Research completed by the Applied Snow and Avalanche Research group at the University of Calgary (ASARC) under the supervision of Dr. Bruce Jamieson successfully forced the Swiss snow cover model SNOWPACK with NWP model outputs (Bartelt & Lehning, 2002; Lehning, Bartelt, Brown, Fierz, & Satyawali, 2002) with Canadian NWP models to simulate the evolution of the seasonal snowpack on the same 2.5 km grid spacing (Bellaire & Jamieson, 2013; Horton, 2015). Incredibly,

this can allow for a glimpse at the snowpack conditions at any desired location within the mountains. As this research is refined, useful computer model tools will become available for avalanche forecasters to assist in their daily hazard assessments of data-sparse regions. Since 2017, the Avalanche Research Program at Simon Fraser University (SARP) is working on upscaling the use of snowpack modelling in Canada and making the simulated observations more accessible to avalanche professionals. Using the research computing resources of Compute Canada, the SARP research team can simulate the evolution of the seasonal snowpack at thousands of locations across western Canada at a resolution of 2.5 km.

However, having large amounts of simulated weather and snowpack observations creates new challenges for avalanche forecasters. Since it is impossible for forecasters to read, analyze and synthesize all of the simulated information, current research at SARP is focusing on how to make the available information more accessible to forecasters and allow them to interact with it efficiently. Some of the key approaches for addressing this challenge are the development of insightful visualizations (Horton, Novak, & Haegeli, 2019) or the development of computer algorithms that can cluster and aggregate simulated observations (Herla, Horton, & Haegeli, In Preparation) to highlight large scale patterns and deviations from them. Another possible approach for addressing the information overload challenge is to develop algorithms that can interpret the simulated observations and summarize it in a way that links it more closely to avalanche risk management.

Another challenge in public avalanche forecasting that has emerged in recent years are inconsistencies in the interpretation of conditions among avalanche warning services and within forecaster teams. Key studies in this research area include the study of Lazar, Trautman, Cooperstein, Greene, and Birkeland (2016) who showed that avalanche forecasters presented with the same observations did not assign the same avalanche danger rating, or the study of Techel et al. (2018) who examined spatial consistency and biases in avalanche forecasts in the European Alps. In an effort to structure and standardize the avalanche forecasting process in Canada, Statham, Haegeli, et al. (2018) created the CMAH to help describe the expert reasoning processes used by industry professionals across all types of avalanche forecasting operations. Since its inception, the CMAH has become the foundation for Canadian avalanche bulletins to help avalanche terrain users mitigate their risk and the risk to

others (Statham, Haegeli, et al., 2018). The CMAH decomposes avalanche hazard into its components, reassembling them into a probability-consequence framework in an effort to reproduce the reasoning process that professionals use to explicitly describe the pathway between the raw observations and the predicted avalanche hazard (Statham et al., 2010a; Statham, Haegeli, et al., 2018). However, recent research by Statham, Holeczi, and Shandro (2018) and Clark (2019) highlighted that inconsistencies in public avalanche bulletins have prevailed in western Canada despite the introduction of the CMAH. Hence, having a better understanding of how the CMAH is applied by public avalanche forecasters and how other factors affect the hazard assessment process is critical for improving the consistency and quality of public avalanche forecasting in the future.

The challenges of creating a meaningful forecasting product from simulated observations for data-sparse regions and developing a better understanding of forecaster practices set the stage for my research. Using Glacier National Park as a pilot study area, the goal of my research is to explore the link between modelled weather and snowpack data and the presence or absence of avalanche problem types published in the public avalanche bulletin. On one side, this research offers a new quantitative perspective on forecaster habits that can potentially be used to develop approaches to improve forecaster consistency. On the other side, the research aims to contribute to the foundation for integrating avalanche problem types into snowpack simulations. Together, the results of this study aim to contribute to helping forecasters identify avalanche conditions more accurately and increase the reliability of daily avalanche bulletins for backcountry recreationists.

Chapter 2. Background

2.1. Conceptual Model of Avalanche Hazard

The CMAH was introduced in Canada in 2010 to provide a streamlined and consistent workflow for assessing avalanche hazard (Statham et al., 2010a; Statham, Haegeli, et al., 2018). The CMAH provides a foundation for forecasters to structure and focus their hazard assessment process which relies on integrating large amounts of weather, snowpack and avalanche observations combined with terrain information. Furthermore, the CMAH provides forecasters with a consistent language to express their assessments both to other avalanche professionals and to the public.

The CMAH breaks the hazard assessment process down into four sequential questions that address key components of avalanche hazard (Figure 2.1):

1. What type of avalanche problem(s) exist?
2. Where are these problems located in the terrain?
3. How likely is it that an avalanche will occur?
4. How big will the avalanche be?

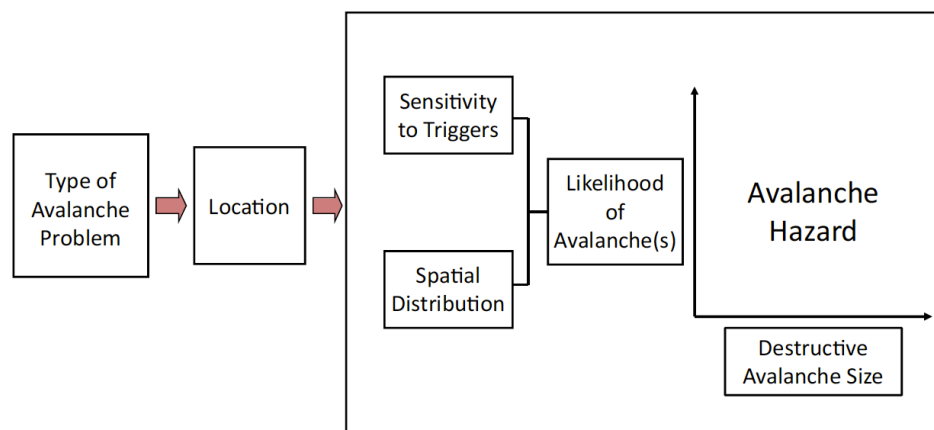


Figure 2.1 Workflow process of the CMAH, defining an avalanche problem by its type, likelihood and size (Statham, Haegeli, et al., 2018).

The concept of avalanche problems and avalanche problem types plays a critical role in the CMAH. The CMAH defines nine separate types of avalanche problems that

are created by different weather and terrain factors and snowpack characteristics (Table 2.1). Each avalanche problem is considered a repeatable pattern that requires distinct risk management techniques (Statham, Haegeli, et al., 2018). The CMAH's avalanche problem types break down the complexity of avalanche prediction into more manageable pieces and allow for prioritizing each avalanche problem individually through the workflow process.

Table 2.1 Types of avalanche problems. Edited from Statham, Haegeli, et al. (2018).

Name	Description	Typical physical characteristics
Dry Loose Avalanche Problem (LDRY)	Cohesionless dry snow starting from a point. Also called a sluff or point release.	
Wet Loose Avalanche Problem (LWET)	Cohesionless wet snow starting from a point. Also called a sluff or point release.	
Storm Slab Avalanche Problem (SS)	Cohesive slab of soft new snow. Also called a direct-action avalanche.	Weak layers of DF or PP in new snow or at new/old snow interface.
Wind Slab Avalanche Problem (WS)	Cohesive slab of locally deep, wind deposited snow	Weak layers of DF or PP in upper snowpack.
Persistent Slab Avalanche Problem (PS)	Cohesive slab of old and/or new snow that is poorly bonded to a persistent weak layer and does not strengthen or strengthens slowly over time. Structure is conducive to failure initiation and crack propagation.	Weak layers of SH, FC, or FC/CR combo in the mid- to upper snowpack.
Deep Persistent Slab Avalanche Problem (DPS)	Thick, hard cohesive slab of old snow overlying an early-season persistent weak layer located in the lower snowpack or near the ground. Structure is conducive to failure initiation and crack propagation. Typically characterized by low likelihood and large destructive size.	Basal or near-basal weak layers of DH, FC, or FC/CR combo.
Wet Slab Avalanche Problem (WET)	Cohesive slab of moist to wet snow that results in dense debris with no powder cloud.	Weak layers vary but often FC or DH at any level in the snowpack.
Glide Slab Avalanche Problem	Entire snowpack glides downslope then cracks, then continues to glide downslope until it releases a full-depth avalanche.	Weak layer of WG or FC at or near the ground.
Cornice Avalanche Problem (CORN)	Overhanging mass of dense, wind-deposited snow jutting out over a drop-off in the terrain.	

Based on their defining characteristics and required risk management approaches, avalanche problem types can be grouped into **surface problems**, such as Storm Slab (SS), Wind Slab (WS), Dry Loose (LDRY), Wet Loose (LWET), and Cornice (CORN) avalanche problem types, and **persistent problems** which include Persistent Slab (PS) and Deep Persistent Slab (DPS) avalanche problem types. SS avalanche problems are characterized by a cohesive slab of new snow that creates a short-term instability either within the newly deposited snow or at an old interface where bonding has yet to occur (Haegeli et al., 2010; Statham, Haegeli, et al., 2018), and therefore mainly occur during and immediately after storms with heavy snowfall and periods of high and fluctuating snowfall intensities. WS avalanche problems occur after sufficient wind has transported surface or falling snow into hard-packed pockets of broken snow crystals predominantly on lee (downwind) slopes and in cross-loaded areas (Haegeli et al., 2010). LDRY and LWET avalanche problems contain loose, cohesionless snow (new snow or old faceted snow) and are confined to the upper surface layers, and the main difference between the two is the liquid water content of the snow. LDRY avalanche problems predominantly occur in early to mid-winter either shortly after a storm when the new snow has settled and gained strength, or after prolonged periods of cold weather that has caused the surface snow to facet and lose cohesion. LWET avalanche problems are most common in late-winter and spring conditions when periods of prolonged melt or rainfall has sufficiently increased the liquid water content of the upper snowpack. CORN avalanche problems can occur at any time during the season but tend to occur more as the season progresses due to the amount of snow and wind needed to create sufficient sized cornices capable of breaking and collapsing. For surface avalanche problems, the main observations that practitioners pay attention to in the field are (McClung & Schaerer, 2006):

- Weather and temperature trends from the previous days
- The height of storm snow (HST, accumulation of precipitation particles (PP) and decomposing fragments (DF) from the most recent storm cycle)
- Weak layer instabilities (e.g. whumpfung, shooting cracks, pinwheeling, snowballing, etc.)
- Natural avalanche activity in the area (distribution and type)

Practitioners will also perform targeted tests (e.g. snowpack tests, ski-cutting, or explosive tests) to check the stability of the storm snow layers and the interfaces between the storm snow and the old snow (Haegeli et al., 2010).

Persistent avalanche problem types (PS and DPS) are considered more difficult to forecast than surface problems (Klassen, 2010). PS avalanche problems are characterized by a cohesive slab losing its bond with an underlying persistent weak layer (PWL) in the mid-pack that can remain unstable for weeks or even months after burial (Haegeli et al., 2010; Statham, Haegeli, et al., 2018). PS avalanches tend to release larger snow masses and are typically more destructive (Conlan, Tracz, & Jamieson, 2014; Statham, Haegeli, et al., 2018). Several types of PWLs can form under differing conditions, including: surface hoar (SH) which forms during long periods of cold, dry weather; and faceted crystals (FC) and depth hoar (DH) which form under strong temperature gradients in the snowpack; and although not a PWL, many PWLs often exist next to melt-freeze crusts (MFcr) which can contribute to PWL formation and avalanche release. PWLs can be widely distributed or form on specific aspects and elevations depending on the weather conditions during formation. They are considered PWLs after they are buried and remain unstable after storm or wind slab instabilities have subsided. These PWLs have the capability of persisting for long periods of time and can reawaken with increasing loads and elevated snowpack temperatures (Conlan et al., 2014). In the field, observations that practitioners typically look for are a cohesive slab (40-150 cm thick) overlying a PWL of SH, FC or FC/MFcr combo of varying thicknesses, and they perform stability tests (e.g. compression tests, extended column tests, propagation saw tests, and Rutschblock tests) to assess the stability of the PWL (Haegeli et al., 2010).

In western Canada, WS, SS and PS avalanche problems are the most common avalanche problem types observed (Shandro, Haegeli, Statham, & Floyer, 2016). Together with DPS, these four avalanche problem types are responsible for more than 80% of the avalanche fatalities in North American (Jamieson, Haegeli, & Gauthier, 2010; Logan & Greene, 2014). More detailed information on all nine avalanche problem types can be found on SARP's website (www.avalancheresearch.ca/avalanche-problem-types/).

Once the types of the existing avalanche problems have been identified, forecasters describe the terrain each avalanche problem might be found in by using common terminology to describe and identify avalanche terrain (Statham, Haegeli, et al., 2018). Public avalanche forecasters commonly describe avalanche terrain by specifying the elevation band and aspect ranges for each avalanche problem type.

Avalanche forecasters then estimate the likelihood of an avalanche occurring by analyzing the spatial distribution of the avalanche problem and its sensitivity to natural or human triggers (Statham, Haegeli, et al., 2018). The spatial distribution can be heavily influenced by the weather systems that create the instabilities (McClung & Schaerer, 2006) and is described using a 3-level ordinal scale ranging from 'isolated' (spotty and found in only a few terrain features) to 'widespread' (found in many locations and terrain features). The sensitivity to triggers gauges the load necessary to release avalanches, which is described by a 4-level ordinal scale ranging from 'unreactive' to 'touchy' (triggering is almost certain). The resulting likelihood, which is described using an ordinal scale from 'unlikely' to 'almost certain' (Figure 2.2), is a forecaster's best guess of the chance of avalanches occurring based on the spatial density of the particular avalanche problem's defining characteristics and any evidence found within the terrain.

Spatial Distribution	Widespread	Unlikely	Possible	Very Likely	Almost certain
	Specific	Unlikely	Possible	Likely	Very Likely
	Isolated	Unlikely	Unlikely	Possible	Likely
		Unreactive	Stubborn	Reactive	Touchy
Sensitivity to Triggers					

Figure 2.2 Likelihood of avalanches as a function of its spatial distribution and its sensitivity to triggers (Statham, Haegeli, et al., 2018).

The magnitude of avalanches is described in the CMAH by providing an estimate of the expected destructive size (CAA, 2014), which is a function of the density, mass

and speed of an avalanche and the length and cross section of avalanche path it could take (Table 2.2). Sizes can range from 1 (relatively harmless to people) to 5 (largest known avalanches, could destroy a village) and requires an assessment of the estimated harm the potential avalanche could cause (CAA, 2014).

Table 2.2 Canadian Avalanche Association size classification (CAA, 2014).

Size	Destructive Potential	Typical mass	Typical path length	Typical impact pressure
1	Relatively harmless to people.	< 10 t	10 m	1 kPa
2	Could bury, injure, or kill a person.	10 ² t	100 m	10 kPa
3	Could bury and destroy a car, damage a truck, destroy a wood-frame house or break a few trees.	10 ³ t	1000 m	100 kPa
4	Could destroy a railway car, large truck, building or a forest of approximately 4 ha.	10 ⁴ t	2000 m	500 kPa
5	Largest snow avalanche known. Could destroy a village or a forest area of approximately 40 ha.	10 ⁵ t	3000 m	1000 kPa

The final step for forecasters in the CMAH's assessment process is to summarize the overall hazard assessment using a hazard chart (Statham, Haegeli, et al., 2018) (Figure 2.3). In addition to providing the best possible estimate of likelihood and destructive size (i.e. typical value) for each avalanche problem, the hazard chart also allows forecasters to represent the uncertainty from the spatial and temporal variability by incorporating minimum, typical and maximum values.

Since its initial introduction in 2008, the CMAH has gained broad acceptance within the North American avalanche community and has been adopted by many avalanche safety operations. In 2011, the CMAH was integrated into the production of the daily avalanche bulletins by the Avalanche Canada and Parks Canada through the public avalanche forecasting system *AvalX* (Statham, Campbell, & Klassen, 2012). In 2013, the CMAH was also integrated into the *InfoEx*, the avalanche hazard information exchange platform used by avalanche safety operations in Canada (Haegeli et al., 2014).

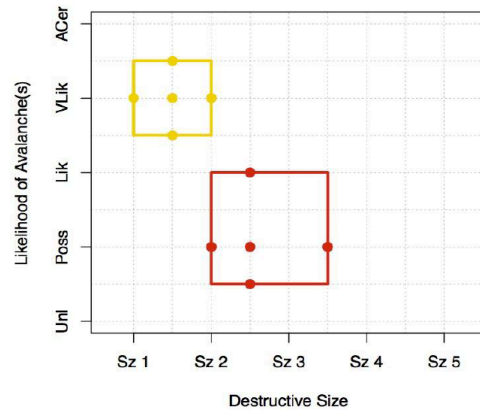


Figure 2.3 Example of a daily hazard chart. The yellow square represents a SS avalanche problem while the red square represents a PS avalanche problem. The middle point represents the typical value while the outer edges represent the minimum and maximum values (Statham, Haegeli, et al., 2018).

2.2. Numerical Weather Prediction Models

NWP models describe the current and future behaviour of the atmosphere by solving a system of differential equations based on the laws of physics on a 3-D grid around the earth (Coiffier, 2011). NWP models can predict future values of the atmosphere's characteristic variables using current meteorological observations. The fundamental variables calculated on the model grid include wind, temperature and humidity (Morin et al., 2019). Derived variables such as cloud coverage, precipitation, and radiation transfer are calculated from the fundamental variables at each grid point through parameterizations (J. Côté et al., 1998; Stull, 2016). Finally, near surface weather variables are statistically calculated including; 2 m air temperature, solar radiation, and 10 m wind speed and direction (Morin et al., 2019).

The Meteorological Service of Canada developed a suit of NWP models called Global Environmental Multiscale (GEM) models to forecast weather systems at all scales in Canada (J. Côté et al., 1998; Erfani et al., 2005; Mailhot et al., 2010; Milbrandt et al., 2016). The High Resolution Deterministic Prediction System (HRDPS) is a GEM model that covers large portions of Canada (including all of BC) with a 2.5 km horizontal grid spacing (J. Côté et al., 1998; Milbrandt et al., 2016). Initial and boundary conditions are provided by the larger scale Regional Deterministic Prediction Systems (RDPS) (Caron

et al., 2015; Milbrandt et al., 2016), with certain fields driven by a high-resolution land data assimilation system to capture small scale processes.

Avalanche forecasters use NWP models extensively to understand future weather conditions in their regions and make predictions of the expected avalanche hazard (Horton, 2015). Schirmer and Jamieson (2015) studied the reliability of NWP models (HRDPS & RDPS) to predict snowfall amounts in mountainous terrain during winter seasons where they compared modelled precipitation outputs to daily observations at more than 100 weather stations in western Canada. They found that even with the finer resolution HRDPS, precipitation values are usually underestimated. To fix these biases, they applied elevation corrections to air temperature, relative humidity and precipitation to account for differences between station and grid elevations, which increased the performance of the models (Schirmer & Jamieson, 2015). Milbrandt et al. (2016) also found that the 2.5 km resolution of the HRDPS provided an overall improvement in modelling of cloud cover and surface fields such as temperature, humidity and precipitations, making this newest NWP model more reliable for weather and avalanche forecasters in Canada.

2.3. SNOWPACK Model

One-dimensional physical snow cover models can simulate the evolution of the snowpack over entire winter seasons using input variables from weather stations or NWP models. Once snow is deposited on the ground, there are many complex interrelated processes involved in the evolution of the snowpack which can be predicted using models (Morin et al., 2019). Individual timeseries of meteorological variables drive the predicted evolution of vertical snow profiles using laws of physics to calculate new snow amounts, settling rates, surface hoar formation, temperature and density profiles, and metamorphic development of snow grains at point locations (Lehning et al., 1999; Morin et al., 2019).

The two most advanced models currently being used are the French CROCUS (Brun, Martin, Simon, Gendre, & Coleou, 1989) and the Swiss SNOWPACK (Lehning et al., 1999). CROCUS was developed to simulate the energy and mass evolution of the snow cover at a given location using meteorological inputs such as precipitation, air temperature, humidity, wind velocity and incoming short-wave and long-wave radiation

(Brun et al., 1989). SNOWPACK shares many basic principles with CROCUS, but contains more features such as explicit representation of surface hoar growth, grain bonds and erosion of snow and does not impose a limit on the amount of numerical layers it calculates (Lehning, Bartelt, Brown, & Fierz, 2002; Lehning, Bartelt, Brown, Fierz, et al., 2002). The main difference between the application of CROCUS and SNOWPACK is the operational scale; CROCUS simulates the snow cover at the scale of mountain ranges (i.e. massifs covering roughly 500 km²) whereas SNOWPACK simulates snow cover at point locations related to the weather station or NWP grid point data (Bellaire & Jamieson, 2013).

SNOWPACK was developed by researchers at the Swiss Federal Institute for Snow and Avalanche Research for the purpose of providing avalanche forecasters with supplementary information for avalanche hazard assessments, especially in cases where obtaining real-time data from snow pits was either impossible or too time-consuming (Bartelt & Lehning, 2002; Lehning, Bartelt, Brown, & Fierz, 2002; Lehning, Bartelt, Brown, Fierz, et al., 2002; Lehning et al., 1999). SNOWPACK, based on a Lagrangian finite element implementation, is a multi-layer physically-based model that numerically solves partial differential equations governing the mass, energy and momentum conservation within the snowpack (Bartelt & Lehning, 2002; Morin et al., 2019). The driving input parameters needed can either be generated from automatic snow stations, NWP models, or a combination of both and includes variables such as air temperature, relative humidity, wind speed, incoming or reflected short-wave radiation, snow surface temperature, and precipitation (Morin et al., 2019). The model output is a series of simulated timeseries of the vertical snow profile of the physical snow properties (Figure 2.4).

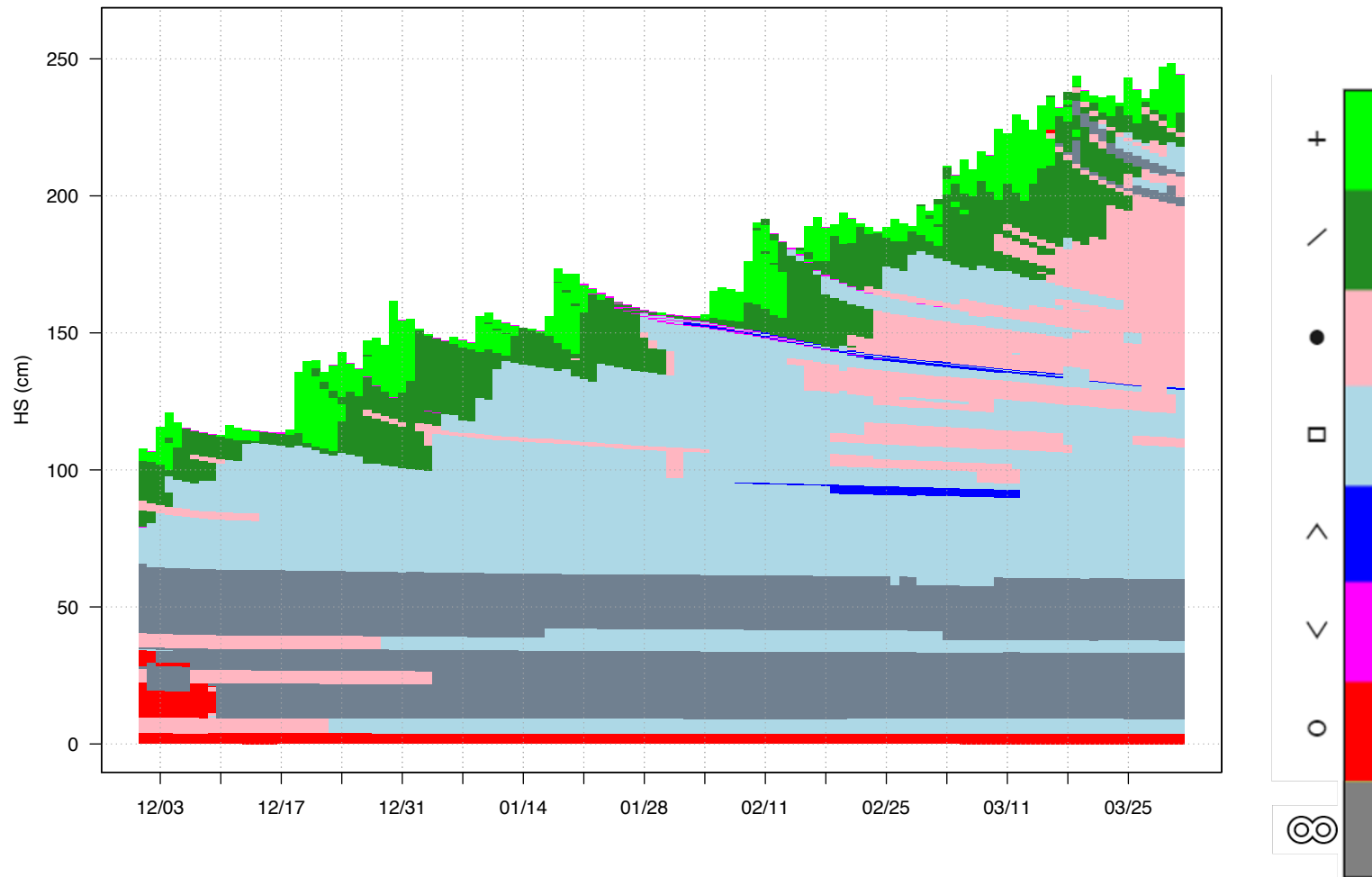


Figure 2.4 Example of SNOWPACK’s timeseries evolution output for one NWP grid point over the duration of one season. Colours are representative of grain type: Precipitation Particles (PP, +), Decomposing Fragments (DF, /), Rounded Grains (RG, •), Faceted Crystals (FC, □), Depth Hoar (DH, ^), Surface Hoar (SH, v), Melt Forms (MF, o), Melt-Freeze Crusts (MFcr, ∞).

2.4. SNOWPACK Research and Application in Canada

The sheer size of Canada's mountainous regions and the sparsity of automated weather stations makes it impossible to use the Swiss version of SNOWPACK in the traditionally intended way. In an effort to create a more meaningful forecasting tool for public avalanche forecasters in Canada, Bellaire, Jamieson, and Fierz (2011) coupled SNOWPACK with Canada's regional forecasting model GEM-15 which predicted weather on a 15 km grid spacing (Erfani et al., 2005; Mailhot et al., 2010) to provide information for avalanche forecasting in regions that would otherwise be data-sparse. In their study area of Glacier National Park (GNP), the authors found a notable overprediction of precipitation, which led to inaccuracies in the simulated snowpack within the models (Bellaire et al., 2011). After pre-processing of the input data using elevation corrections, the SNOWPACK model was run and extensive comparisons between modelled and observed snow profile data were completed. The results indicated that snow depth and new snow events were well modelled and many (over 50%) of the relevant critical layers were reproduced (Bellaire et al., 2011).

More recently, weather data from the HRDPS (GEM-LAM) (Milbrandt et al., 2016) has been coupled with SNOWPACK, increasing the spatial resolution from 15 km to 2.5 km (Bellaire & Jamieson, 2013; Horton & Jamieson, 2016). The increase in resolution allows for better modelling of localized atmospheric effects in complex terrain and a better representation of the variability of the snowpack at a regional scale. Projects currently being worked on at SARP by Herla et al. (In Preparation) and Horton et al. (2019) have the potential to provide avalanche forecasters with large amounts of relevant snowpack information in a meaningful and efficient way in the future.

2.5. Modelling of Avalanche Hazard

Existing studies modelling avalanche hazard have used a wide range of different statistical approaches using different input parameters. Early studies tried to distinguish if a given day was susceptible to avalanches or not by using discriminant analysis and nearest-neighbour methods. For example, Obled and Good (1980) introduced the use of the nearest-neighbour method to estimate the probability of an avalanche occurrence within a ski area in Switzerland. The authors' idea was to compare current avalanche

conditions with recorded avalanche conditions in the past. McClung and Tweedy (1994) predicted avalanche occurrences using Bayesian statistics in their discriminant analysis model. The authors also incorporated clustering techniques and the nearest-neighbour method to analyze the avalanche occurrences. Brabec and Meister (2001) used the nearest-neighbour method to assess regional avalanche danger from manual weather station observations such as aspect, elevation and avalanche activity. Results indicate that their model failed most often over periods when snow-cover stability was important. Floyer and McClung (2003) incorporated canonical discriminant analysis with a one-way analysis of variance to study which physical variables were important to avalanche prediction. The authors were able to differentiate and classify time periods into avalanche and non-avalanche periods by identifying important variables such as new precipitation amounts, snowpack depth and air temperature.

Other studies incorporated machine learning techniques such as support vector machines (SVM), artificial neural networks, Bayesian additive trees and classification trees to predict avalanche hazard. Schirmer, Lehning, and Schweizer (2009) used SNOWPACK model outputs and meteorological variables to examine the link between weather and snowpack conditions and regional avalanche danger. Although the authors tried numerous statistical methods (i.e. classification trees, artificial neural networks, SVM, hidden Markov models and nearest-neighbour methods), the nearest-neighbour method achieved the best results when incorporating the avalanche hazard from the previous day as additional input. Pozdnoukhov, Matasci, Kanevski, and Purves (2011) incorporated local weather observations, modelled snowpack variables and avalanche observations into an SVM approach. Using a 10 m resolution the authors were able to produce avalanche forecasts for a small forecast region in Scotland based on a probability framework from unlikely (0%) to certain (100%). Bellaire and Jamieson (2013b) also used classification trees to model avalanche danger ratings from SNOWPACK model outputs and estimates of the regional avalanche danger from experienced forecasters. Using four parameters derived from the simulated profiles (maximum new snow amounts over 24-hours and 3-days and measures of likelihood, and; expected avalanche size based on skier stability index and depth of a critical layer), the authors estimated avalanche danger with an accuracy ranging between 70 – 77%. Likewise, Hendrikx, Murphy, and Onslow (2014) used classification trees, but incorporated 28 years of weather, snowpack and avalanche activity observations to

identify the key variables responsible for days with significant avalanche activity. The authors propose that the model could provide avalanche forecasters with an additional tool to assist with decision making. More recently, Blattenberger and Fowles (2017) employed a Bayesian additive tree model to predict whether or not an avalanche would cross the main highway at a specific location in Utah. By incorporating 17 years of winter data the authors' method outperformed traditional statistical methods and reduced losses arising from misclassification. Building on the existing research, Clark (2019) used conditional inference trees (CIT) to explore the relationship between avalanche hazard assessments and the danger rating assignments in Canadian public avalanche bulletins. The author extracted key decision rules and the important components of the CMAH that influenced danger rating assessments and created a foundation for critically reviewing current forecaster practice.

Since forecasted regional avalanche assessments can cover large amounts of terrain (usually $>100 \text{ km}^2$), Jamieson, Haegeli, and Schweizer (2009) used classification and regression trees (CART; Breiman, Friedman, Olshen, & Stone, 1984) to estimate the local avalanche danger at the scale of a recreational ski tour ($\sim 10 \text{ km}^2$). The authors identified simple weather, snowpack and avalanche observations that are used by recreationists to assess the current avalanche hazard in the field without having to dig a snow pit (e.g. whumpfung, shooting cracks, recent avalanche activity, etc.). The recreational snow observations were incorporated with the regional avalanche danger level to create a more representative local avalanche danger level. Building on this body of work, Haladuick (2014) incorporated a much larger dataset and used multivariate classification trees to assess the relationships between the recreational snow observations and the local avalanche danger for each avalanche problem type identified by the CMAH. The author's results indicated that the trees could be used to predict the current local avalanche danger for each avalanche problem based on the decision rules that emerged.

Expert systems such as MÉPRA (Giraud, 1992) emulate the human avalanche forecasting and decision-making processes and are perhaps a more effective approach to predicting avalanche hazard. Data is processed based on pre-determined decision rules to interpret simulated snow profile data and derive an avalanche hazard rating. MÉPRA is the final model of a chain of models (including the meteorological analysis system SAFRAN (Durand et al., 1993) and the snow cover model CROCUS (Brun et al.,

1989)) that evaluates the avalanche hazard based on modelled weather and snowpack conditions. Similarly, Schweizer and Föhn (1996) also created two separate expert system models to evaluate avalanche hazard based on the elevation and aspect of avalanche prone slopes and on weather and snowpack observations in Switzerland. The DAVOS model was strictly data-based and achieved an accuracy of 60%, while the MODUL model was a combination of data- and rules-based and achieved an accuracy of 70 – 75%.

Chapter 3. Methods

3.1. Study Area

The study area for my research was Glacier National Park (GNP), a Canadian national park which is located in the Columbia Mountain range between the towns of Revelstoke and Golden in the interior of BC (Figure 3.1). The mountainous terrain in GNP ranges from dense vegetation in the valleys to open glades at treeline (~2000 m.a.s.l.) and glaciated mountain tops (~3000 m.a.s.l.).

Based on the snow and avalanche climate scheme described by Armstrong and Armstrong (1987) and further refined in a Canadian context by Haegeli and McClung (2003) and McClung and Schaerer (2006), the Columbia Mountains (and GNP) have a '*transitional*' snow climate with a strong '*maritime*' influence. The snowpack in a '*transitional*' snow climate is typically quite deep and exhibits several PWLs throughout the season. However, these characteristics can vary considerably from year to year due to the '*maritime*' influence. On average, Rogers Pass in GNP sees roughly 140 snowfall days per year which bring approximately 10 m of snow at treeline per season (Parks Canada, 2019).

The combination of excessive amounts of powder snow and accessibility make GNP a popular destination for backcountry skiers, and the presence of a critical transcontinental railway (completed in 1885) and the Trans-Canada Highway (completed in 1962) have made Rogers Pass a focal point of Canadian avalanche risk mitigation. Within the park, Parks Canada is responsible for both managing avalanche risk on the transportation corridor and producing a public avalanche bulletin for backcountry recreationists. Due to the large amount of snowfall, highway staff record approximately 2000 avalanche events each winter on approximately 140 avalanche paths that impact the highway and railway (Parks Canada, 2019). From a public avalanche forecasting perspective, GNP is a relatively small forecast region (1349 km²).

Rogers Pass has also been the location for many avalanche research projects, including work done by Schweizer, Jamieson, and Skjonsberg (1998), Bellaire and Jamieson (2013), and K. Côté, Madore, and Langlois (2017). In addition, much of the

SNOWPACK model validation work done by Bruce Jamieson's research group has been completed in GNP (Bellaire et al., 2011; Horton & Jamieson, 2016).

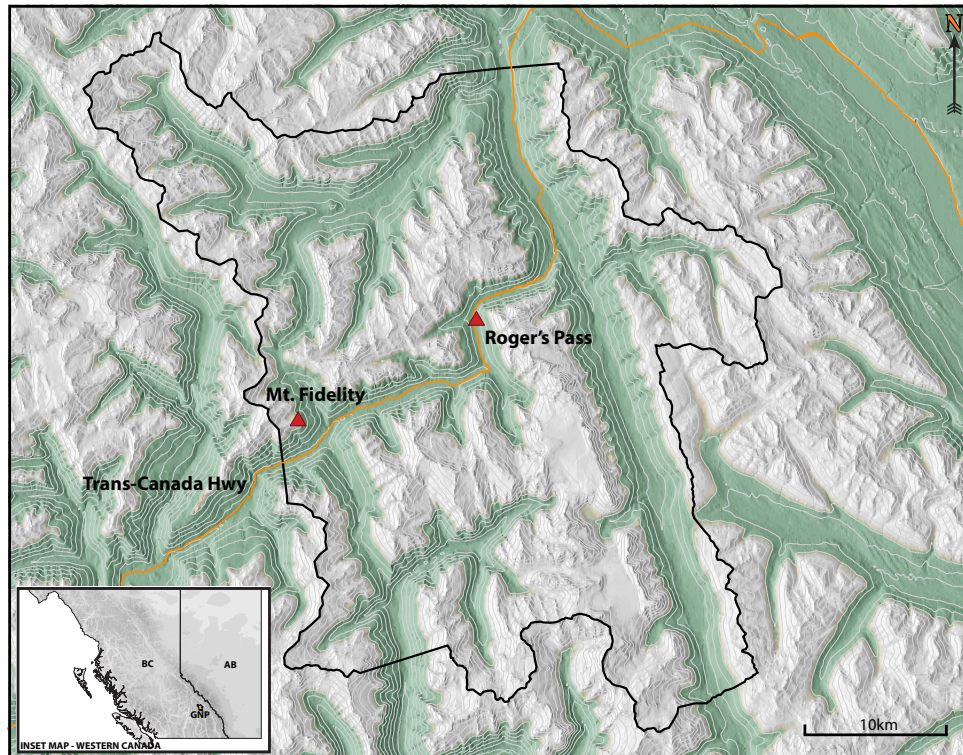


Figure 3.1 Study Area - Glacier National Park of British Columbia. Parks Canada study plots at Mt. Fidelity and Roger's Pass are shown.

3.2. Study Period

My study covers the six winter seasons from 2013 to 2018 (December 1st to March 31st). These winters cover a wide variety of weather and avalanche conditions giving my dataset a meaningful sample of the variability of conditions experienced within GNP.

The 2013 season was a classic example of a '*transitional*' snow climate and was characterized by multiple WS, SS, LDRY and PS avalanche problems. Abundant early season snow and formation of PWLs increased the avalanche hazard rating to high by the beginning of December. Cold, dry spells during mid-end of December and early-mid January created additional PWLs and by early March. The combination of many PWLs

in the snowpack and large amounts of snowfall increased the occurrences of SS and PS avalanche problems and elevated the avalanche hazard rating to high and extreme.

The 2014 season leaned more towards a '*continental*' snow climate with more frequent periods with clear skies and less snowfall which resulted in longer cold spells and a thinner snowpack. These conditions were conducive to the creation of many PWLs and the majority of days had forecasted WS, SS and PS avalanche problems. The combination of numerous PWLs and a large storm cycle at the beginning of January elevated the avalanche hazard rating to high and extreme. A long cold snap from mid-January to early February resulted in a relatively calm period of avalanche hazard but created a PWL that persisted through to the end of the season and caused elevated avalanche hazard.

The 2015 season was an interesting season that saw a strong '*maritime*' influence. Periods of warm temperature brought heavy rainfall above the treeline elevation several times throughout the season which saturated the snowpack and temporarily elevated the avalanche hazard rating before colder temperatures stabilized the snowpack. PS avalanche problems were dominant and persisted most of the season. There was also an increase in LWET avalanche problems. The rainfall events and warmer weather contributed to a very thin seasonal snowpack.

The 2016 season saw a return to the standard '*transitional*' snow climate with frequent periods of clear skies and colder temperatures. The season was dominated by WS and SS avalanche problems and although there were many periods of cold dry spells conducive to PWL formation, there was not many occurrences of PS avalanche problems. Comparatively, this season also seemed to be safer compared to other years with many periods of low to moderate avalanche hazard.

The 2017 season continued the standard '*transitional*' snow climate trend, highlighted by colder temperatures and intermittent snowfall. Also dominated by WS and SS avalanche problems, the avalanche hazard remained relatively low for the first half of the season. An increase in temperatures and snowfall amounts in early February, buried a couple of PWLs that contributed to a few periods of elevated avalanche hazard and identified PS avalanche problems.

The 2018 season began with early season PWL formation and was again a standard '*transitional*' snow climate. These PWLs contributed to an extended period from mid-December to late February where PS avalanche problems were continuously identified. SS avalanche problems were also dominant, especially throughout the middle part of the season where the bulk of the snowfall occurred. Overall, the avalanche hazard remained low to considerable with the exception of the mid-season storm cycles that elevated the hazard to high on multiple occasions.

3.3. Dataset

Since the winter season of 2013, the avalanche forecasting team in GNP has consistently applied the CMAH using the *AvalX* software (Statham et al., 2012) to record observations and produce daily avalanche bulletins. Hence, complete avalanche hazard characterizations according to the CMAH are available for my entire study period. Simulated meteorological data was extracted from the HRDPS and used as inputs to simulate the snow cover using SNOWPACK. Modelled weather and snowpack data were then merged with avalanche hazard assessment data from the GNP public avalanche bulletins by date to produce the analysis dataset for the study.

3.3.1. Avalanche Bulletins from Parks Canada

Avalanche bulletin data from *AvalX* consists of three main components: metadata, avalanche problem type characteristics, and associated avalanche danger ratings for each day. Metadata contains information on the authoring forecaster, date of publication and the associated region and mountain range. Avalanche problem type data contains information from the application of the CMAH, including: a) the minimum, typical and maximum values of likelihood and destructive size; b) avalanche problem location based on elevation bands and aspects; c) the spatial distribution, and; d) the sensitivity to triggering. The overall avalanche hazard assessment is represented by an avalanche danger rating for each elevation band on the day the bulletin is released and also includes a forecast for the following two days (Figure 3.2).

Avalanche Bulletin - Glacier National Park - Thu Jan 01, 2015

Issued: Thu Jan 01, 2015 08:09

Valid Until: Fri Jan 02, 2015 08:00

Special Avalanche Warning in Effect... [Click Here](#)

“The Special Avalanche Warning has been extended. The potential for human triggered avalanches on the December 17th surface hoar layer continues. Conservative route selection is advised.” [PW]

[Weather Stations](#) [map of region](#) [Print](#) [CAAML Data Source](#) [disclaimer](#)

Public Avalanche Forecast

Forecast Details



[Weather Observations](#)

[learn more about danger ratings...](#)

Problem 1: Persistent Slabs



The December 17th surface hoar layer is still reactive. Avalanches continue to be triggered even in locations previously skied. Some areas offer few clues of the instability but the potential for large avalanches continues.

Travel and Terrain Advice

Use conservative route selection, choose moderate angled and supported terrain with low consequence. Choose conservative lines and watch for clues of instability.

Figure 3.2 Sample of a daily avalanche bulletin from GNP (Parks Canada, 2019).

A custom *R* package was designed by the SARP lab to easily extract the data from the *AvalX* database and make it accessible for analysis. The extracted data from *AvalX* for the six winter seasons was a list of three data frames; *Bulletins*, containing all metadata; *AvProblems*, containing avalanche problem data for each elevation band, and; *DngRating*, containing the current and forecasted danger ratings data for each elevation band.

The daily avalanche hazard assessments were converted and split into separate wide format tables for each elevation band. Each row of the table was for a unique day and columns were added to represent the presence of each avalanche problem type with binary values for the present (1) and absence (0) of that problem. Each problem

type column contained the binary value of their presence on each of the eight aspects of that elevation band (eight cardinal and intermediate directions).

3.3.2. NWP Model

Hourly weather data from the HRDPS was compiled for 225 NWP grid points that fell within the boundaries of GNP and written into a SARP research database for easy access. The HRDPS provides an updated weather forecast every 6 hours, and so 6 hours of data were taken from each forecast to produce a continuous hourly timeseries for all six winter seasons. Variables extracted included air temperature ($^{\circ}\text{C}$, 2 m above the surface), wind speed and direction (m/s, azimuth degrees, 10 m above the surface), relative humidity (% of maximum, 2 m above the surface), precipitation (mm/h), and incoming short-wave and long-wave radiation (W/m^2). All grid points were labelled with the elevation bands used by Parks Canada in their avalanche assessments in GNP; Below Treeline (BTL, 0 – 1800 m.a.s.l.), Treeline (TL, 1800 – 2100 m.a.s.l.), and Alpine (ALP, above 2100 m) (Parks Canada, personal communication, 2018). Each grid point is given a *Station ID #* (eg. 086523), and once in the SARP database, data for each grid point can be queried using these identifiers.

For the present study, one NWP grid point for each elevation band was chosen to keep the analysis relatively simple. Grid points were selected near the Trans-Canada Highway since Parks Canada mainly uses observations from locations near the highway for their avalanche assessments (Table 3.1). Additional criteria for the selection of the grid points was a) their location being in the middle of GNP, and b) their elevation being roughly located in the middle of their respective elevation bands (Figure 3.2). The simplification of only focusing on a single grid point per elevation band seems reasonable since weather among grid points at similar elevations are highly correlated.

Table 3.1 Station ID #s - 2013 – 2017 Seasons

Station ID #	Elevation Band	Elevation (m.a.s.l.)
158676	BTL	1436
158681	TL	1904
155942	ALP	2141

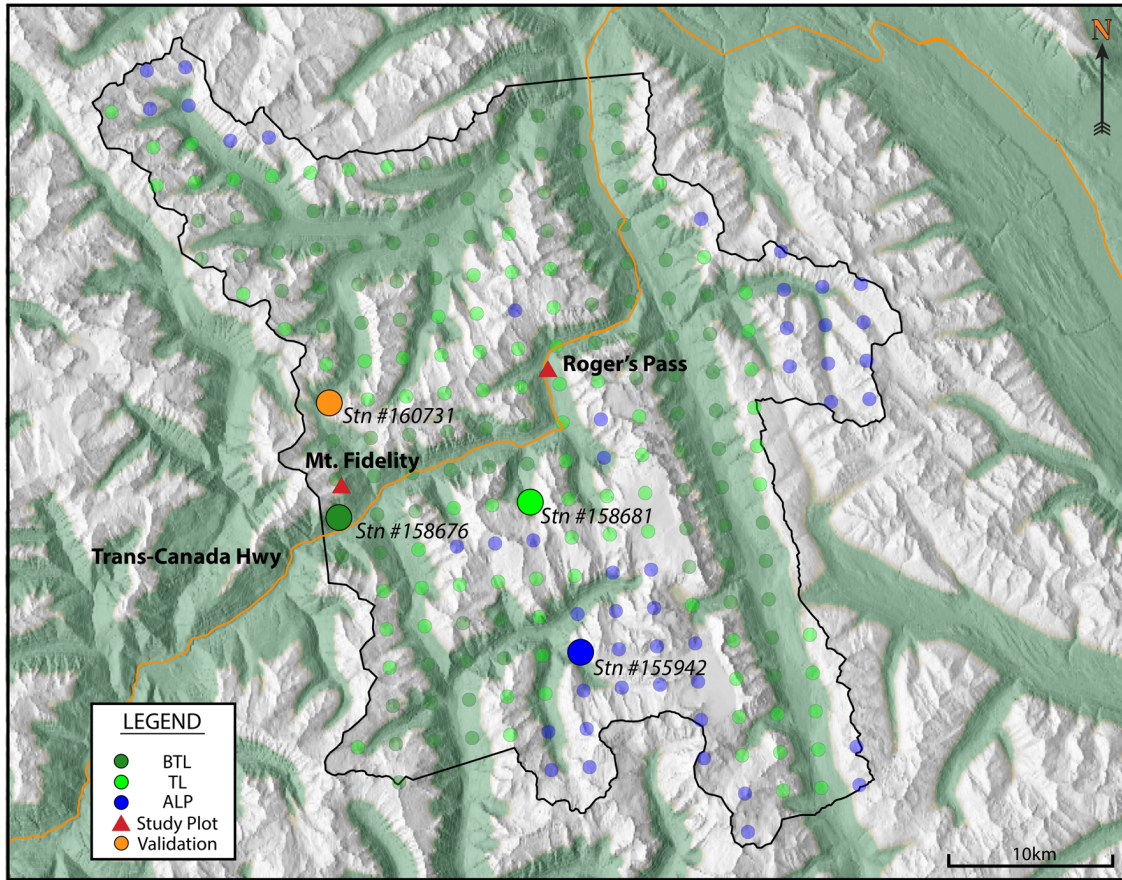


Figure 3.3 2013-2017 NWP grid point locations.

An upgrade to the HRDPS prior to the 2018 winter season changed the location of all grid points, therefore new grid points were chosen for the last two seasons under the same premise (Table 3.2, Figure 3.3).

Table 3.2 Station ID #s - 2018 Season

Station ID #	Elevation Band	Elevation (m.a.s.l.)
080856	BTL	1499
082514	TL	1875
078657	ALP	2227

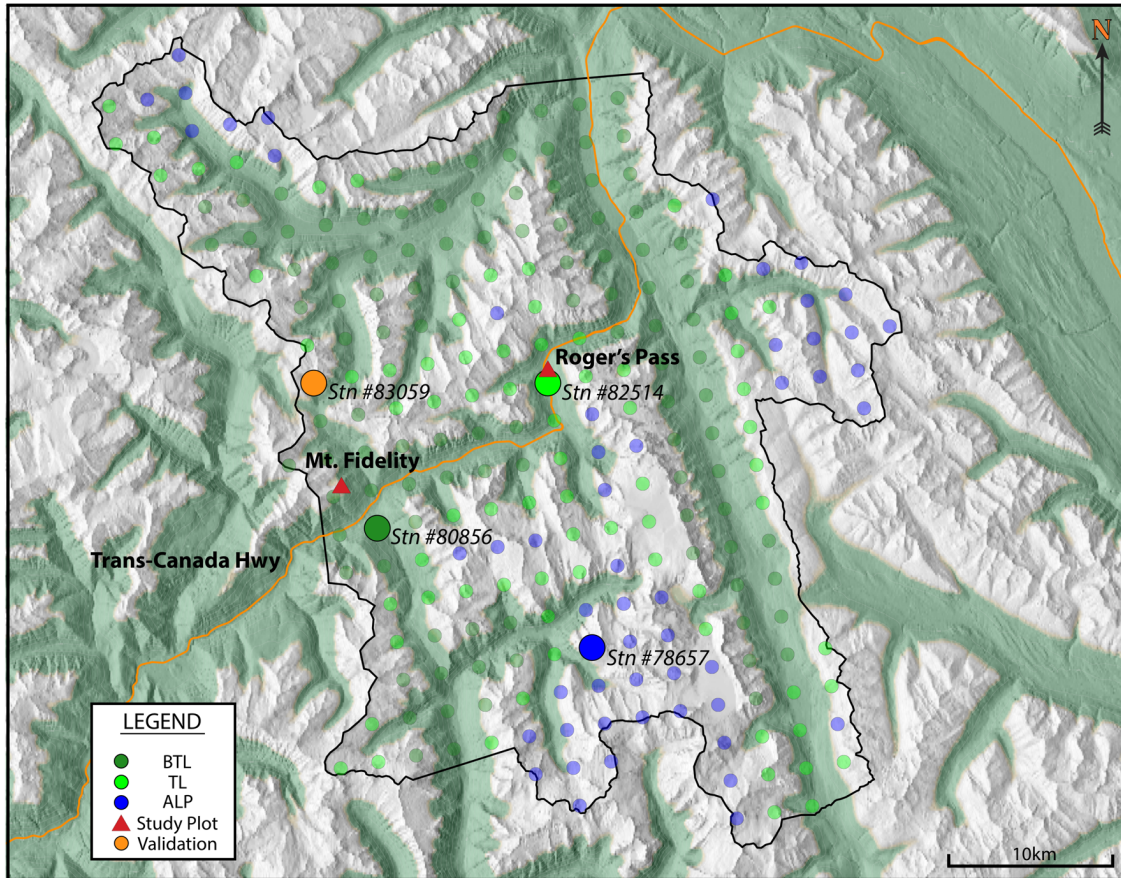


Figure 3.4 2018 NWP grid point locations.

3.3.3. SNOWPACK Model

The modelled meteorological data from the HRDPS (air temperature, wind, relative humidity, precipitation, incoming short-wave and long-wave radiation) was used as inputs for the SNOWPACK model to simulate a single flat-field (horizontal) snow profile at the three chosen NWP model grid points for all six winter seasons. Default SNOWPACK settings were used in the simulations, with wind transport disabled to simulate conditions in sheltered terrain. SNOWPACK outputs consisted of snow layers at every timestep and timeseries of modelled weather and key variables.

Daily simulated weather and snowpack observations at 8:00 a.m. were extracted and written to the SARP research database to match the approximate time when avalanche bulletins are published in GNP (Parks Canada, personal communication,

2018). Each profile consisted of snow layers with the following properties: height, deposition date, density, temperature, grain size, grain type, hand hardness, and a structural stability index based on the derivation of Schweizer, Bellaire, Fierz, Lehning, and Pielmeier (2006). The number of layers in each profile was reduced using SNOWPACK's internal layer aggregation routine that merges layers with similar properties. In addition to the daily snow profiles, timeseries of the hourly input weather data from the HRDPS were compiled into a data frame along with a few key variables from SNOWPACK (height of snowpack (HS), height of settled snow from the previous 24 h (HN24), and height of settled snow from the previous 72 h (HN72)), which was also written to the SARP research database.

3.3.4. Weather Observations

Within GNP, Parks Canada also operates several automatic weather stations at different elevations relevant to avalanche forecasting along the Trans-Canada Highway corridor. Along with gathering weather data, numerous locations include study plots where manual snow profiles are recorded at regular intervals to document the evolution of the snow cover over the entire season. Mt. Fidelity and Rogers Pass (see Figure 3.1 for locations) both contain flat field study plots where information on the conditions of the snow cover are reported to the InfoEx regularly and there is 10+ years of consistent weather and snowfall data. The study plot at Mt. Fidelity is located in a clearing at treeline (1905 m.a.s.l.), and is sheltered from the wind (Horton, 2015). The study plot at Rogers Pass is in a large sheltered clearing below treeline, surrounded by dense forest (1305 m.a.s.l.). To validate the simulated snowpack variables produced by my model chain, Parks Canada shared relevant weather and snowpack observations (air temperature, snow surface temperature, wind speed and direction, HS, HN24, and HST) with the research team.

3.4. Data Preparation and Manipulation

The dataset was converted into two separate structures to facilitate the analysis of surface avalanche problems and persistent slab avalanche problem types separately. Due to the unique characteristics of these avalanche problem types, each was approached differently. Additional derived variables were computed from the original

model output variables to better represent what avalanche forecasters might be looking for when assessing the hazard of different avalanche problem types.

3.4.1. Surface Avalanche Problem Types

The relatively simple nature of surface avalanche problem types allowed me to extract variables and the surface avalanche problems (WS, SS, LDRY, LWET, WET, CORN) from the three representative grid points for all six seasons into a single table with a wide format where each day was represented by three rows, one for each elevation band (BTL, TL, and ALP). The status of each surface avalanche problem was labelled *Absent* or *Present* based on whether it was currently being identified in each respective elevation band. The status from the previous day for each avalanche problem was also recorded. Since WET avalanche problems were only identified on two days in the entire dataset, I did not include this avalanche problem type in the analysis. The resulting data frame was wide format with columns for each modelled weather and snowpack variable from the representative NWP grid point for that elevation band (Table 3.3).

The NWP output data was used to calculate a few extra weather variables that were chosen to strengthen the dataset and offer different perspectives. To mimic the HN24 precipitation variable calculated by SNOWPACK, a rain sum variable was calculated to keep track of the amount of rainfall for every day. Also, in an effort to create more meaningful wind variables, wind run values were calculated as the sum of hourly wind speed values over defined periods of time (24 h, 48 h and 72 h) to represent the total amount of wind experienced at a location. These variables were added to the surface avalanche problem dataset. Several additional snowpack variables were also calculated from the SNOWPACK output to include variables in the analysis that reflect how practitioners examine the real snowpack. First, a key variable that forecasters and practitioners observe for their avalanche hazard assessments is the amount of snow that has accumulated through the duration of each storm using storm boards, height of storm snow (HST; CAA, 2014). To produce this observation from the modelled data, I created a function that calculates HST and the properties of the storm snow from the snow profiles modelled by SNOWPACK. The function determines the bottom HST

Table 3.3 Modelled and calculated variables for surface avalanche problem types

Variable Name	Units	Source	Description
StatusWIND		Bulletin	Problem status of WS avalanche problem
StatusSTORM		Bulletin	Problem status of SS avalanche problem
StatusLDRY		Bulletin	Problem status of LDRY avalanche problem
StatusLWET		Bulletin	Problem status of LWET avalanche problem
StatusCORN		Bulletin	Problem status of CORN avalanche problem
StatusSTORMPrev		Bulletin	Previous day problem status of SS
StatusWINDPrev		Bulletin	Previous day problem status of WS
StatusLDRYPrev		Bulletin	Previous day problem status of LDRY
StatusLWETPrev		Bulletin	Previous day problem status of LWET
StatusCORNPprev		Bulletin	Previous day problem status of CORN
SeasonDay		Bulletin	Day of the season (from October 1 st)
SeasonMonth		Bulletin	Month of the season (from October)
ta_avg	°C	NWP	Average hourly temperature over last 24 h
ta_max	°C	NWP	Maximum hourly temperature over last 24 h
ta_min	°C	NWP	Minimum hourly temperature over last 24 h
vw_avg	m/s	NWP	Average hourly wind speed over last 24 h
vw_max	m/s	NWP	Maximum hourly wind speed over last 24 h
vw_min	m/s	NWP	Minimum hourly wind speed over last 24 h
rain_sum	mm	NWP	Total rainfall over last 24 h
wr24	m	NWP	Wind run of last 24 h
wr48	m	NWP	Wind run of last 48 h
wr72	m	NWP	Wind run of last 72 h
tss	°C	SNOWPACK	Snow surface temperature
hs	cm	SNOWPACK	Height of snowpack
hn24	cm	SNOWPACK	New snow over last 24 h
hn72	cm	SNOWPACK	New snow over last 72 h
ski_pen	cm	SNOWPACK	Ski penetration from surface
hst_thickness	cm	SNOWPACK	Total thickness of storm snow
hst_density	kg/m ³	SNOWPACK	Weighted average density of storm snow
hst_ssi_bottom		SNOWPACK	SSI of layer under storm snow
hst_ssi_min		SNOWPACK	Minimum SSI of storm snow
hst_grain_type_below		SNOWPACK	Grain type below storm snow
hst_grain_size_below	mm	SNOWPACK	Grain size below storm snow
hn48_thickness	cm	SNOWPACK	Total thickness of 48 h snowfall
hn48_density	kg/m ³	SNOWPACK	Weighted average density of 48 h snowfall
hn48_ssi_bottom		SNOWPACK	SSI of layer under 48 h snowfall
hn48_ssi_min		SNOWPACK	Minimum SSI of 48 h snowfall
hn48_grain_type_below		SNOWPACK	Grain type below 48 h snowfall
hn48_grain_size_below	mm	SNOWPACK	Grain size below 48 h snowfall
hn72_thickness	cm	SNOWPACK	Total thickness of 72 h snowfall
hn72_density	kg/m ³	SNOWPACK	Weighted average density of 72 h snowfall
hn72_ssi_bottom		SNOWPACK	SSI of layer under storm 72 h snowfall
hn72_ssi_min		SNOWPACK	Minimum SSI of 72 h snowfall
hn72_grain_type_below		SNOWPACK	Grain type below 72 h snowfall
hn72_grain_size_below	mm	SNOWPACK	Grain size below 72 h snowfall

interface layer in the snow profile by determining the starting day for a new storm cycle. New storm snow cycle periods were initialized after each day with zero precipitation. The function then computed the overlying storm slab properties including; slab thickness, maximum and average hardness, maximum and average density, and minimum structural stability index (SSI). It also attached the SSI, grain type and grain size of the interface layer below the storm snow. All slab average values were calculated using a product sum to properly account for the varying thicknesses of the layers. To gain insight into how different time periods of recent snowfall affected surface avalanche problems, I created two additional sets of surface snow layers for my analysis. Interfaces defined by HN48 and HN72 were used to calculate the slab properties of all layers deposited within the last 48 h and 72 h, respectively. All three extra groups of calculated variables were added to the existing data frame to complete the surface avalanche problem properties (Table 3.3).

3.4.2. Persistent Slab Avalanche Problem Types

Since PS and DPS avalanche problems are inherently linked to PWLs within the snowpack, a meaningful analysis of these avalanche problems required a different data structure than what was used for the surface avalanche problems. Instead of focusing on days and examining whether a specific avalanche problem existed or not, the analysis of PS and DPS avalanche problems tracked all storm interfaces with the potential to turn into PWLs and examined their link to different avalanche problem types over time. Hence, creating this dataset required a) identifying potential PWLs, and b) tracking their characteristics and the properties of the associated overlying slab as they evolved over the entire season.

Since the SNOWPACK model reproduces PWLs most accurately at the TL elevation band (Horton & Jamieson, 2016), only the TL elevation grid point for all six seasons was analyzed (Table 3.1 and Table 3.2). It is important to note that to simplify the present analysis, DPS and PS avalanche problem types were merged in the present study. This was done because a) the number of days with DPS avalanche problems was relatively small (only 38 days for all seasons), b) they are directly related to the same PWLs as PS avalanche problems, and c) operational experience has shown that forecasters have challenges distinguishing between PS the DPS avalanche problem types (Klassen, 2014).

To ensure the capturing of all potential interfaces that could be related to PS and DPS avalanche problems in the SNOWPACK model, a function was created to determine the last day before a new storm cycle began. Since each new storm cycle had the potential to bury a possible weak layer (e.g. SH, DH, FC, or MFcr grain types created on the surface and subsequently buried by new snowfall), every storm cycle start date was compared to the daily avalanche bulletins to make sure that the dates of all PWLs that were explicitly discussed in the bulletin text throughout all six seasons were captured. Due to the fact that SNOWPACK merges adjacent layers of similar characteristics for efficiency reasons by default, it is possible that the date of a particular PWL of concern may not be explicitly represented in every simulated snow profile at the chosen grid point. To address this issue, I manually assigned a meaningful date range to each potential interface (based on days with no snowfall leading up to the next storm cycle) that would look through SNOWPACK profiles and find the weakest layer within the date range using the SSI of the layer (Schweizer et al., 2006). Similar to the function for extracting HST characteristics from the surface avalanche problems, a function was created that extracted all the characteristics for an associated interface and the overlying slab from the simulated SNOWPACK profiles (Table 3.4). In addition, the age of each interface was calculated by counting the number of days between the initial burial of the layer and the day of the forecast. Each interface captured by SNOWPACK was labeled with the date of burial taken from the daily avalanche bulletin analysis or from the storm cycle analysis.

Finally, I created a variable named ProbStatus to describe the link of the tracked interface to PS and DPS avalanche problems throughout the season. To understand which of the existing interfaces was associated with each forecasted occurrence of PS/DPS avalanche problems, I manually interpreted each daily public avalanche forecast from Parks Canada keeping track of the date of burial of the interfaces and when they were considered problems. Klassen (2014) describes the common progression for the creation of a PS avalanche problem as a) the formation of a potential weak layer on the snowpack surface, b) the interface is buried by a storm cycle where it usually becomes a surface problem (i.e. SS avalanche problems), and c) the overlying snow becomes a cohesive slab and the interface becomes a PWL susceptible to natural and human triggers. As time progresses, the PWL heals or becomes dormant deep in the snowpack before it potentially wakes up again in the spring. Accordingly, three

different stages of an interface were recorded in the ProbStatus column. Interfaces and the overlying snowpack were considered a *Surface* problem from their date of burial to the last day before they were associated with a PS/DPS avalanche problem in the bulletin. If an interface was never assigned as a PS/DPS problem throughout the season, it remained a *Surface* problem. The ProbStatus of an interface was labeled as *Present* for the duration of time that the PS/DPS avalanche problem was actively considered an issue in the bulletin. Once the PS/DPS avalanche problem was considered healed or dormant (i.e. not mentioned in the bulletin anymore), the status of the interface was labeled *Absent* (Figure 3.5).

The properties of each interface for each day of the season were merged by stacking them together and combined with the tracked interfaces from the rest of the seasons creating a long data frame. Since I was only interested in the dates after interfaces were formed, this data frame did not necessarily cover all the dates between the December 1st – March 31st for every season in the study period. In addition, many dates contained more than one record as multiple storm interfaces and potential PWLs would be tracked at the same time. Therefore, each observation record in the data frame for the PS/DPS analysis contained information on the interface and the overriding slab at the TL elevation band for a given day.

Table 3.4 Modelled and calculated variables for PS avalanche problem types

Variable Name	Units	Source	Description
ProbStatus		Bulletin	Problem status of PS/DPS avalanche problem
SeasonMonth		Bulletin	Month of the season (from October)
SeasonDay		Bulletin	Day of the season (initialized on October 1 st)
ta_avg	°C	NWP	Average hourly temperature over last 24 h
ta_max	°C	NWP	Maximum hourly temperature over last 24 h
ta_min	°C	NWP	Minimum hourly temperature over last 24 h
vw_avg	m/s	NWP	Average hourly wind speed over last 24 h
vw_max	m/s	NWP	Maximum hourly wind speed over last 24 h
vw_min	m/s	NWP	Minimum hourly wind speed over last 24 h
rain_sum	mm	NWP	Total rainfall over last 24 h
wr24	m	NWP	Wind run of last 24 h
wr48	m	NWP	Wind run of last 48 h
wr72	m	NWP	Wind run of last 72 h
hs	cm	SNOWPACK	Height of snowpack
hn24	cm	SNOWPACK	New snow over last 24 h
hn72	cm	SNOWPACK	New snow over last 72 h
wkl_density	kg/m ³	SNOWPACK	Average density of PWL
wkl_lwc	% of vol.	SNOWPACK	Liquid water content of PWL
wkl_grain_size	mm	SNOWPACK	Grain size of PWL
wkl_hardness		SNOWPACK	Hardness of PWL
wkl_ssi		SNOWPACK	SSI of PWL
wkl_grain_type		SNOWPACK	Grain type of PWL
wkl_thickness	cm	SNOWPACK	Thickness of PWL
wklage	days	SNOWPACK	PWL age in days since burial
crust_below		SNOWPACK	MFcr below PWL (y/n)
slab_top	cm	SNOWPACK	Height at top of slab
slab_bottom	cm	SNOWPACK	Height of bottom of slab
slab_thickness	cm	SNOWPACK	Total thickness of PS
slab_maxhardness		SNOWPACK	Maximum hardness within PS
slab_avghardness		SNOWPACK	Weighted mean hardness of all layers in PS
slab_maxtemp	°C	SNOWPACK	Maximum temperature within PS
slab_avgtemp	°C	SNOWPACK	Average temperature within PS
slab_minssi		SNOWPACK	Minimum SSI within PS

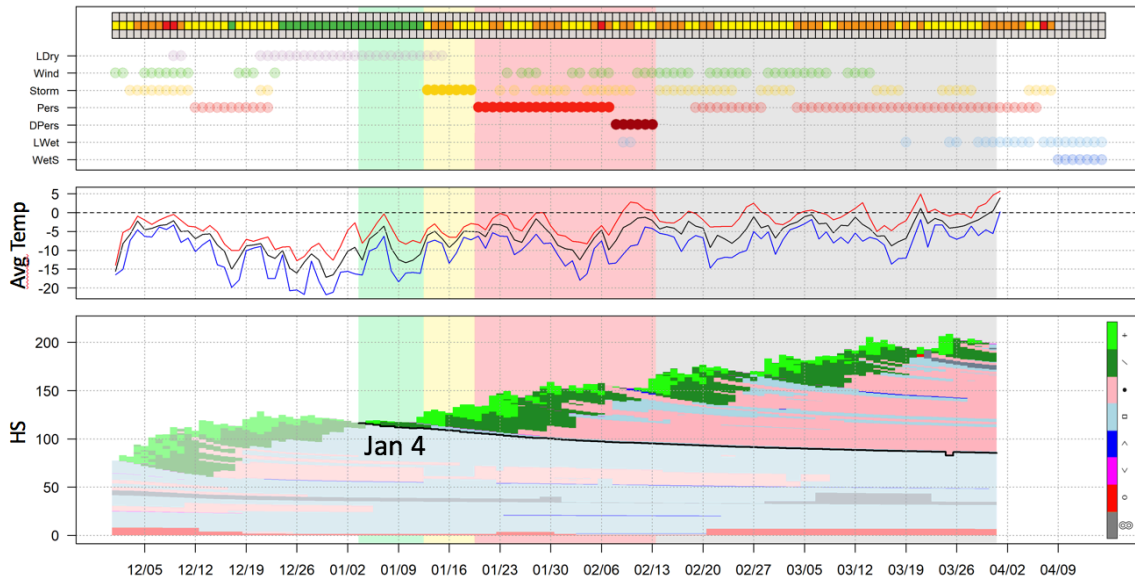


Figure 3.5 Sample (2016 Season @ TL) of how each tracked interface (January 4th PWL shown) was labelled according to the text descriptions from the daily avalanche bulletins (*Surface* problem = green and yellow bands, *Present* problem = red band, *Absent* problem = grey band).

3.5. Statistical Analysis

I started my analysis with a general exploratory analysis to get a feel of the dataset and examine interactions between all variables. A simple SNOWPACK model validation was then conducted to explore the accuracy of some of the major modelled variables. Finally, Conditional Inference Tree (CIT) models were estimated to explore the relationships between modelled variables and forecasted avalanche problem types. All of the statistical analyses included in this study were performed in *R* (R Core Team, 2019)

3.5.1. Exploratory Data Analysis

Exploratory data analysis was used to conduct initial investigations and to detect patterns or anomalies within the data. Interactions between weather and snowpack variables and avalanche problem types were examined using boxplots, scatter plots and correlations. All of these methods are standard applications of exploratory data analysis that help show the complex interactions of all the variables and is an important step prior

to quantitative analysis. Particular attention was paid to examining the distributions of each variable that was to be included in the CIT model with respect to avalanche problem type to understand the specific characteristics of each avalanche problem type and their differences. These explorations provided critical information for guiding the analysis and interpreting the results in a meaningful way.

3.5.2. Model Validation

SNOWPACK model validation was conducted using the NWP grid point closest to the Mt. Fidelity study plot and located within the same elevation band (Mt. Fidelity - *VIR160731* (TL), (Figure 3.3). Due to NWP grid changes, the representative grid point for Mt. Fidelity was updated for the 2018 season (*VIR083059*), (Figure 3.4). Using the same method for extracting data used in the surface problem analysis, weather and snowpack data was gathered for the NWP grid point location and merged with observational data from the Mt. Fidelity study plot. Scatter plots and box plots of modelled versus observed data (HS, HN24 and HST) were analyzed to examine how well the modelled values corresponded to the observed values. The measurement of the spread of predicted values around the regression line, the Root Mean Square Error (RMSE), was calculated by

$$RMSE = \sqrt{\frac{\sum_{i=1}^n (\hat{y}_i - y_i)^2}{n}} \quad (1)$$

where y_i is the observed value for the i th observation and \hat{y}_i is the predicted value. The bias and coefficient of determination (r^2) values for each observation was also calculated to determine the accuracy of the modelled data.

3.5.3. Conditional Inference Trees

Decision or classification trees are a statistical method used to model complex non-linear relationships with decision rules that offer tangible and easy to interpret insights. Previous avalanche studies that have also incorporated decision trees as part their analysis include Schirmer et al. (2009) and Bellaire and Jamieson (2013b). These studies used the Breiman et al. (1984) Classification and Regression Tree (CART) approach to partition their datasets using the Gini Index as splitting criteria. Three main issues have been identified with the CART approach: a) a lack of stopping criteria can

lead to overfitting of data, b) pruning based on interpretation of performance indicators is required to be effective, and c) interpretation of trees is affected by a selection bias towards covariates with many possible splits (Hothorn, Hornik, & Zeileis, 2006). To avoid these issues, the CIT model introduced by Hothorn et al. (2006) and recently applied by Clark (2019) in the avalanche context, recursively splits the dataset based on statistical hypothesis testing. The CIT approach of using statistically motivated stopping criteria is equivalent to the performance of optimally pruned trees using the CART approach but offers a computationally efficient and intuitive solution to the stated issues related to CART. The CIT approach also differs from the CART approach in that the splits in the dataset are based on a variable's influence on the dependent variable and not an information criterion. Because of these advantages, the CIT method was chosen for my analysis.

The CIT method begins the splitting process by calculating a quadratic linear test statistic for the differences in dependent variable distributions for all possible partitions within the dataset (Hothorn et al., 2006). Since the test statistic alone provides little information for determining the possible split, permutation framework tests are used to evaluate the calculated values. Permutation tests offer a way of shuffling through numerous samples of the dataset and calculating corresponding test statistics for each of the random splits. The resulting distribution of quadratic linear test statistics is then used to compare to the original test statistic and derive a p-value to assess the statistical significance of the proposed split. All possible splits are ranked by p-value and the overall lowest p-value is determined as the split with the highest significance and chosen by the algorithm. This process is repeated until none of the possible splits is significant anymore. Once complete, the terminal nodes of each branch will contain a distribution of the dependent variable that can be used to make predictions. The resulting tree can be easily visualized and offers intuitive interpretation of the partitioning and allows for extraction of decision rules. The position of where the split occurs reflects the statistical significance and shows the importance of each individual variable. Therefore, decision rules located higher in the tree are more significant while decision rules further down are responsible for fine-tuning.

To explore my dataset, separate CIT analyses were conducted on all avalanche problem types using a significance level of 5% ($\alpha = 0.05$). CIT analyses were applied to determine the presence or absence of surface avalanche problems and for

understanding the transition from surface to present PS/DPS avalanche problems and the transition from present to absent PS/DPS avalanche problems. Each CIT analysis computed numerous decision rules that split the dataset into many distinct terminal nodes.

Chapter 4. Results

The complete dataset consisted of 725 days with Parks Canada avalanche hazard assessments from the six winter seasons during my study period (2013 to 2018 seasons). The results of my analysis are presented in the following manner. First, I discuss the validation results for some of the key modelled weather and snowpack observations to provide insight into the accuracy of the model simulations. Next, I elaborate on the results of my main analysis of the presence of the different avalanche problem types in detail. Because the dataset used in the analysis for surface avalanche problem types (SS, WS, LDRY, LWET, CORN) is different from the dataset used for persistent avalanche problem types, the results of these analyses are presented in separate sections. Both of the main results are organized in the following way. I first describe the distributions of the predictor variables as well as timeseries explorations and univariate comparisons to explore patterns seen in the data. Afterwards, the CIT model outputs for each avalanche problem type are explained in detail, highlighting the strongest predictors first and then describing specific outlier cases.

4.1. Validation of Model Data

Observed weather and snowpack data from the Mt. Fidelity treeline study plot was compared against model output from the nearest NWP grid point. For the entire study period (2013-2018 winter seasons) the NWP and SNOWPACK models provided relatively accurate forecasts for air temperature and 24 h snowfall, but under-estimated snowpack height (Table 4.1, Figure 4.1).

Table 4.1 Model validation calculations

Variable	Bias	RMSE	R ²
Minimum Air Temperature	-1.8	3.1	0.96
Maximum Air Temperature	-0.6	2.0	0.91
HN24	-2.4	6.2	0.73
HS	-79.6	90.5	0.96

The relatively large bias (the tendency for values to either be over- or under-estimated) seen with snowpack height and the lower R² value (how close the data are to the fitted regression line) for recent snow can be explained by the fact that the NWP grid point is

not located exactly at the Mt. Fidelity study plot (elevation difference: 2013-2017 season = 102 m; 2018 season = 86 m), however the model provides reasonable representations of the actual values. Because of the differences between modelled and observed weather and snowpack variables, it is important to remember that the relationships between avalanche problems and modelled weather and snowpack variables presented in this study may differ from the relationships with actual observed values.

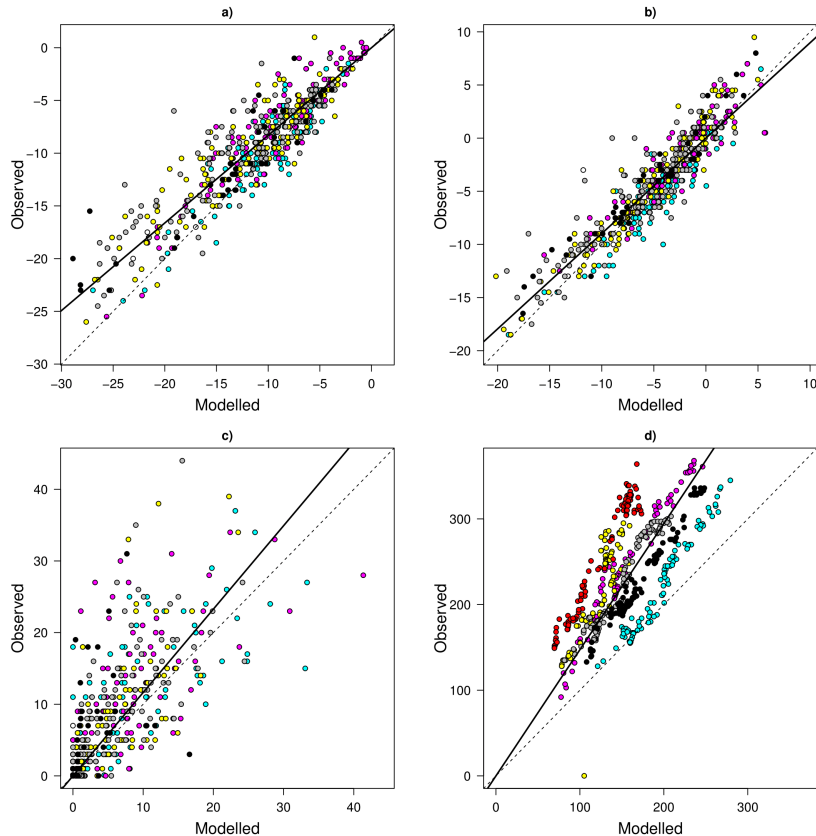


Figure 4.1 Scatterplots of observed versus modelled data from Mt. Fidelity study plot and matched NWP grid point. a) minimum air temperature (°C); b) maximum air temperature (°C); c) 24 hour snowfall (HN24, cm); and d) height of snowpack (cm). Colours represent separate seasons. Dashed line represents 1-to-1 trendline, and solid line is line of best fit.

4.2. Surface Avalanche Problem Types

4.2.1. Analysis Dataset Overview

An analysis of the number of days when surface avalanche problems were present reveals substantial differences in the prevalence of the different avalanche problem types (Figure 4.2). The most common surface avalanche problem types in my dataset were SS and WS avalanche problems. When the assessments from all elevation bands were pooled, SS avalanche problems were present on a total of 934 elevation band days, which is equivalent to 43% of the days included in my dataset, and WS avalanche problems were present on 677 elevation band days (31% of my dataset). While SS avalanche problems were distributed throughout all elevation bands fairly evenly, WS avalanche problems were predominantly forecasted in the alpine and at treeline (Figure 4.2). CORN, LDRY and LWET avalanche problems were forecasted much less frequently. The number of elevation band days when these surface avalanche problems were present were 83 (4%), 319 (15%) and 156 (7%) respectively. Similar to WS avalanche problems, CORN avalanche problems occurred mainly in the alpine, whereas LDRY avalanche problems occurred at all elevation bands, and LWET avalanche problems occurred more frequently at lower elevations (Figure 4.2). Based on the coefficient of variability (Table 4.1), the seasonal variability of the presence of avalanche problems is smallest for SS, which means that their presence is most consistent from year to year. LWET avalanche problems exhibit the largest season variability, whereas the variability of WS, CORN and LDRY are in the middle.

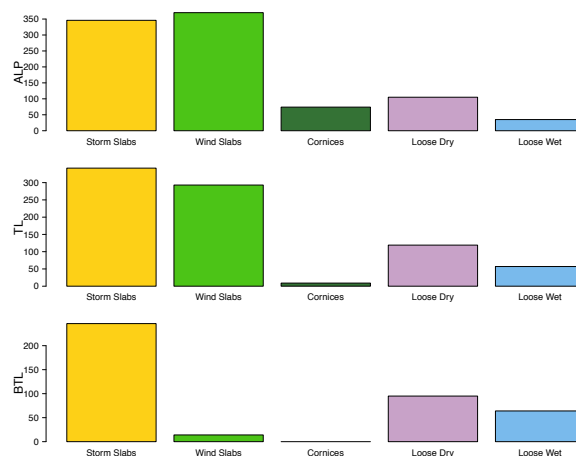


Figure 4.2 Distribution of surface avalanche problems per elevation band for all seasons within the study period.

Table 4.2 Surface avalanche problem type hazard assessment summary by elevation band and season.

Avalanche Problem	Season	Days Present			Elevation Band Days
		ALP	TL	BTL	
Wind Slab Avalanche Problem	2013	79	64	0	
	2014	78	72	10	
	2015	30	20	0	
	2016	66	49	0	
	2017	81	59	3	
	2018	36	29	1	
	AVG	61.67	48.83	2.33	
	SD	22.90	20.47	3.93	
	CoefVar	0.37	0.42	1.69	
TOTALS	370	293	14	677	
%	51%	40%	2%	31%	
Storm Slab Avalanche Problem	2013	51	51	36	
	2014	68	68	53	
	2015	60	53	27	
	2016	54	57	44	
	2017	53	53	46	
	2018	60	60	40	
	AVG	57.67	57.00	41.00	
	SD	6.28	6.29	8.94	
	CoefVar	0.11	0.11	0.22	
TOTALS	346	342	246	934	
%	48%	47%	34%	43%	
Dry Loose Avalanche Problem	2013	28	29	30	
	2014	9	18	17	
	2015	5	8	7	
	2016	28	28	17	
	2017	21	21	18	
	2018	14	15	6	
	AVG	17.50	19.83	15.83	
	SD	9.73	7.99	8.75	
	CoefVar	0.56	0.40	0.55	
TOTALS	105	119	95	319	
%	14%	16%	13%	15%	
Cornice Avalanche Problem	2013	13	5	0	
	2014	17	0	0	
	2015	4	0	0	
	2016	21	4	0	
	2017	8	0	0	
	2018	11	0	0	
	AVG	12.33	1.50	0.00	
	SD	6.12	2.35	0.00	
	CoefVar	0.50	1.56	n/a	
TOTALS	74	9	0	83	
%	10%	1%	0%	4%	
Wet Loose Avalanche Problem	2013	2	6	6	
	2014	2	1	0	
	2015	13	22	25	
	2016	5	8	10	
	2017	1	5	10	
	2018	12	15	13	
	AVG	5.83	9.50	10.67	
	SD	5.34	7.66	8.33	
	CoefVar	0.92	0.81	0.78	
TOTALS	35	57	64	156	
%	5%	8%	9%	7%	

My exploratory analysis of the modelled independent weather and snowpack variables provided general insights about the modelled weather and snowpack conditions at the three NWP grid points included in my study between 2013 and 2018 (Figure 4.3). The daily average modelled air temperatures in GNP ranged from -27.0 °C to +4.1 °C during the study period, with a median modelled air temperature of -7.1 °C. Minimum modelled air temperatures, which usually occurred overnight, ranged from -31 °C to +0.8 °C with a median of -10.5 °C, while maximum modelled air temperatures, which usually occurred during the day, ranged from -25.0 °C to +8.9 °C with a median of -4.4 °C. Modelled snow surface temperatures ranged from -45.3 °C to 0.0 °C, with a median of -11.2 °C. The median modelled average daily wind speed was 1.7 m/s, with maximum modelled wind speeds reaching 13.8 m/s. Calculated wind run values from the previous 24 h ranged from 4.2 m/s·h to 269.4 m/s·h with a median value of 40.7 m/s·h. Calculated wind run values from the previous 48 h ranged from 11.9 m/s·h to 509.9 m/s·h with a median value of 84.9 m/s·h. Calculated wind run values the previous 72 h ranged from 23.7 m/s·h to 725.6 m/s·h with a median value of 130.8 m/s·h.

Modelled snowfall over the previous 24 h occurred on approximately 75% of days within the study period and ranged from many days with 0.1 - 5 cm (ALP = 313 days, TL = 240 days, BTL = 237 days) to very few days with more than 20.0 cm (ALP = 35 days, TL = 27 days, BTL = 23 days) with a median snowfall of 4.7 cm and maximum snowfall of 41.4 cm. The snowfall accumulation contributed to a median modelled height of the snowpack of 145.0 cm with a maximum of 345.0 cm which was simulated during the 2013 season. Modelled ski penetration depth ranged from 8.0 cm to 58.0 cm with a median of 21.0 cm. Rainfall throughout the study period was modelled during two days at the ALP elevation band, 30 days at the TL elevation band, and 90 days at the BTL elevation band. The majority of the rainfall days saw less than 5.0 mm with a median rainfall of 0.3 mm and maximum rainfall of 30.0 mm which occurred in the 2015 season.

The thickness of the modelled HST layer had a median of 16.3 cm (minimum = 0.1 cm, maximum = 116.8 cm) and had a median density of 132.1 kg/m³ (minimum = 34.1 kg/m³, maximum = 383.0 kg/m³). The modelled interface layer below the HST layer consisted mainly of FC (26%), DF (24%), and SH (21%) with a median grain size of 0.9 mm (minimum = 0.3 mm, maximum = 9.9 mm) and a median simulated stability index of 6. The median of the minimum stability index within the HST layer was also 6. The median modelled thickness of the HN48 layer of surface snow was 3.5 cm

(minimum = 0.0 cm, maximum = 64.6 cm) and had a median density of 101.2 kg/m³ (minimum = 30.0 kg/m³, maximum = 383.0 kg/m³). The modelled interface layer below the HN48 layer consisted mainly of DF (45%), PP (26%), and FC (12%) with a median grain size of 0.5 mm (minimum = 0.3 mm, maximum = 7.6 mm). Both the median minimum stability index within the HN48 layer as well as the median stability index of the interface layer below was 6. Finally, the median thickness of the simulated HN72 layer of surface snow was 6.5 cm (minimum = 0.0 cm, maximum = 77.4 cm) and had a median density of 108.8 kg/m³ (minimum = 30.0 kg/m³, maximum = 383.0 kg/m³). The interface layer below the HN72 layer consisted mainly of DF (52%), FC (15%), and PP (11%) with a median grain size of 0.6 mm (minimum = 0.3 mm, maximum = 7.2 mm). Similar to the HST and HN48 layers, the median minimum stability index within the HN72 layer and the median stability index of the interface layer below were also 6. Stability indexes for all new snow time periods were heavily skewed to the value 6, with the majority of the values equal to 6 (Figure 4.4; HST ~70% of dataset, HN48 ~95% & HN72 ~90%). This is because the rules included in the SNOWPACK model automatically gives a stability index of 6 to any layers that are near the surface and within the ski penetration depth. Hence the simulated stability index values do not reflect the true stability of these layers. For this reason, I omitted the stability index variables from the surface avalanche problem analysis.

Explorations of seasonal differences in the independent variables revealed a few patterns that are important to consider when interpreting the results of my analysis. Several variables indicated that the 2015 season was an anomalous winter. During this winter, the amount of rainfall was exceptionally high, the daily average air temperature was warmer, the ski penetration depth was lower than normal, and the HST layer was thinner than normal (Figure 4.5). Another important observation is the sudden jump in wind speed values from the 2014 season to the 2015 season and beyond (Figure 4.6). Further investigation revealed that this dramatic change in wind speeds was related to an update of the HRDPS model, which included refinements to the wind speed model and produced more realistic wind speed values in subsequent years (Milbrandt et al., 2016).

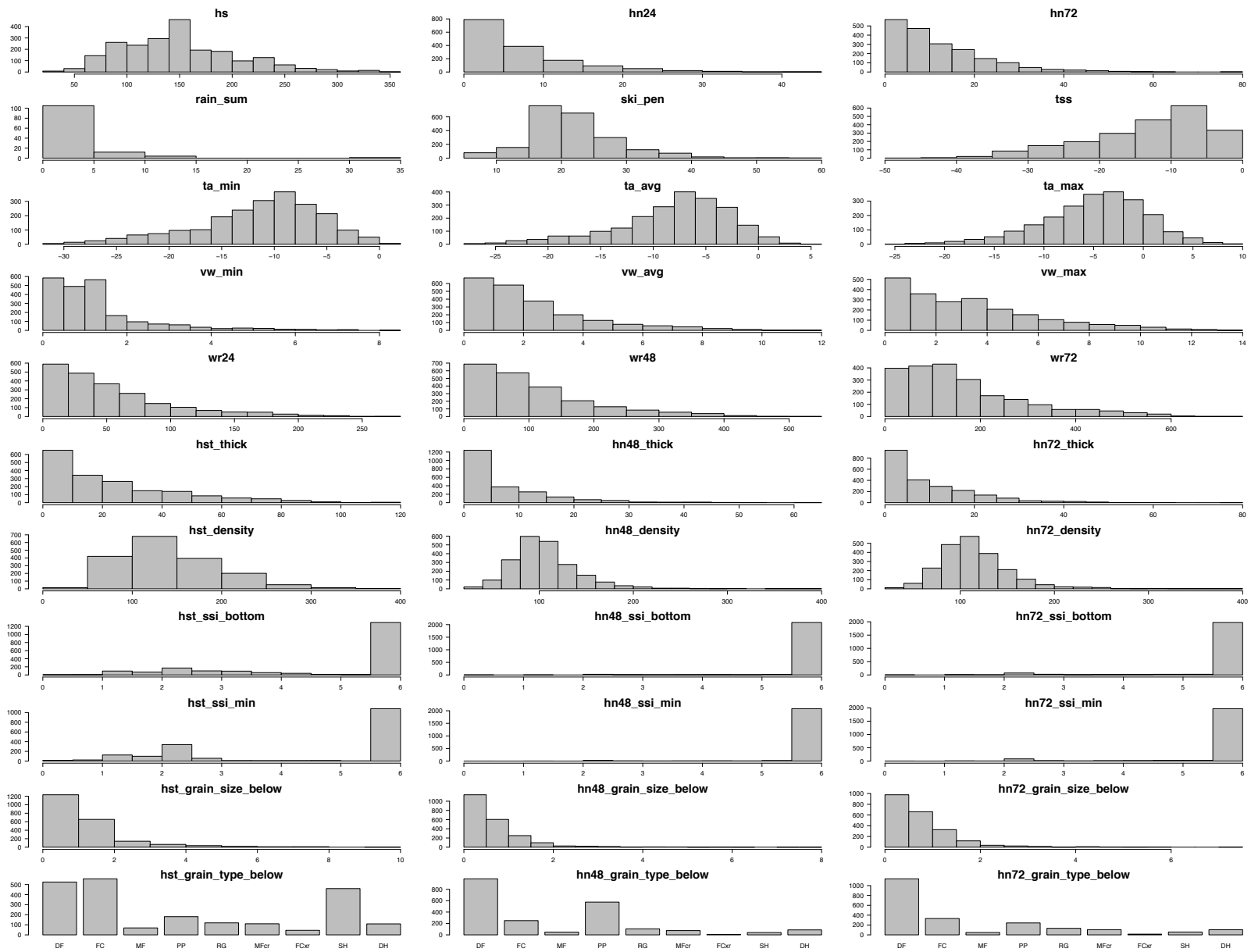


Figure 4.3 Frequency distribution of all variables in the Surface Avalanche Problems Types dataset. Zero precipitation values (hn24, hn72 & rain_sum variables) are omitted to show distributions more clearly.

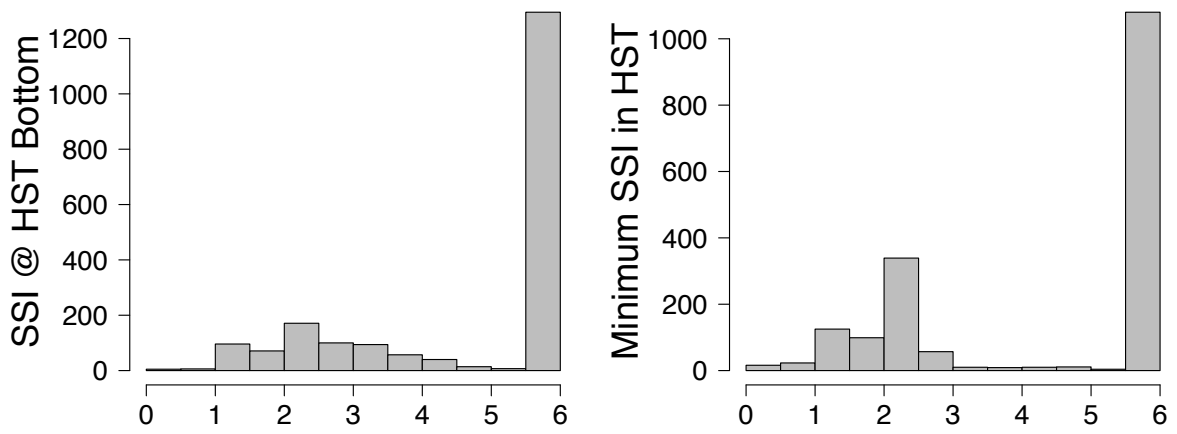


Figure 4.4 Sample of frequency distributions of stability indexes from interface at the bottom of HST and the minimum within the HST.

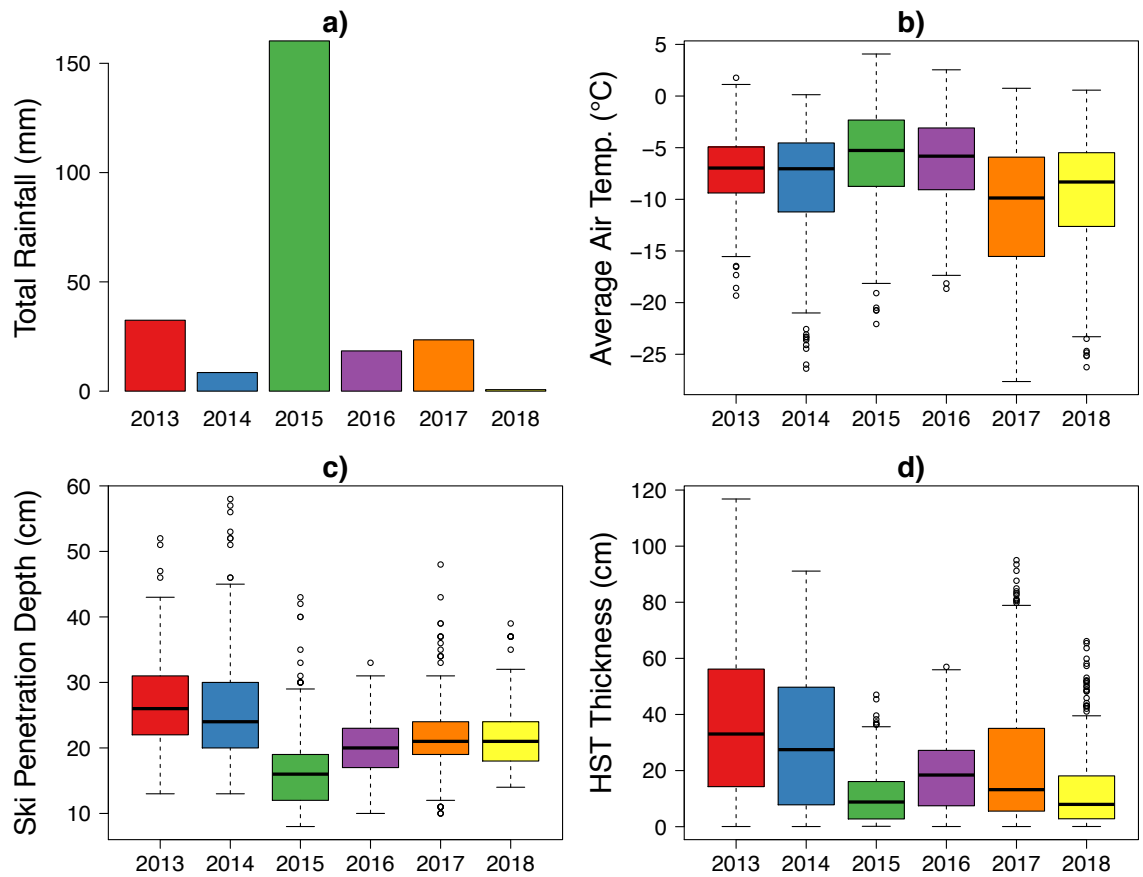


Figure 4.5 a) Summary of total rainfall per season; Frequency distribution for all seasons of: b) average air temperatures; c) Ski penetration per season; d) HST thickness per season.

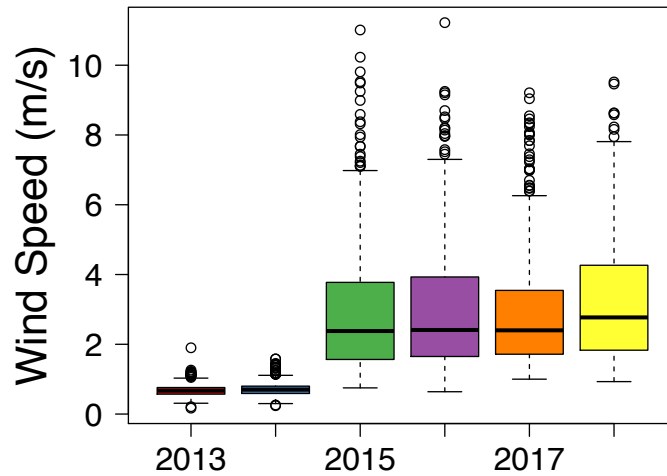


Figure 4.6 Wind speed distributions per season.

There are considerable correlations between the simulated weather and snowpack variables included in my analysis (Figure 4.7). Strong positive relationships existed between several variables: all wind speed variables were strongly correlated with each other (R^2 ranging from +0.83 to +1.00); and not surprisingly the thickness of new snow layers (HST_thick, HN48_thick and HN72_thick) were also moderately to strongly correlated with the recent snowfall variables (HN24 and HN72), ranging from +0.43 to +0.97. These positive correlations are the direct result of how the thickness variables were extracted from the model simulations. Weaker positive correlations existed between air temperature variables and the thicknesses and densities of the new snow layers (HST, HN48 and HN72), ranging from +0.16 to +0.30. The correlation between temperature and layer thickness is likely related to the fact that the coldest temperatures typically occur during high pressure periods when precipitation is rare. The correlation between temperature and layer density is likely due to higher temperature promoting a faster transformation of precipitation particles to rounded grains. Moderate negative relationships existed between ski penetration and the wind variables (ranging from -0.36 to -0.29), and weak negative relationships existed between the thickness of new snow layers and recent snowfall amounts, and the wind speed and calculated wind variables (ranging from -0.21 to -0.08).

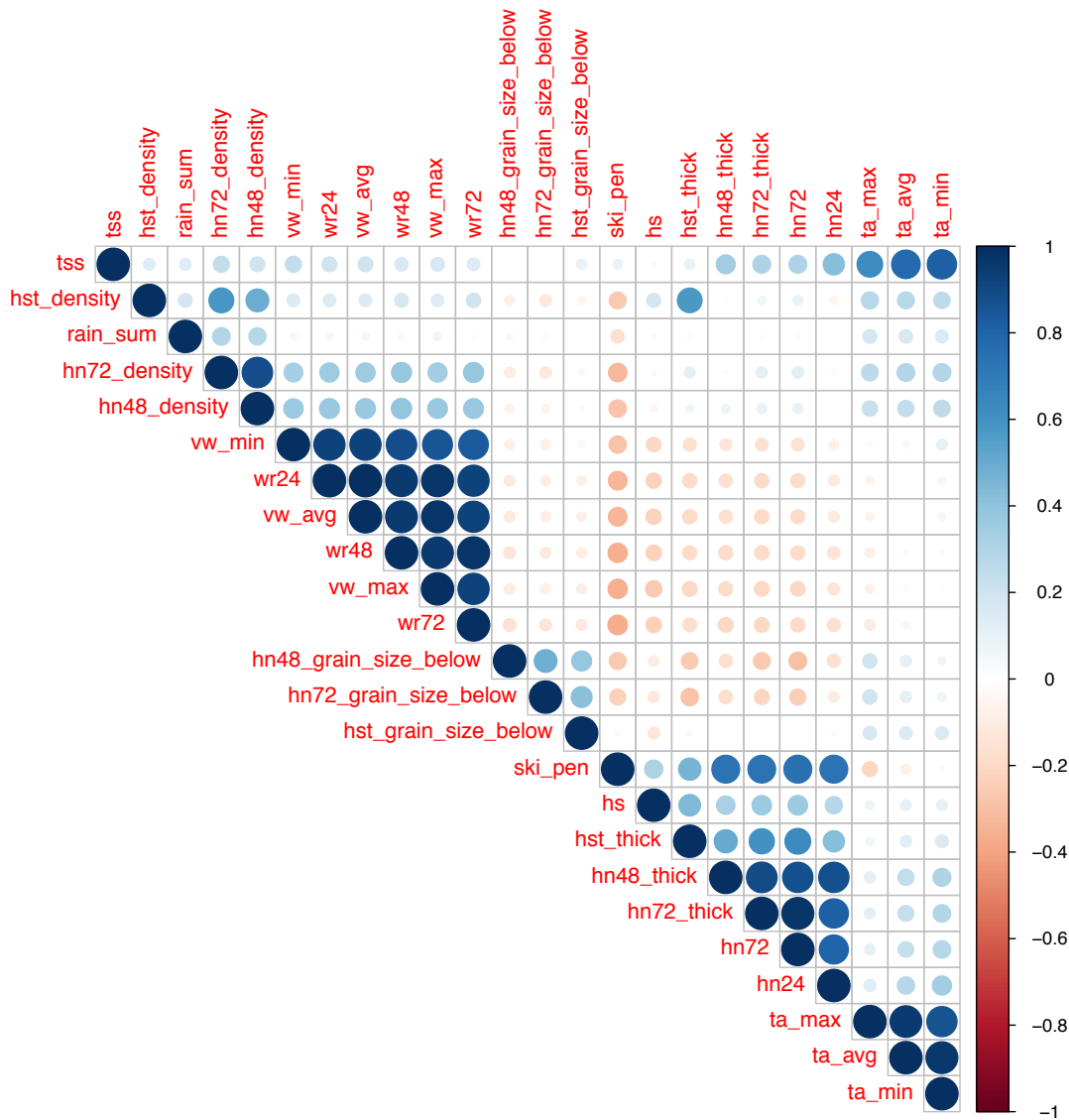


Figure 4.7 Correlation plot of all numeric weather and snowpack variables included in the Surface Avalanche Problem Type dataset.

4.2.2. Wind Slab Avalanche Problems

WS Avalanche Problem Dataset and Timeseries Analysis

Due to the HRDPS wind model upgrade, the 2013 and 2014 seasons were omitted from the WS avalanche problem analysis. Over the adjusted study period from the 2015 to 2018 season, WS avalanche problems were identified by forecasters in the alpine elevation band an average of 9 periods per winter season with an average

duration of 6 days (Table 4.2). Overall, the alpine elevation band had a total of 213 days with a WS avalanche problem present, which represents a seasonal average of 53 days per season (Table 4.2). The treeline elevation band exhibited a similar pattern (not shown), whereas WS avalanche problems were extremely rare below treeline.

As expected, a visual examination of the weather and SNOWPACK profile timeseries plots showed that WS avalanche problem occurrences aligned well with wind and snowfall events (Figure 4.8), which indicates that a combination of sufficient wind and new snow was required for forecasters to be concerned about WS avalanche problems. Later seasons (e.g. 2018 season shown in Figure 4.8) also show a relationship between WS avalanche problems (green dots) and the presence or absence of SS avalanche problems (yellow dots). WS avalanche problems were usually not forecasted during times where SS avalanche problems were forecasted. Exploratory univariate comparisons revealed additional, but weaker relationships between other possible predictor variables and the presence of WS avalanche problems. For example, average modelled air temperatures were lower on days when WS avalanche problems were present (WS present: median = -9.0 °C, WS absent: median = -6.4 °C, Mann-Whitney-Wilcoxon Test: p- value < 0.01); and accumulated 72 h wind run values were increased on days when WS avalanche problems were present (WS present: median = 134.3 m/s·h, WS absent: median = 129.8 m/s·h, Mann-Whitney-Wilcoxon Test: p- value < 0.01), (Figure 4.9).

Table 4.3 Season Summaries – WS Avalanche Problem Type – Alpine Elevation

Season	WS Av. Prob. occurrences	Avg. Duration (days)	Minimum Length (days)	Maximum Length (days)	Total days with WS (days)
2013*	9	8.8	1	27	79
2014*	8	9.8	1	26	78
2015	5	6.0	1	19	30
2016	11	6.0	1	17	66
2017	10	8.1	1	20	81
2018	9	4.0	1	9	36
Average	8.75	6.0	1	16.3	53.3
Totals	35	NA	NA	NA	213

* omitted from analysis

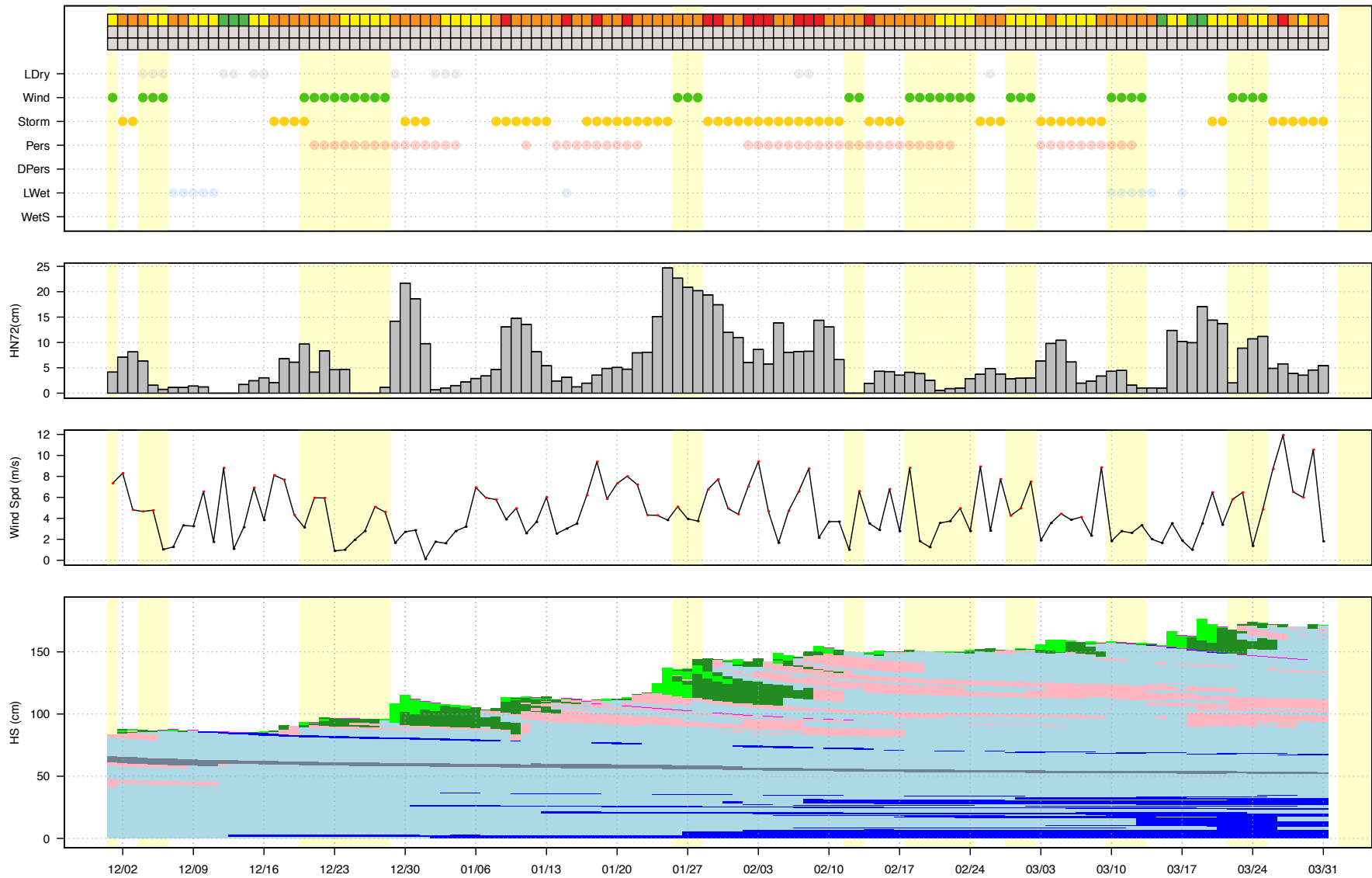


Figure 4.8 Timeseries (2018 Season - Alpine) of WS avalanche problems, associated weather variables (HN72 and wind speed) and snowpack evolution. Yellow bands represent the presence of a WS avalanche problem on any given day.

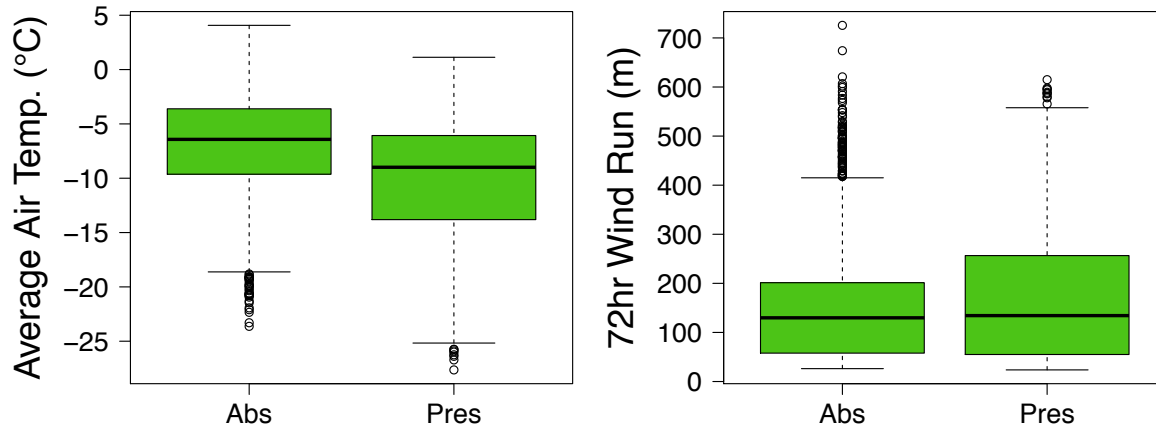


Figure 4.9 Distribution of average air temperature and 72 h wind run when WS avalanche problems were absent or present (2015-2018 Seasons).

Representing WS avalanche problem relationships with a CIT model

The WS avalanche problem CIT analysis for the 2015-2018 seasons computed 9 decision rules that split the dataset into 10 distinct terminal nodes (Figure 4.10). The first and most significant split in the CIT model was the WS avalanche problem status from the previous day. When an WS avalanche problem was *Present* on the previous day, there was an 80% probability that forecasters’ concerns about a WS avalanche problem persisted ($n = 278$). When, on the other side, a WS avalanche problem was *Absent* on the previous day, there was a 93% probability that a WS avalanche problem remained absent. While this first split indicates that persistence plays an important role in the forecasting of WS avalanche problems, the subsequent branches offer valuable insight on when the WS avalanche problems are “turned-on” (left branch) or “turned-off” (right branch).

Following the “turning-on” or left branch, when WS avalanche problems were *Absent* the day before, the first and most important decision rule related to elevation band, which separated the BTL elevation band from ALP and TL. This split showed that there was almost no chance of a WS avalanche problem being forecasted below treeline (Node 12, $n = 481$, 0.4% probability). The large amount of cases in this node and the fact that it basically includes all the BTL observations highlights that this is a strong predictor. This result reflects that WS avalanche problems were forecasted predominantly at higher elevations which are more exposed to prevailing winds. At the

TL and ALP elevation bands, the next decision rule related to whether avalanche forecasters were concurrently concerned with SS avalanche problems in the same elevation band. This terminal node shows that forecasters were unlikely to identify a WS avalanche problem when they were concerned about SS avalanche problems at the same time (Node 11, $n = 335$, 4% probability). The remaining nodes on the branch when a SS avalanche problem was absent (Nodes 7, 8, 9 & 10) outline specific circumstances when forecasters would possibly be concerned about WS avalanche problems. First, significant modelled winds over the past 72 h (> 320 m/s·h, equivalent to an average hourly windspeed of > 4.5 m/s·h) were associated with a 56% probability of WS avalanche problems being predicted that day. However, it is important to note that with $n = 26$, this is a relatively small terminal node. When the modelled winds over the last 72 h were lower, modelled HN72 was responsible for the next split in the tree. Values of modelled HN72 > 2.3 cm resulted in 27% probability of WS avalanche problems being identified, whereas lower amounts were associated with only a 4% probability of WS avalanche problems. The last split in the tree along the *Absent* branch was related to average modelled air temperatures. Days with average modelled air temperatures below -19 °C had a higher prevalence of WS avalanche problems (Node 7, $n = 7$, 43% probability), than warmer days (Node 8, $n = 88$, 1% probability). Since most of the terminal nodes with higher probabilities of WS avalanche problems only include few observations, generalizing the observed thresholds is questionable. However, the observed splits still offer valuable insight about the importance of individual variables in existing forecasting practices.

Following the “turning-off” or right branch when WS avalanche problems were *Present* the previous day, the first and most important decision rule was related to whether there was a SS avalanche problem identified the same day. When forecasters were concerned about an SS avalanche problem that day, there was only an 56% probability that the WS avalanche problem would persist (Node 17, $n = 117$). This is the terminal node with the lowest probability of a WS avalanche problem in the *Present* branch of the tree. When forecasters were not concerned about SS avalanche problems that day, the probability that they would identify a WS avalanche problem increased to 90%. The final decision rule on this branch related to whether they were concurrently concerned about LWET avalanche problems (Nodes 15 & 16). WS avalanche problems were significantly less prevalent when a LWET avalanche problem was present (67%

versus 92%). Interestingly, none of the modelled weather and snowpack observations included in the analysis emerged as significant predictors on this side of the WS avalanche problem tree.

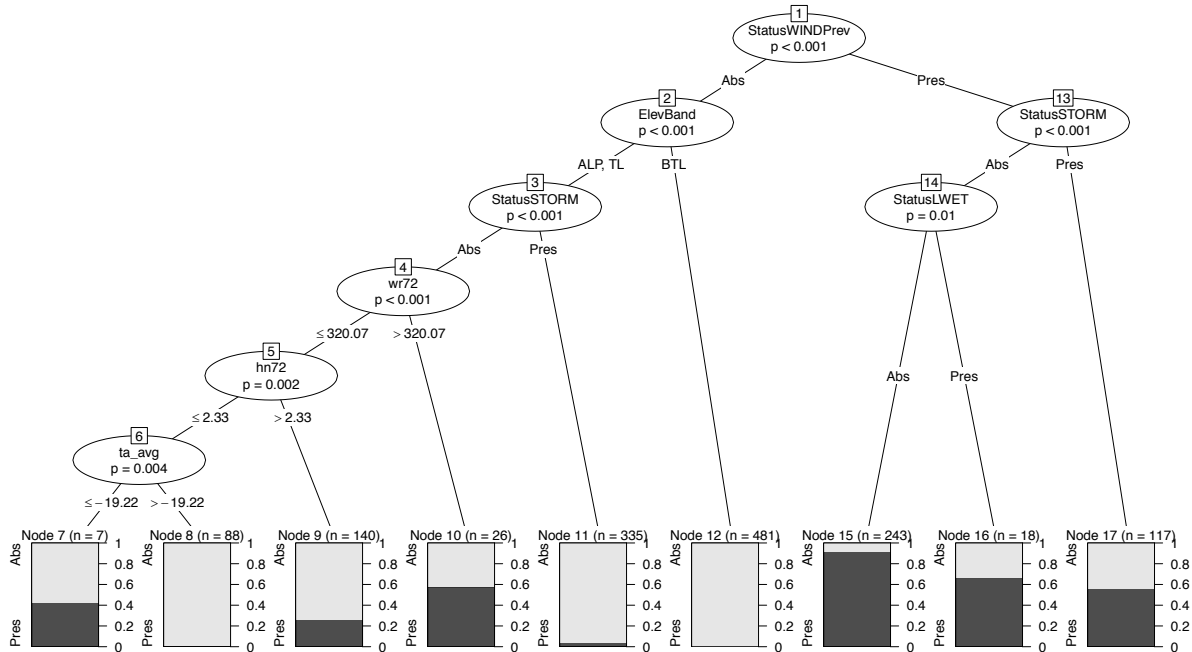


Figure 4.10 Conditional Inference Tree for WS avalanche problems (2015-2018 Seasons).

4.2.3. Storm Slab Avalanche Problems

SS Avalanche Problem Dataset and Timeseries Analysis

Over the study period, SS avalanche problems were identified by forecasters in the treeline elevation band an average of 10 periods per winter season with an average duration of 6 days (Table 4.3). Overall the treeline elevation band had a total of 342 days with a SS avalanche problem present, which resulted in a seasonal average of 57 days per season (Table 4.3). The alpine elevation band exhibited a similar pattern (not shown), while SS avalanche problems were slightly less prevalent below treeline (not shown) (Table 4.1).

As expected, the visual examination of the weather and SNOWPACK profile timeseries plots showed that SS avalanche problem occurrences aligned well with

snowfall events (Figure 4.11), as thick layers of precipitation particles (PP) and decomposing fragments (DF) are the primary reason for forecasters to be concerned about SS avalanche problems. Air temperatures also aligned well with snowfall and rain events, as the coldest temperatures occurred during dry periods in the winter. As found with WS avalanche problems, SS avalanche problems were rarely forecasted at the same time as WS avalanche problems (e.g. 2018 season shown in Figure 4.11).

Exploratory univariate comparisons also revealed the expected relationships between possible predictor variables and the presence of SS avalanche problems. For example, 24 h and 72 h snowfall amounts were higher on days when SS avalanche problems were present (HN24: SS present: median = 5.6 cm, SS absent: median = 0.7 cm, Mann-Whitney-Wilcoxon Test: p-value < 0.01; HN72: SS present: median = 15.2 cm, SS absent: median = 4.0 cm, Mann-Whitney-Wilcoxon Test: p-value < 0.01); the simulated snow layer from the past 48 h was thicker on days when SS avalanche problems were present (SS present: median = 8.6 cm, SS absent: median = 1.0 cm, Mann-Whitney-Wilcoxon Test: p-value < 0.01); and ski penetration depth was deeper on days when SS avalanche problems were present (SS present: median = 24.0 cm; SS absent: median = 20.0 cm, Mann-Whitney-Wilcoxon Test: p-value < 0.01), (Figure 4.12).

Table 4.4 Season Summaries – SS Avalanche Problem Type – TL Elevation

Season	SS Av. Prob. occurrences	Avg. Duration (days)	Minimum Length (days)	Maximum Length (days)	Total days with SS (days)	Tracked Storm Interfaces
2013	9	5.7	1	11	51	11
2014	10	6.8	1	26	68	15
2015	9	5.9	2	11	53	20
2016	11	5.2	1	11	57	13
2017	9	5.9	1	12	53	15
2018	11	5.5	2	14	60	21
Average	9.8	5.8	1.3	14.2	57	15.8
Totals	59	NA	NA	NA	342	95

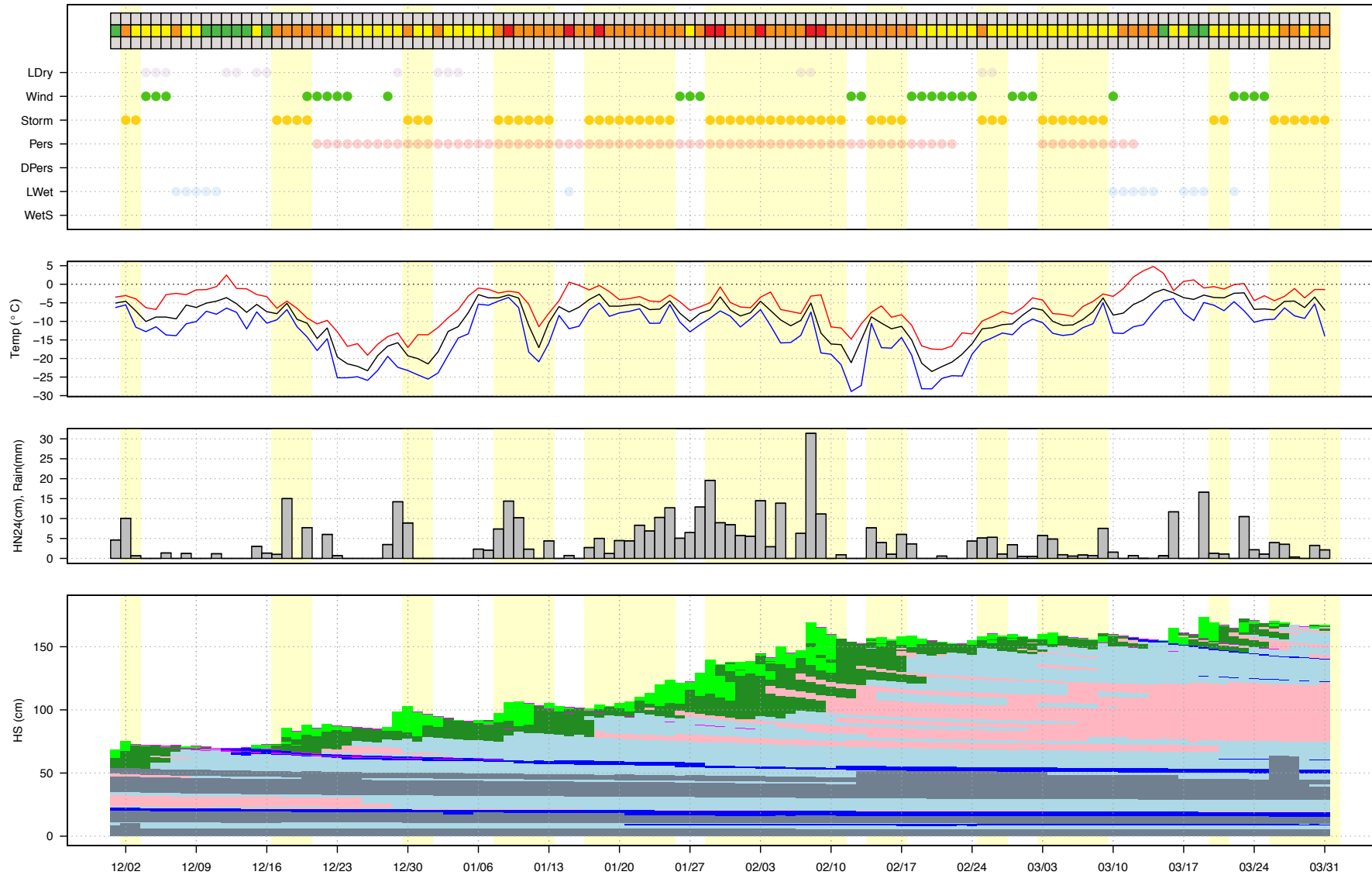


Figure 4.11 Timeseries (2018 Season - Treeline) of SS avalanche problems, associated weather variables (air temperatures, HN24 and rain) and snowpack evolution. Yellow bands represent the presence of a SS avalanche problem on any given day. Air temperature timeseries colours are defined as: red = maximum, black = average, blue = minimum.

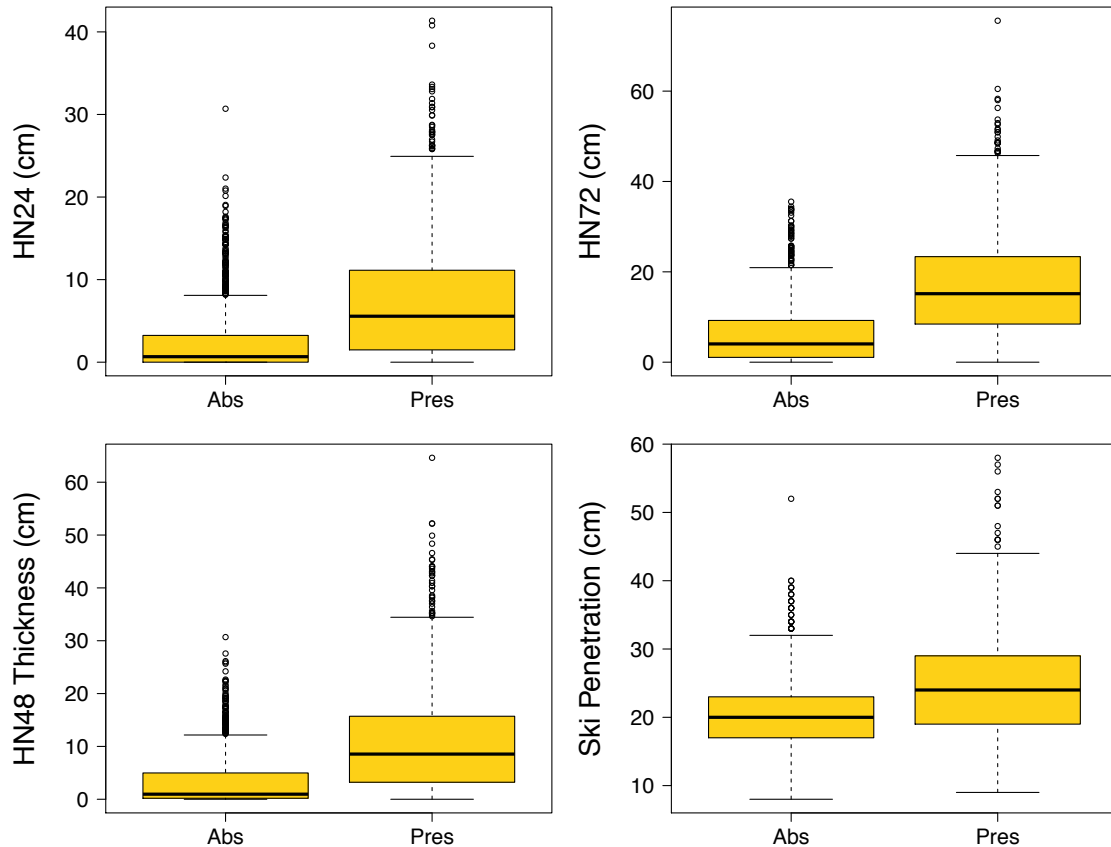


Figure 4.12 Distribution of snowfall amounts (HN24 & HN72), HN48 layer thickness and ski penetration depth when SS avalanche problems were absent and present (2013 - 2018 Seasons).

Representing SS avalanche problem relationships with a CIT model

The SS avalanche problem CIT analysis for the complete study period computed 18 decision rules that split the dataset into 19 distinct terminal nodes (Figure 4.13). The first and most significant split in the CIT model was the status of SS avalanche problems from the previous day. When a SS avalanche problem was *Present* on the previous day, there was an 82% probability that forecasters' concerns about a SS avalanche problem persisted ($n = 931$). On the other side, when a SS avalanche problem was *Absent* on the previous day, there was an 86% probability that a SS avalanche problem remained absent ($n = 1244$). Consistent with the WS avalanche problem analysis, these results indicate that persistence again plays an important role in the forecasting of SS avalanche problems and the subsequent branches offer valuable insight on when SS avalanche problems are “turned-on” (left branch) or “turned-off” (right branch).

Following the “turning-on” or left branch when SS avalanche problems were *Absent* the day before, the first and most important decision rule related to recent snowfall amounts. With more than 7.3 cm of modelled 24 h snowfall there was a 41% probability that forecasters would identify a SS avalanche problem. Although when forecasters assessed a WS avalanche problem on the same day, the probability of a SS avalanche problem being identified dropped to 16% (Node 22, n = 67). When forecasters were not concerned with WS avalanche problems that day, they were more likely to identify a SS avalanche problem at the TL and ALP elevation bands (Node 16, n = 32, 72% probability) than at the BTL elevation band (Node 17, n = 38, 40% probability). Forecasters were much less concerned about SS avalanche problems when HN24 was below the 7.3 cm threshold (Nodes 6, 8, 9, 12, 13, 14, 16 & 17, n = 1029, 8% probability). The large number of cases in these nodes highlights that recent snowfall is a strong predictor, which confirms that SS avalanche problems are predominantly reliant on large amounts of snowfall to be “turned-on”. The remaining nodes outline additional factors that contribute to forecasters’ concerns about SS avalanche problems. First, on windy days (24 h wind run > 129.9 m/s·h) the probability of forecasters being concerned about SS avalanche problems was strongly related to whether they identified concurrent WS avalanche problems (WS present: 21% probability, WS absent: 78% probability). On days with less wind, characteristics of the modelled HN48 snow layer became relevant; when the layer was thicker than 2.6 cm the probability of forecasters identifying a SS avalanche problem increased slightly to 14% (Nodes 12, 13 & 14) where the WS avalanche problem status played a role again (WS present: 4% probability, WS absent: 19% probability) with an additional split on days without WS avalanche problems with windier days having a higher probability of SS avalanche problems (Nodes 12, 13% probability; Node 13, 44% probability). However, the split on the 24 h wind run needs to be interpreted with caution due to the discontinuity in the simulated wind information caused by the upgrade to the HRDPS between the 2014 and 2015 seasons. While I only included the seasons after the upgrade in the WS analysis, I used the entire dataset for all other surface and persistent avalanche problems where I expected wind to only play a secondary role. Hence, care should be taken when interpreting any of the wind information. Finally, when the modelled HN48 snow layer was thinner, the density of this layer was important. Whereas a less dense HN48 layer ($\leq 145 \text{ kg/m}^3$) meant there was almost no chance of a SS avalanche problem being identified by forecasters (Node 6, 1% probability), denser

HN48 snow layers increased chance of a SS avalanche problem being identified (Nodes 8 & 9, 7% probability). The final split on this node related to the amount of recent snow, where $HN24 > 1.8$ cm was associated with a higher probability of a SS avalanche problem (Node 9, 38% probability).

Following the “turning-off” or right branch when SS avalanche problems were *Present* the previous day, the first and most important decision rule was related to the amount of snowfall over the previous 72 h. With small amounts of snowfall ($HN72 \leq 4.2$ cm), there was 46% probability of a SS avalanche problem persisting (Nodes 25 & 26), which was further affected by the presence or absence of a concurrent WS avalanche problem (WS present: 15% probability, WS absent: 58% probability). These are the terminal nodes with the lowest probability of a SS avalanche problem in the *Present* branch of the CIT analysis. As expected, larger amounts of snowfall ($HN72 > 4.2$ cm) were associated with higher concerns for SS avalanche problems (86% probability). The remaining nodes of this branch describe additional factors affecting forecasters’ concerns about SS avalanche problems (Nodes 29, 32, 33, 34, 36 & 37). First, recent snowfall > 2.6 cm was associated with a 93% probability of an SS avalanche problem being predicted that day (Nodes 36 & 37). This node further divided according to minimum daily temperature with warmer temperatures being associated with higher probabilities of SS avalanche problems (> -16 °C, 94% probability). I attribute this final split to the fact that slabs formed more slowly at lower temperatures. Minor amounts of recent snowfall (≤ 2.6 cm) is associated with a 74% probability of a SS avalanche problem persisting that day. Additional splits were based on significant modelled winds over the previous 72 h (> 60.6 m/s·h, 78% probability; ≤ 60.6 m/s·h, 53% probability) and the presence of assessed LWET avalanche problems (LWET present: 47% probability, LWET absent: 81% probability).

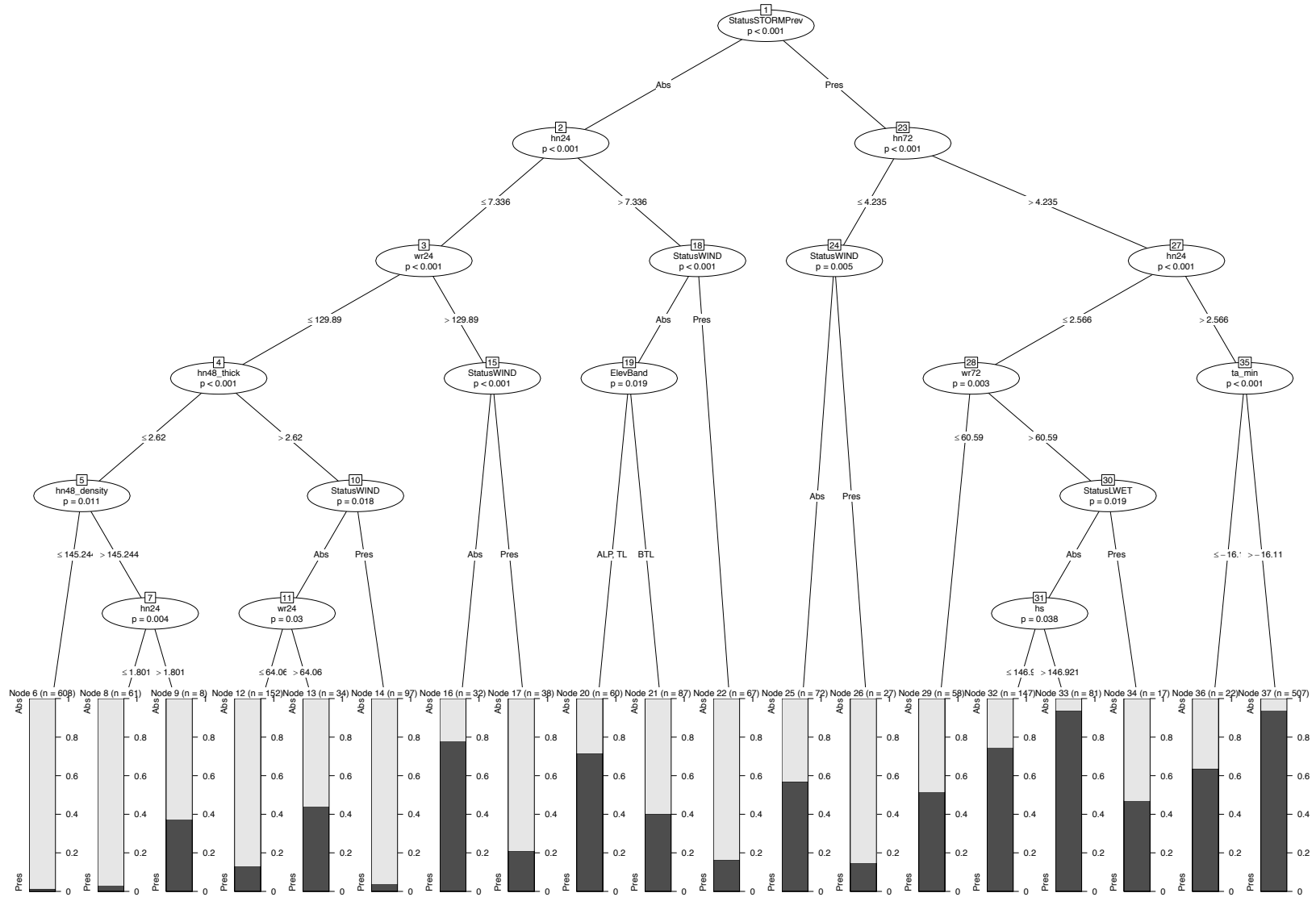


Figure 4.13 Conditional Inference Tree for SS avalanche problem types

4.2.4. Loose Dry Avalanche Problems

LDRY Avalanche Problem Dataset and Timeseries Analysis

Over the study period, LDRY avalanche problems were identified by forecasters in the treeline elevation band an average 7 times per winter with an average duration of 4 days (Table 4.4). Overall, the treeline elevation band had a total of 119 days with a LDRY avalanche problem present, which resulted in a seasonal average of 20 days per season (Table 4.4). The alpine and below treeline elevation bands exhibited similar patterns (not shown).

Visual examination of the weather and SNOWPACK profile timeseries plots showed the LDRY avalanche problem occurrences aligned with snowfall events and lower air temperatures (Figure 4.14), which indicated that a combination of sufficient new snow and colder temperatures was required for forecasters to be concerned about LDRY avalanche problems. Exploratory univariate comparisons confirmed these observations and revealed strong relationships to other possible predictor variables and the presence of LDRY avalanche problems. For example, maximum modelled air temperatures were lower on days when LDRY avalanche problems were present (LDRY present: median = -6.6 °C, LDRY absent: median = -3.9 °C; Mann-Whitney-Wilcoxon Test: p-value < 0.01); modelled storm slab densities were lower on days when LDRY avalanche problems were present (LDRY present: median = 107.7 kg/m³, LDRY absent: median = 138.3 kg/m³, Mann-Whitney-Wilcoxon Test: p-value < 0.01); and ski penetration depths were higher on days when LDRY avalanche problems were present (LDRY present: median = 24.0 cm, LDRY absent: 21.0 cm, Mann-Whitney-Wilcoxon Test: p-value < 0.01) (Figure 4.15).

Table 4.5 Season Summaries – LDRY Avalanche Problem Type – TL Elevation

Season	LDRY Av. Prob. occurrences	Avg. Duration (days)	Minimum Length (days)	Maximum Length (days)	Total days with LDRY (days)
2013	11	2.9	1	12	29
2014	6	3.0	1	4	18
2015	5	2.0	1	5	8
2016	2	14.0	2	26	28
2017	8	2.3	1	5	21
2018	7	2.1	1	3	15
Average	6.5	4.4	1.2	9.2	19.8
Totals	39	NA	NA	NA	119

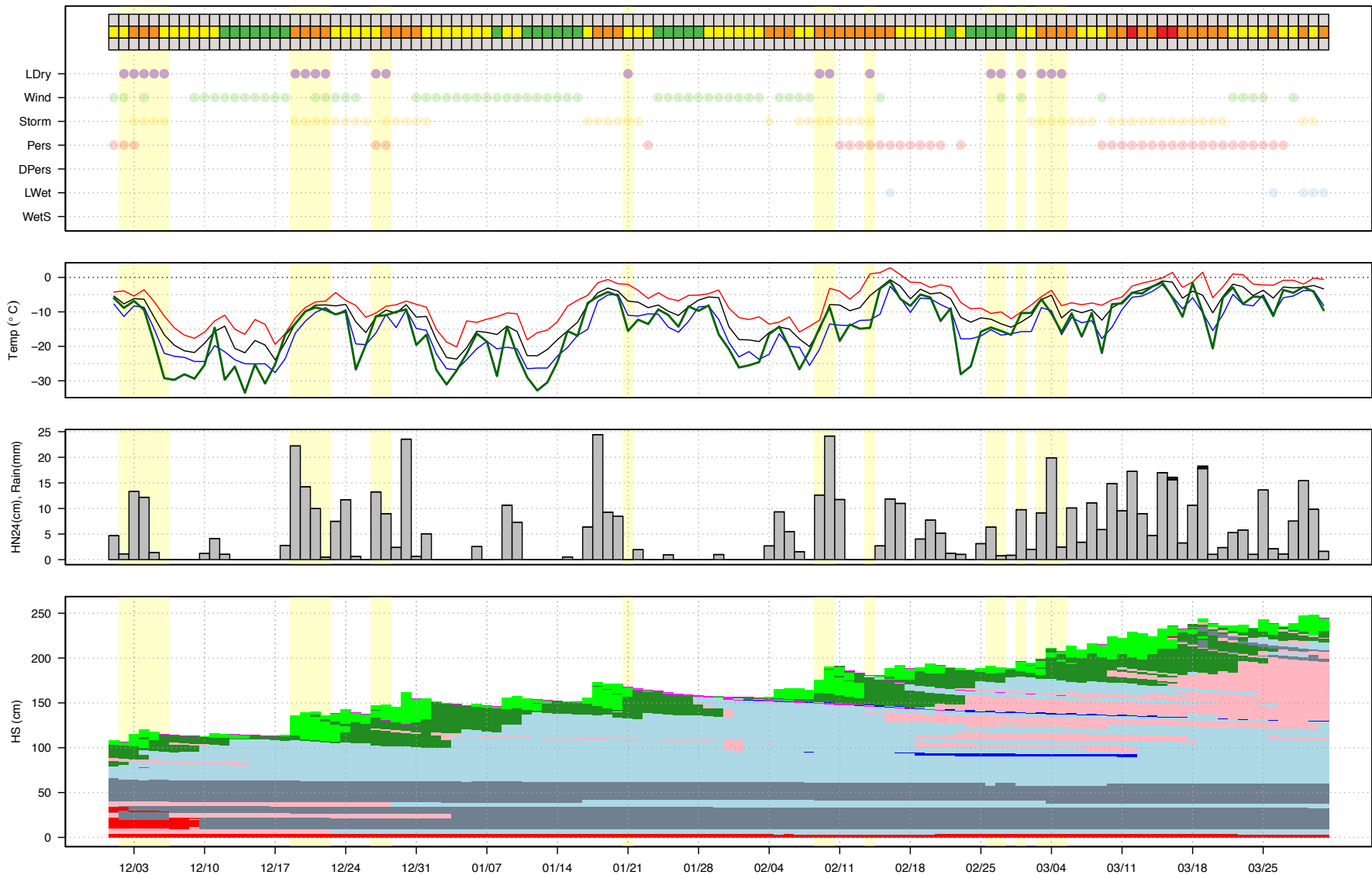


Figure 4.14 Timeseries (2017 Season - Treeline) of LDRY avalanche problems, associated weather variables (air temperature, HN24 and rainfall) and snowpack evolution. Yellow bands represent the presence of a LDRY avalanche problem on any given day. Air temperature timeseries colours are defined as: red = maximum, black = average, blue = minimum, & snow surface temperature = green.

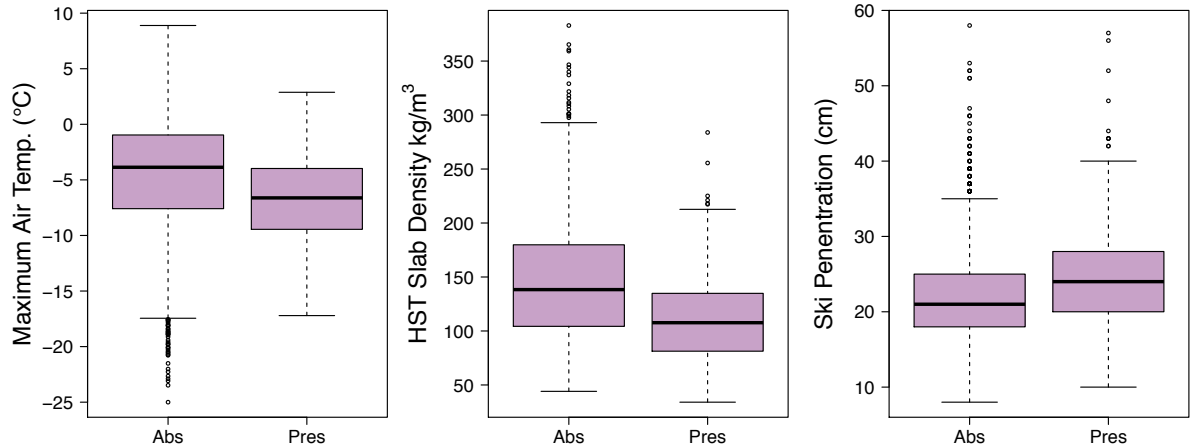


Figure 4.15 Distribution of maximum air temperature, HST slab density and ski penetration depth when LDRY avalanche problems were absent and present (2013 - 2018 Seasons).

Representing LDRY avalanche problem relationships with a CIT model

The LDRY avalanche problem CIT analysis for the 2013-2018 seasons computed 11 decision rules that split the dataset into 12 distinct terminal nodes (Figure 4.16). Just like the other avalanche problem analyses, the first and most significant split in the LDRY CIT model was the status of LDRY avalanche problems from the previous day. If a LDRY avalanche problem was *Present* on the previous day, there was a 65% probability that forecasters' concerns about a LDRY avalanche problem persisted (n=324). If, on the other side, a LDRY avalanche problem was *Absent* on the previous day, there was a 94% probability that a LDRY avalanche problem remained absent.

Following the “turning-on” or left branch when LDRY avalanche problems were *Absent* the day before, the first and most important decision rule related to the day of the season. Day of the season was initiated on October 1st of every season, therefore this split occurred at the beginning of March (154 = March 3rd, except on leap years) and indicated that LDRY avalanche problems were unlikely later in the season (1% probability). LDRY avalanche problems were only identified late in the season on days where the modelled snow surface temperature was below -26.1 °C (Node 13, 21% probability). The probability of a LDRY avalanche problem being turned on during the earlier part of the season (i.e. before March 3rd) was at 7%. The remaining nodes on this branch (Nodes 4, 8, 9, 10 & 11) highlight other factors that affect forecasters' concerns

about LDRY avalanche problems. First, shallower modelled ski penetration depths (≤ 23 cm) was associated with a lower probability of LDRY avalanche problems being predicted that day (5% probability). When modelled ski penetration depth was higher (> 23 cm, 11% probability), maximum modelled air temperature was responsible for the next split in the tree. Values of maximum modelled air temperatures above -9.0 °C resulted in an 8% probability of LDRY avalanche problems being identified, whereas lower maximum air temperatures were associated with a 26% probability of LDRY avalanche problems. This was further refined by the presence of WS avalanche problems where the presence of a WS avalanche problem resulted in a decrease in probability of a LDRY avalanche problem being identified (Node 10, 11% probability) and the absence of a WS avalanche problem resulted in a 50% probability of a LDRY avalanche problem being identified. The final split in the branch with WS avalanche problems being absent related to HN24. At this node, the probability of a LDRY avalanche problem being identified was significantly higher when there was sufficient recent snowfall ($\text{HN24} > 3.3$ cm; 81% versus 21%). Therefore, for forecasters to be concerned about LDRY avalanche problems, the conditions needed to be cold and calm with sufficient recent snow. Again, the terminal nodes with higher probabilities of LDRY avalanche problems only have few observations, which might indicate that we are looking at special cases.

Following the “turning-off” or right branch when LDRY avalanche problems were *Present* the previous day, the first and only important decision rule was related to density values of the modelled storm snow. Lower slab densities (≤ 130.2 kg/m³) were associated with higher probabilities of LDRY avalanche problems persisting that day (Node 16; 71% probability), whereas higher slab densities (> 130.2 kg/m³) were associated with lower probabilities of LDRY avalanche problem persisting that day (Node 17; 49% probability). Although the probabilities are relatively high in either instance, this confirms forecasters become less concerned about LDRY avalanche problems as the top layers of snow evolve (i.e. settlement, wind transport, etc.). At this point, forecasters might become concerned with other types of avalanche problems.

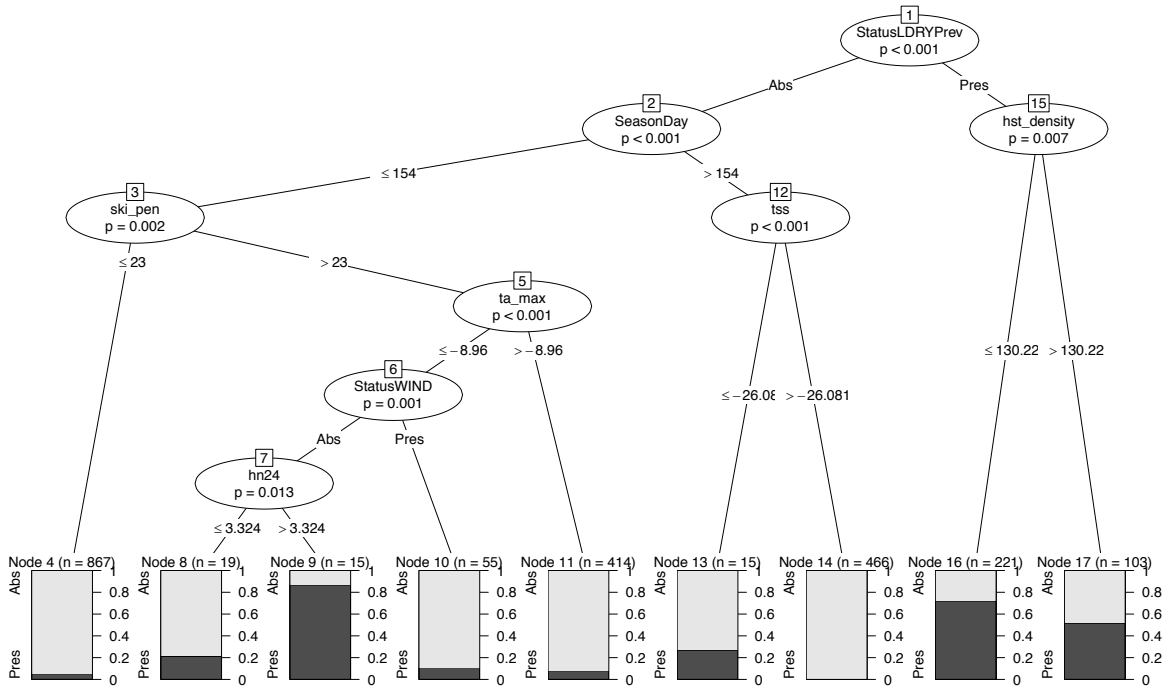


Figure 4.16 Conditional Inference Tree for LDRY avalanche problem types

4.2.5. Cornice Avalanche Problems

CORN Avalanche Problem Dataset and Timeseries Analysis

CORN avalanche problem types were identified by forecasters in the alpine elevation band an average of 3.5 periods per winter season with an average duration of 3.6 days (Table 4.6). Over the entire study period, the alpine elevation band had a total of 72 days with a CORN avalanche problem present, which resulted in an average of 12 days per season (Table 4.6). CORN avalanche problems were rarely identified in the treeline elevation band and never identified below treeline (not shown).

Visual examination of the weather and SNOWPACK profile timeseries plots showed that CORN avalanche problem occurrences aligned with higher sustained wind events later in the season when snowpack heights were elevated (Figure 4.17), which indicates that it took sustained large wind events time to build up cornices which produced CORN avalanche problems predominantly later in the season. While my exploratory univariate comparisons confirmed these observations, it also revealed

relationships to additional possible predictor variables. For example, modelled snowpack heights were significantly elevated on days when CORN avalanche problems were present (CORN present: median = 191.6 cm, CORN absent: median = 143.5 cm, Mann-Whitney-Wilcoxon Test: p-value < 0.01); maximum modelled wind speeds were slightly higher on days when CORN avalanche problems were present (CORN present: median = 4.01 m/s, CORN absent: median = 2.7 m/s, Mann-Whitney-Wilcoxon Test: p-value = 0.04); accumulated 72 h wind run values were slightly increased on days when LDRY avalanche problems were present (CORN present: median = 198.7 m/s·h, CORN absent: median = 130.0 m/s·h, Mann-Whitney-Wilcoxon Test: p-value = 0.07); and storm slab densities were significantly higher on days when LDRY avalanche problems were present (CORN present: median = 186.7 kg/m³, CORN absent: median = 131.3 kg/m³, Mann-Whitney-Wilcoxon Test: p-value < 0.01), (Figure 4.18).

Table 4.6 Season Summaries – CORN Avalanche Problem Type – ALP Elevation

Season	CORN Av. Prob. occurrences	Avg. Duration (days)	Minimum Length (days)	Maximum Length (days)	Total days with CORN (days)
2013	4	2.8	1	4	11
2014	3	5.7	3	11	17
2015	1	4.0	4	4	4
2016	6	3.5	1	5	21
2017	3	2.7	1	4	8
2018	4	2.8	1	4	11
Average	3.5	3.6	1.8	5.3	12
Totals	21	NA	NA	NA	72

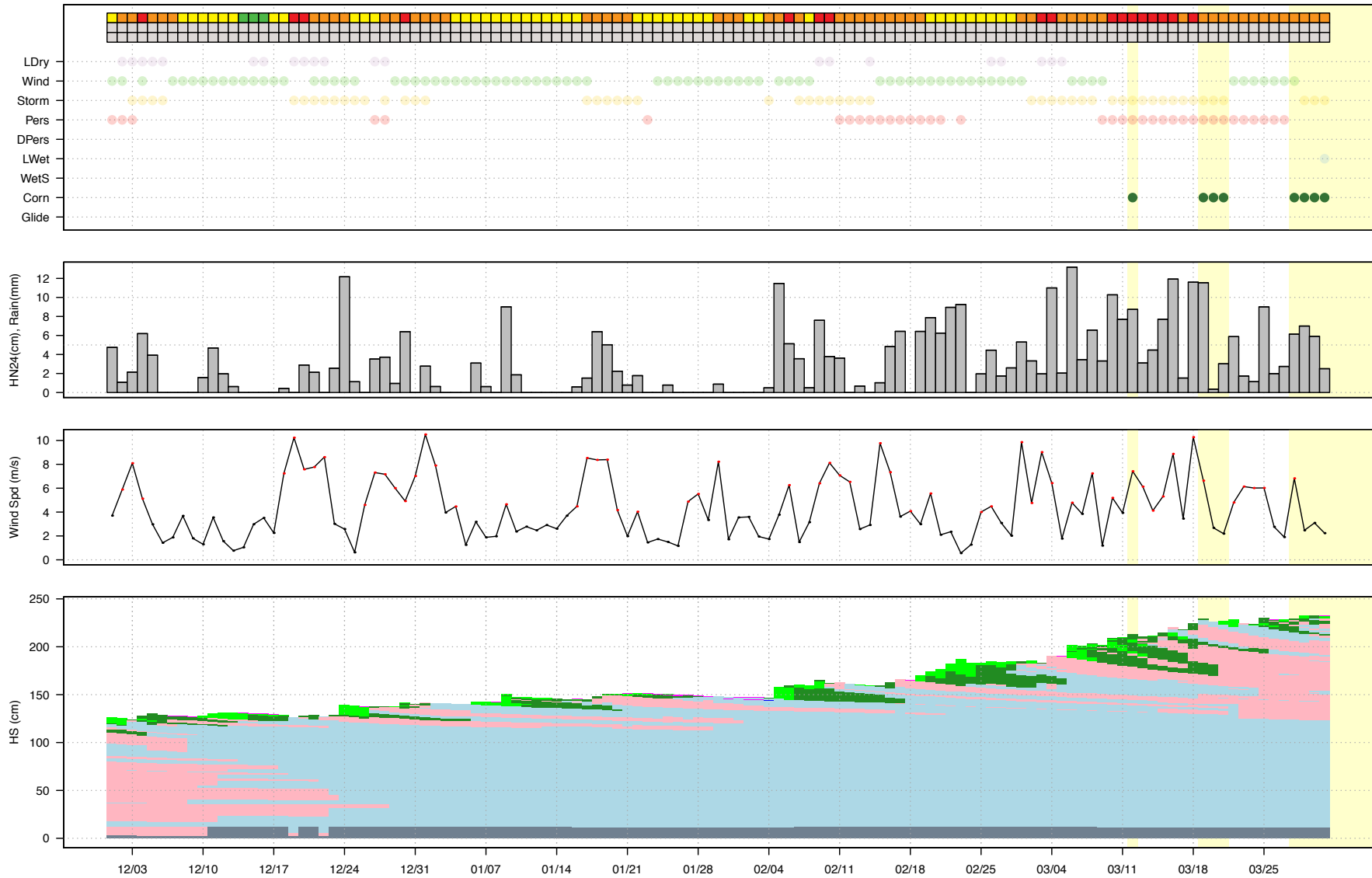


Figure 4.17 Timeseries (2017 Season - Alpine) of CORN avalanche problems, associated weather variables (HN24, rain, and wind speed) and snowpack evolution. Yellow bands represent the presence of a CORN avalanche problem on any given day.

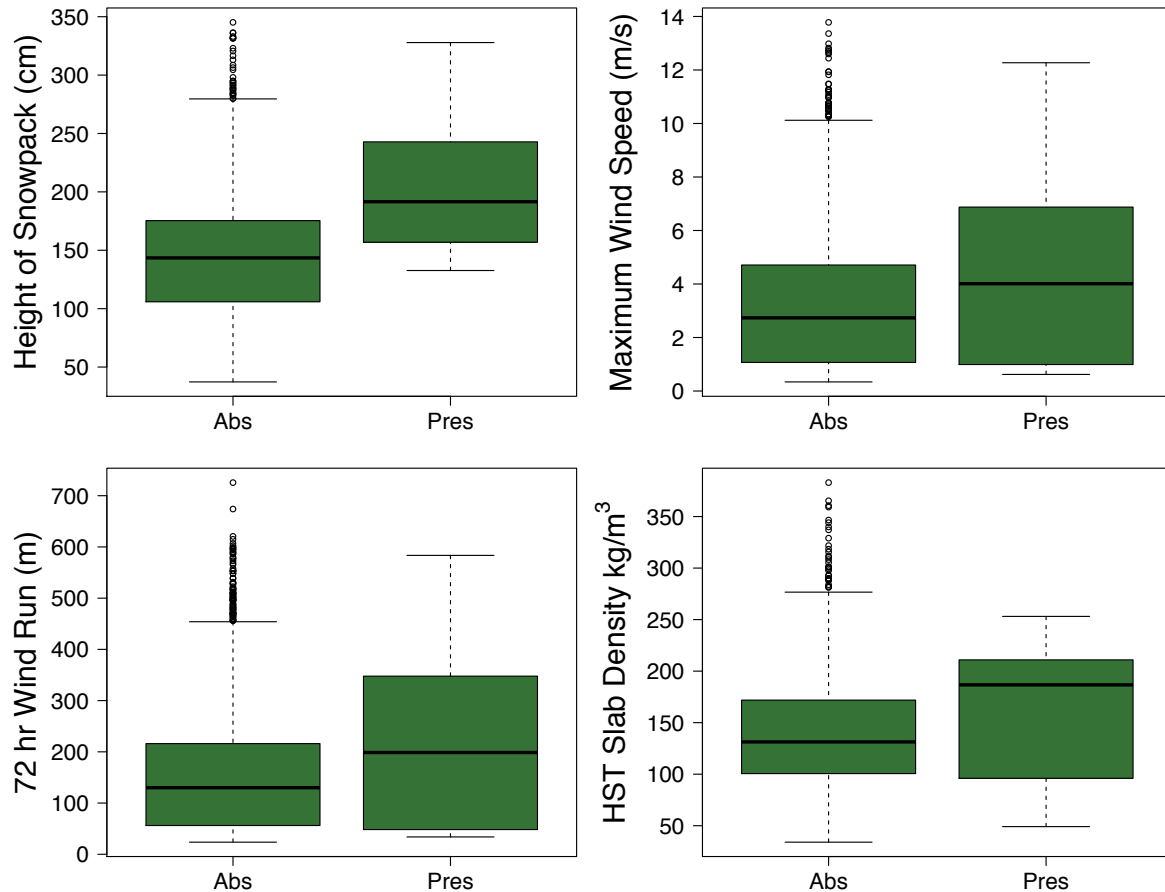


Figure 4.18 Distribution of height of snowpack, maximum wind speed, 72 h wind run and HST slab density when CORN avalanche problems were absent and present (2013 - 2018 Seasons).

Representing CORN avalanche problem relationships with a CIT model

The CORN CIT analysis for 2013-2018 seasons computed 4 decision rules that split the dataset into 5 distinct terminal nodes (Figure 4.19). The first and most significant split in the CIT model was the CORN avalanche problem status from the previous day. When a CORN avalanche problem was *Present* on the previous day, there was a 76% probability that forecasters' concerns about a CORN avalanche problem persisted (n=79). When a CORN avalanche problem was *Absent* on the previous day, there was a 99% probability that a CORN avalanche problem remained absent. Again, these results indicate that persistence plays an important role in the forecasting of CORN avalanche problems.

Following the “turning-on” or left branch when CORN avalanche problems were *Absent* the day before, the first and most important decision rule related to elevation band, which separated the ALP elevation band from TL and BTL. This split showed that there was no chance of a CORN avalanche problem being forecasted at treeline or below (Node 8, n = 1441, 0% probability). This node reflects that CORN avalanche problems were forecasted predominantly at higher elevations which are more exposed to prevailing winds. The remaining nodes on the branch (Nodes 5, 6 & 7) highlight additional factors contributing to forecasters’ CORN avalanche problem assessments in the ALP elevation band. First, the next decision rule related to day of the season, which like LDRY avalanche problems, indicated a split at the beginning of March (155 = March 4th, except on leap years), where later in the season was associated with a higher probability of CORN avalanche problems being identified (Node 7; n = 119; 11% probability) than earlier in the season (1% probability). Finally, in the rare instances that forecasters were concerned about CORN avalanche problems earlier in the season, MFcr and DH grain types below the 72 h storm snow increased their probability of being present to 13% (Node 6; n = 15). This rule is potentially based around the fact that forecasters may be worried more about cornice falls initiating avalanches on weak layers with these grain types within the snowpack. However, since this particular terminal node only includes a small amount of observations, it might simply represent a special situation.

No additional rules were found in the “turning-off” or right branch when CORN avalanche problems were *Present* the previous day. This means that once cornices have been created and become significant enough to be a cause for concern, there is a high probability that the assessed CORN avalanche problem persists regardless of any current weather and snowpack conditions.

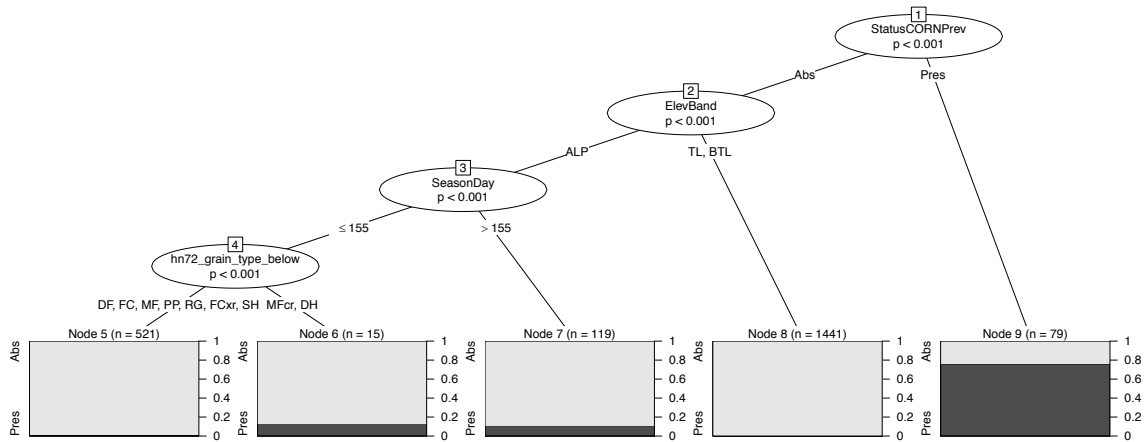


Figure 4.19 Conditional Inference Tree for CORN avalanche problem types

4.2.6. Wet Loose Avalanche Problems

LWET Avalanche Problem Dataset and Timeseries Analysis

In my study dataset, LWET avalanche problem were identified by forecasters more frequently in the below treeline elevation band (Figure 4.2) on an average of 3 periods per winter season with an average duration of 3 days (Table 4.6). Overall, the below treeline elevation band had a total of 64 days with a LWET avalanche problem present, which resulted in an average of 11 days per season (Table 4.6). The treeline and alpine elevation bands had lower occurrences of LWET avalanche problems (not shown) (Table 4.1).

Visual examination of the weather and SNOWPACK profile timeseries plots showed that LWET avalanche problem occurrences aligned well with rainfall events and after or during periods with relatively high air temperatures (Figure 4.20), which indicated that the surface snow had to be wet for forecasters to be concerned with LWET avalanche problems. My exploratory univariate comparisons provided additional insight into possible predictor variables for the presence of LWET avalanche problems. For example, modelled recent snowfall amounts were lower on days when LWET avalanche problems were present (LWET present: median = 0.5 cm, LWET absent: median = 2.1 cm, Mann-Whitney-Wilcoxon Test: p-value < 0.01); average modelled air temperatures were higher on days when LWET avalanche problems were present

(LWET present: median = -1.9 °C, LWET absent: median = -7.4 °C, Mann-Whitney-Wilcoxon Test: p-value < 0.01); modelled ski penetration depths were lower on days when LWET avalanche problems were present (LWET present: median = 14.0 cm, LWET absent: median = 22.0 cm, Mann-Whitney-Wilcoxon Test: p-value < 0.01); and modelled storm snow densities were higher on days when LWET avalanche problems were present (LWET present: median = 154.0 kg/m³, LWET absent: median = 130.8 kg/m³, Mann-Whitney-Wilcoxon Test: p-value < 0.01) (Figure 4.21).

Table 4.7 Season Summaries – LWET Avalanche Problem Type – BTL Elevation

Season	LWET Av. Prob. occurrences	Avg. Duration (days)	Minimum Length (days)	Maximum Length (days)	Total days with LWET (days)
2013	1	6.0	6	6	6
2014	0	0.0	0	0	0
2015	7	3.6	1	6	25
2016	5	2.0	1	4	10
2017	3	3.3	1	6	10
2018	3	4.3	1	11	13
Average	3.2	3.2	1.7	5.5	10.7
Totals	19	NA	NA	NA	64

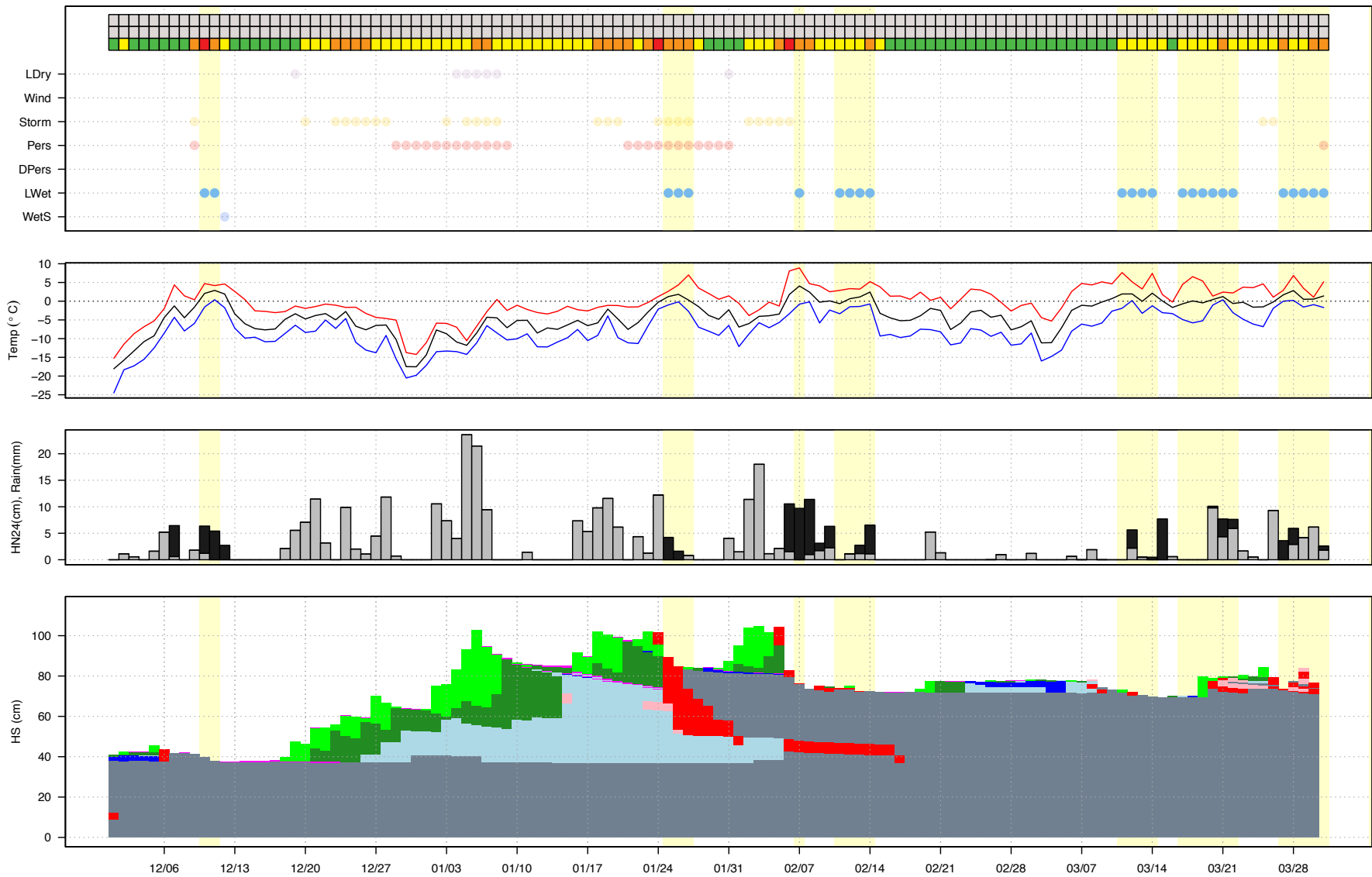


Figure 4.20 Timeseries (2015 Season – Below Treeline) of LWET avalanche problems, associated weather variables (air temperature, HN24 = grey bars, and rainfall = black bars) and snowpack evolution. Yellow bands represent the presence of a LWET avalanche problem on any given day. Air temperature timeseries colours are defined as: red = maximum, black = average, blue = minimum.

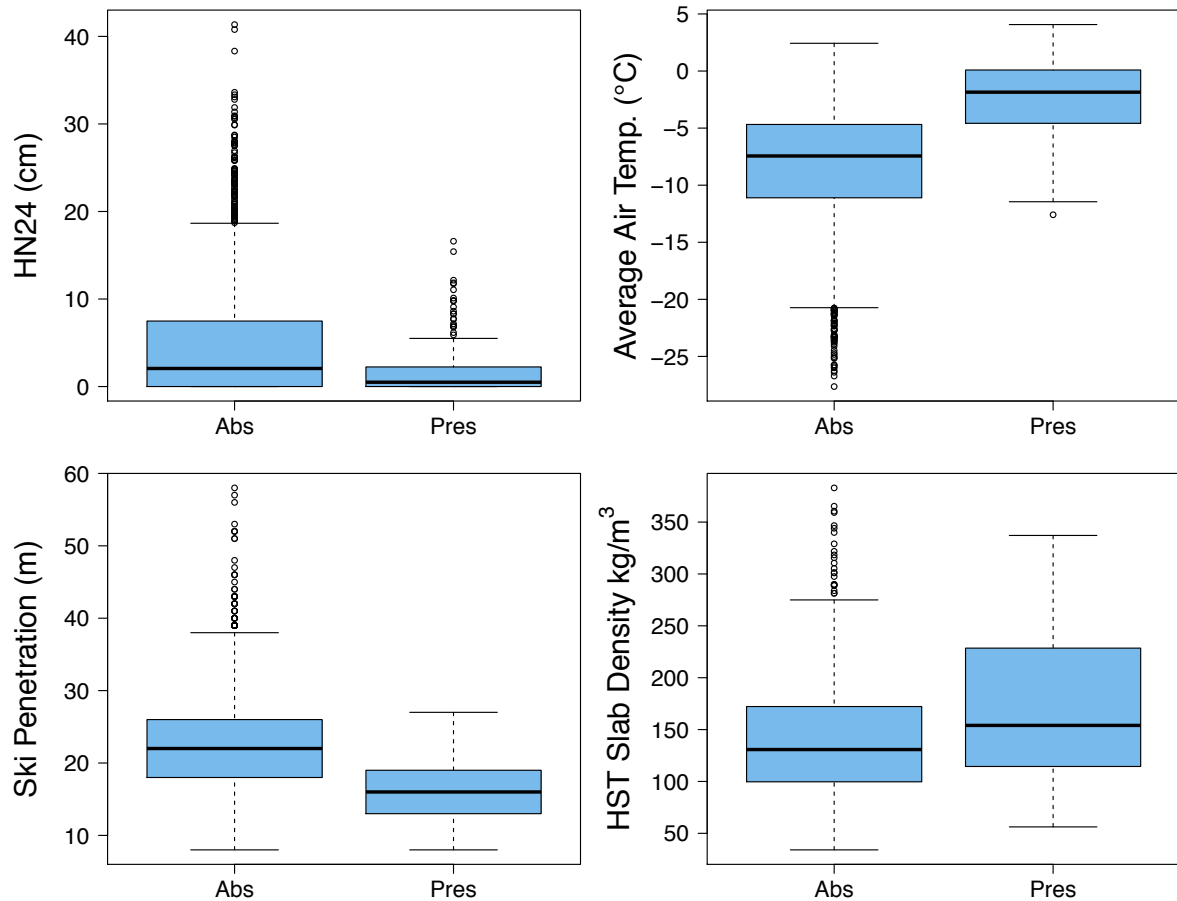


Figure 4.21 Distribution of HN24, average air temperature, ski penetration depth and HST slab density when LWET avalanche problems were absent and present (2013 - 2018 Seasons).

Representing LWET avalanche problem relationships with a CIT model

The LWET avalanche problem CIT analysis computed 8 decision rules that split the dataset into 9 distinct terminal nodes (Figure 4.22). Similar to all the other surface avalanche problems, the first and most significant split in the CIT model was the LWET avalanche problem status from the previous day. When a LWET avalanche problem was *Present* on the previous day, there was a 66% probability that forecasters' concerns about a LWET avalanche problem persisted (n=145). When a LWET avalanche problem was *Absent* on the previous day, there was a 97% probability that a LWET avalanche problem remained absent.

Following the “turning-on” or left branch when LWET avalanche problems were *Absent* the day before, the first and most important decision rule related to maximum modelled air temperature. This split showed that if the maximum modelled air temperature from the previous 24 h was above $-2.6\text{ }^{\circ}\text{C}$ there was 32% probability that a LWET avalanche problem was identified by forecasters. This probability increased to 88% if the minimum air temperature of the previous 24 h (i.e. the previous night) was also above $-1.8\text{ }^{\circ}\text{C}$ (Node 16, $n = 8$). Although there were only few cases when these two thresholds were met, they represent the situation when the snowpack warmed considerably during the day and did not have a substantial refreeze over-night to strengthen the surface layers of the snowpack again. When the maximum modelled air temperature was below $-2.6\text{ }^{\circ}\text{C}$ there was almost no chance of a LWET avalanche problem being forecasted (Nodes 5, 7, 9, 10, 12 & 13, 2% probability). However, the CIT algorithm found a few additional factors affecting forecasters’ likelihood of identifying a LWET avalanche problem. In general, late season (end of March or after) was associated with a higher probability of LWET avalanche problems being predicted (13% probability), whereas the grain size of the layer below the HN72 interface further split the sample with larger grain sizes ($> 1.2\text{ mm}$) being associated with higher probabilities of LWET avalanche problems (Node 13; $n = 26$; 35% probability). Earlier in the season (before the end of March) there was only a very small chance of a LWET avalanche problem being forecasted (1% probability), but in the rare cases where a LWET avalanche problem was predicted, the maximum modelled air temperature over the previous 24 h needed to be above $-2.9\text{ }^{\circ}\text{C}$ and either be in the ALP elevation band (Node 7; $n = 68$; 10% probability), or if in the TL and BTL elevation bands the grain type of the interface below HN72 snow layer needed to be either RG or SH (Node 10; $n = 22$; 13% probability). In other words, while warm temperatures were sufficient to increase the likelihood of a LWET avalanche problem in the alpine, the present of RG or SH further enhanced the likelihood at treeline and below.

No additional splitting rules were identified in the “turning-off” or right branch when LWET avalanche problems were *Present* the previous day. With no subsequent splits in the data, once LWET avalanche problems have been identified, more often than not they will persist until weather or snowpack variables change drastically.

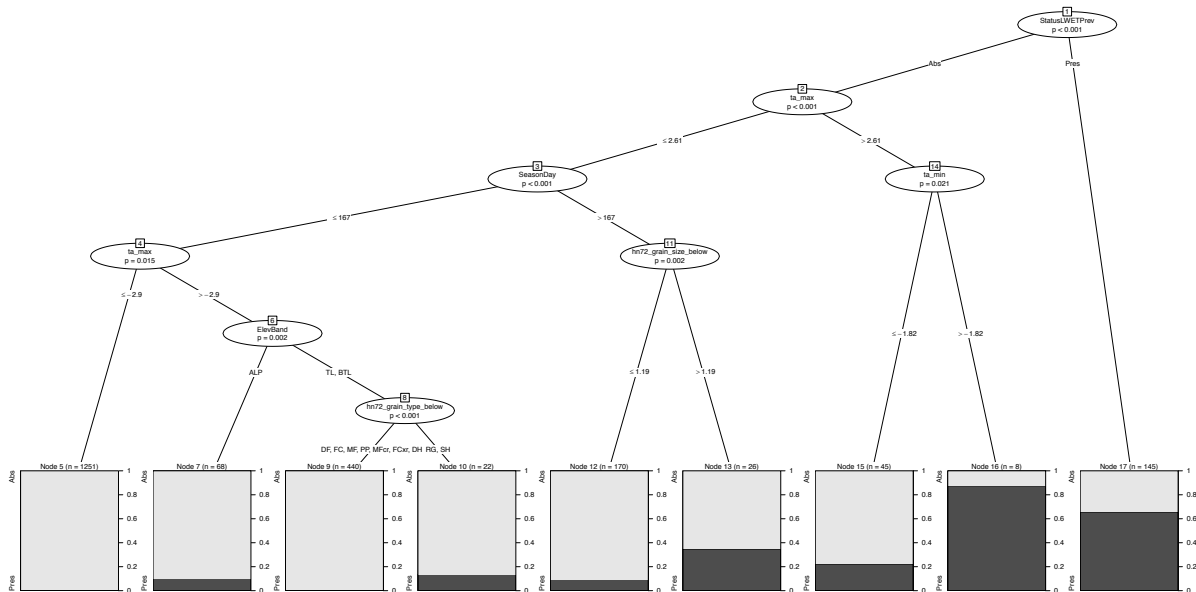


Figure 4.22 Conditional Inference Tree for LWET avalanche problem types

4.3. Persistent Avalanche Problems

4.3.1. Analysis Dataset Overview

A comparison of the number of days when persistent avalanche problems were present (Figure 4.23) reveals substantial differences in the prevalence of PS and DPS avalanche problems. The most common persistent avalanche problem type in GNP over the study period was PS avalanche problems. When the assessments from all elevation bands were pooled, PS avalanche problems were present on a total of 1080 elevation band days, which is equivalent to 50% of the days included in my dataset, and DPS avalanche problems were only present on 58 elevation band days (3% of my dataset). While PS avalanche problems were present in all elevation bands, they were most prevalent at treeline followed by the alpine and below treeline elevation bands. DPS avalanche problems, on the other hand, tended to be more prevalent at treeline and above (Figure 4.23). Based on the coefficient of variability (Table 4.8), the seasonal variability of the presence of persistent avalanche problems was smaller for PS avalanche problems than for DPS avalanche problems, which means that their presence was more consistent from year to year. Due to the limited presence of DPS avalanche

problems, the two persistent slab problems (PS and DPS) were amalgamated together for ease of analysis. Once PS and DPS were pooled together, persistent avalanche problems were present on 1138 elevation band days (52% of my dataset).

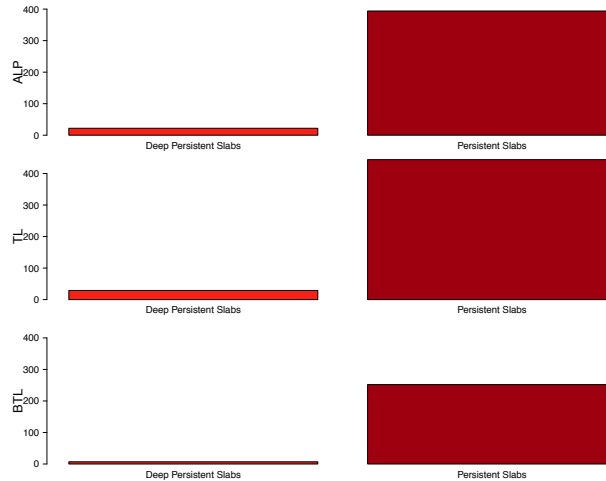


Figure 4.23 Distribution of DPS and PS avalanche problems per elevation band for all seasons within the study period.

Exploratory analysis of the modelled weather and snowpack variables included in the persistent avalanche problem analysis again provided an overview about the modelled weather and snowpack conditions at the treeline elevation band for some NWP grid points used for the analysis of surface avalanche problems (Figure 4.24). An overview of the modelled air temperature, wind speed and precipitation trends are discussed at length in the surface avalanche problem dataset (Section 4.2.1.) and since the dataset for PS/DPS avalanche problems duplicates entries for each day depending on the number of layers tracked, these trends are not discussed further.

The characteristics of the tracked modelled weak layers and the overlying slab were extracted from SNOWPACK. The tracked weak layers had a median age of 41 days (minimum = 1, maximum = 146), a median modelled temperature of -2.7 °C (minimum = -26.1 °C, maximum = 0.0 °C), and a median liquid water content of 0.0 (minimum = 0.0, maximum = 6.0). The thickness of the tracked weak layers had a median of 2.3 cm (minimum = 0.1 cm, maximum = 30.2 cm) and had a median density of 309.0 kg/m³ (minimum = 32.0 kg/m³, maximum = 507 kg/m³), a median hardness of 2.3 (minimum = 1.0, maximum = 5.0) and a median simulated stability index of 3.3

(minimum = 0.2, maximum = 6). The tracked weak layers consisted mainly of FC (23.6%), FCxr (21.9%), MFcr (15.6%), DH (13.5%), RG (9.3%), DF (5.8%) and SH (4.7%) with a median grain size of 1.1 mm (minimum = 0.3 mm, maximum = 6.2 mm). The modelled overlying slab had a median average temperature of -4.8 °C (minimum = -39.8 °C, maximum = 0.0 °C) and a median maximum temperature of -2.5 °C (minimum = -26.1 °C, maximum = +0.4 °C). The median thickness of the simulated slab was 69.6 cm (minimum = 0 cm, maximum = 232.6 cm) and had a median average hardness of 2.0 (minimum = 1.0, maximum = 4.5), a median maximum hardness of 3.5 (minimum = 1.0, maximum = 5.0), a median average density of 236.8 kg/m³ (minimum = 40.0 kg/m³, maximum = 446.8 kg/m³), and a median maximum density of 349.0 kg/m³ (minimum = 40.0 kg/m³, maximum = 574.0 kg/m³). The minimum simulated stability indexes within the overlying slab ranged from 0.5 to 6 with a median value of 1.69.

Table 4.8 Persistent avalanche problem type hazard assessment summary by elevation band and season.

Name	Season	Days Present			Elevation Band Days
		ALP	TL	BTL	
Persistent Slab Avalanche Problem	2013	52	71	46	
	2014	87	85	36	
	2015	104	104	25	
	2016	54	68	51	
	2017	37	37	32	
	2018	56	74	61	
	AVG	65.00	73.17	41.83	
	SD	25.14	22.05	13.29	
CoefVar	0.39	0.30	0.32		
TOTALS	390	439	251	1080	
%	54%	61%	35%	50%	
Deep Persistent Slab Avalanche Problem	2013	0	1	1	
	2014	12	12	0	
	2015	10	10	0	
	2016	0	6	6	
	2017	0	0	0	
	2018	0	0	0	
	AVG	3.67	4.83	1.17	
	SD	5.72	5.31	2.40	
CoefVar	1.56	1.10	2.06		
TOTALS	22	29	7	58	
%	3%	4%	1%	3%	
Persistent and Deep Persistent Slab Avalanche Problems Combined	2013	52	72	47	
	2014	99	97	36	
	2015	114	114	25	
	2016	54	74	57	
	2017	37	37	32	
	2018	56	74	61	
	AVG	68.67	78.00	43.00	
	SD	30.43	26.10	14.35	
CoefVar	0.44	0.33	0.33		
TOTALS	412	468	258	1138	
%	57%	65%	36%	52%	

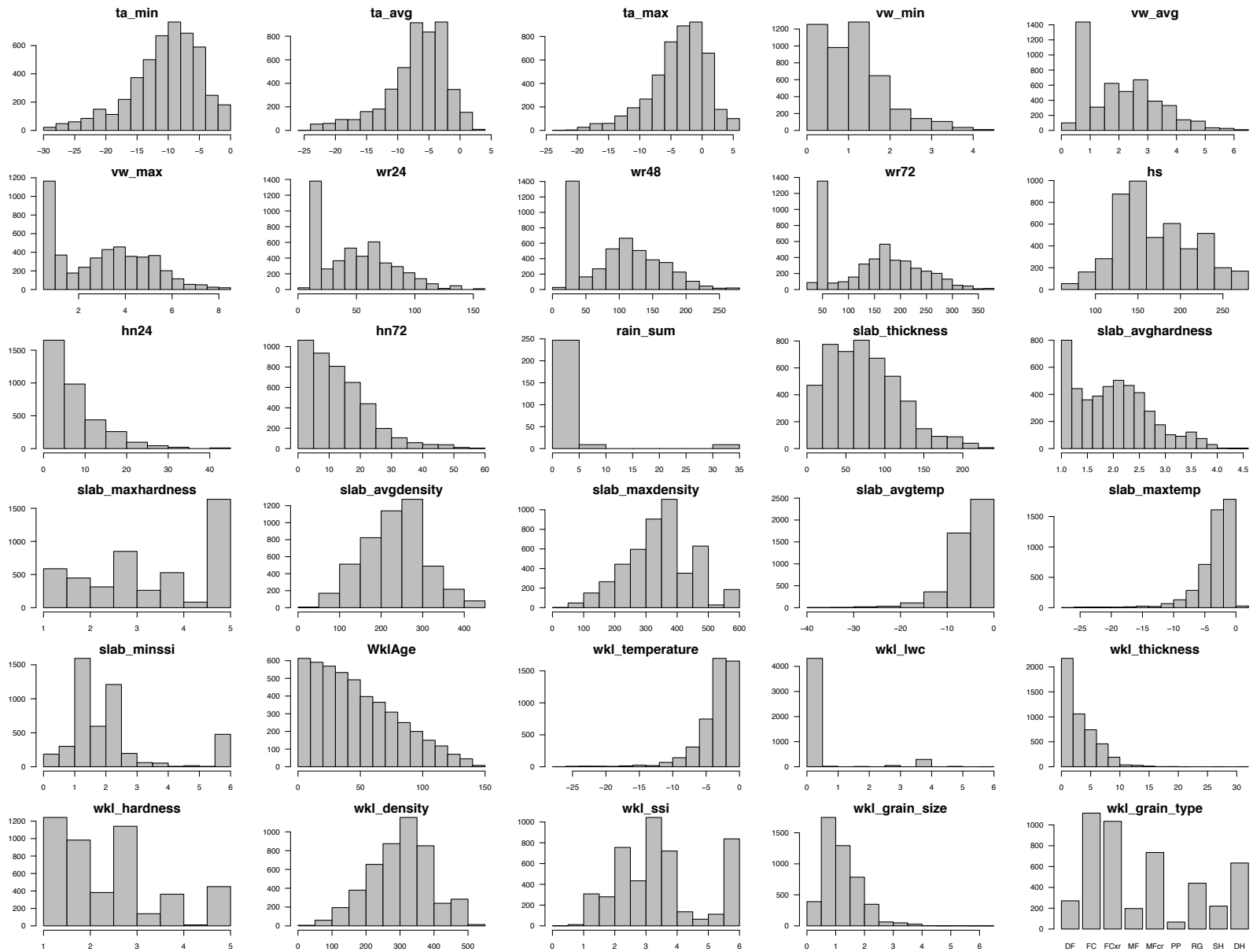


Figure 4.24 Frequency distribution of all variables in the Persistent Avalanche Problems Types dataset. Zero precipitation values (hn24, hn72 & rain_sum variables) are omitted to clearly show distributions

In the persistent avalanche problem type dataset, there are also considerable correlations between the simulated weather and snowpack variables included in my analysis (Figure 4.25). The main pattern that stands out is the high correlation between weak layer age and many of the overlying slab variables (slab thickness = +0.87; slab maximum hardness = +0.63; slab average hardness = +0.74; slab maximum density = +0.77; slab average density = +0.82). These correlations are not surprising as overall, the slabs above weak layers are expected to become thicker and stronger as the winter progresses.

As in the surface avalanche problem analysis, all wind speed variables (vw_min , vw_avg , vw_max , $wr24$, $wr48$, $wr72$) were strongly correlated with each other (ranging: +0.83 to +1.00), but the modelled wind variables also had weak positive correlations with modelled slab and weak layer temperatures (range: +0.12 to +0.25) and weak negative correlations with modelled slab thickness (range: -0.15 to -0.22). Modelled air temperature variables (ta_min , ta_avg , ta_max) were not surprisingly moderately to strongly correlated with modelled slab temperatures (range: +0.49 to +0.73) and moderately correlated to modelled weak layer temperature as well (range: +0.45 to +0.49). Modelled air temperatures were also weakly correlated with the modelled slab and weak layer hardness and density variables (range: +0.12 to +0.32). The modelled slab temperatures were strongly correlated with modelled weak layer temperatures (range: +0.86 to +0.98) and moderately correlated with the modelled slab and weak layer hardness and density variables (range: +0.36 to +0.66). The modelled weak layer temperature was also moderately correlated with the modelled slab and weak layer hardness and density variables (range: +0.47 to +0.68). These positive correlations between modelled temperatures and modelled slab and weak layer variables are the direct result of how air and snowpack temperatures influence snow metamorphism and grain changes which directly impact the hardness and density of snow layers.

Not surprisingly, the modelled HN24 and HN72 variables are strongly correlated (+0.78), but these snowfall variables also have a weak positive correlation with modelled slab thickness (range: +0.17 to +0.23) and weak negative correlations with modelled slab average hardness and average density variables (range: -0.14 to -0.16). This shows that when there is lots of new snow, a large portion of the slab above a layer is composed of soft low-density new snow which will cause a reduction in the weighted average hardness and density. Once it stops snowing the slab hardness and density will

likely increase after a few days of settling. The modelled minimum SSI within the slab had moderate negative correlations with the modelled slab and weak layer temperatures and hardness and density variables (range: -0.42 to -0.59) and weak negative correlations with the modelled air temperature variables (range: -0.17 to -0.18). The modelled SSI of the weak layer had weak to moderate positive correlations with weak layer thickness, density and hardness and liquid water content variables (range: +0.08 to +0.43) and weak negative correlations with modelled snowfall variables HN24 and HN72, slab thickness and weak layer temperature and grain size (range: -0.07 to -0.25).

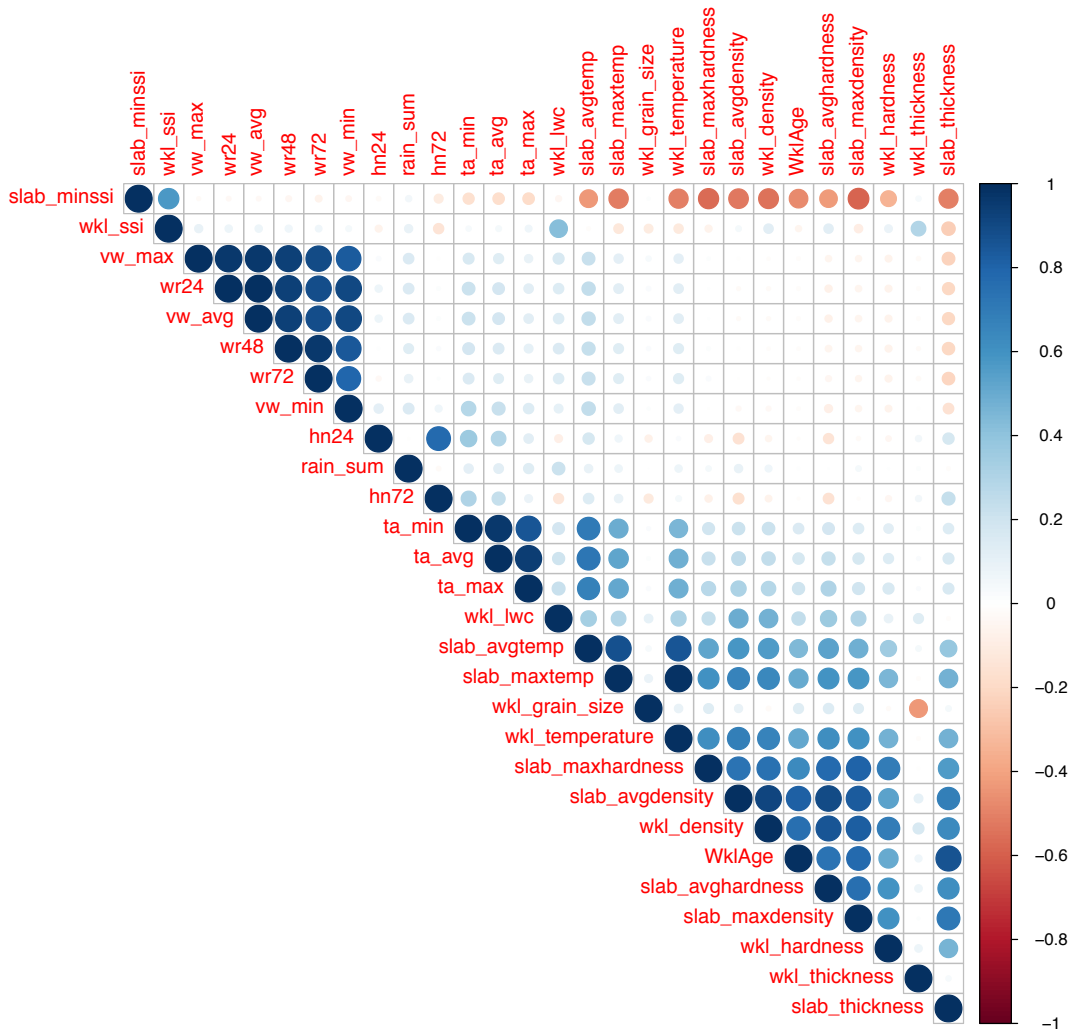


Figure 4.25 Correlation plot of all numeric weather and snowpack variables included in the Persistent Avalanche Problem Type dataset.

To further minimize the PS/DPS avalanche problem dataset, certain variables that were highly correlated with other similar variables were removed to simplify the complex CIT model output into an interpretable and manageable result. These included:

- Slab hardness versus slab density
 - Average slab hardness versus average slab density: Spearman's Rank Correlation: $\rho = 0.89$; $p\text{-value} < 0.01$
 - Maximum slab hardness versus maximum slab density: Spearman's Rank Correlation: $\rho = 0.88$; $p\text{-value} < 0.01$
- Temperature variables
 - Weak layer temperature versus maximum slab temperature: Spearman's Rank Correlation: $\rho = 0.99$; $p\text{-value} < 0.01$
 - Weak layer temperature versus average slab temperature: Spearman's Rank Correlation: $\rho = 0.85$; $p\text{-value} < 0.01$
 - Weak layer temperature versus average air temperature: Spearman's Rank Correlation: $\rho = 0.62$; $p\text{-value} < 0.01$
 - Weak layer temperature versus minimum air temperature: Spearman's Rank Correlation: $\rho = 0.60$; $p\text{-value} < 0.01$
 - Weak layer temperature versus maximum air temperature: Spearman's Rank Correlation: $\rho = 0.59$; $p\text{-value} < 0.01$
 - Average air temperature versus maximum air temperature: Spearman's Rank Correlation: $\rho = 0.95$; $p\text{-value} < 0.01$
 - Average air temperature versus minimum air temperature: Spearman's Rank Correlation: $\rho = 0.96$; $p\text{-value} < 0.01$
 - Average slab temperature versus maximum slab temperature: Spearman's Rank Correlation: $\rho = 0.86$; $p\text{-value} < 0.01$
 - Weak layer temperature, maximum air temperature, and minimum air temperature were omitted from the analysis
- Wind variables:
 - Average wind speed versus maximum wind speed: Spearman's Rank Correlation: $\rho = 0.97$; $p\text{-value} < 0.01$
 - Average wind speed versus minimum wind speed: Spearman's Rank Correlation: $\rho = 0.91$; $p\text{-value} < 0.01$

- Average wind speed versus 24 hr wind run: Spearman's Rank Correlation: $\rho = 1.0$; $p\text{-value} < 0.01$
- Average wind speed versus 48 hr wind run: Spearman's Rank Correlation: $\rho = 0.94$; $p\text{-value} < 0.01$
- Average wind speed versus 72 hr wind run: Spearman's Rank Correlation: $\rho = 0.88$; $p\text{-value} < 0.01$
- Maximum wind speed, minimum wind speed and all three wind run variables were omitted from the analysis.

Due to the high correlation between many of the weather and snowpack variables, the only variables kept for the CIT analysis out of the ones listed above were: a) average and maximum slab hardness, b) slab average and maximum temperature, c) average air temperature, and; d) average wind speed. The removal of all highly correlated variables created a manageable model output that was much easier to interpret.

4.3.2. Persistent Slab/Deep Persistent Slab Avalanche Problems

PS/DPS Avalanche Problem Dataset and Timeseries Analysis

My analysis of the GNP bulletins revealed that PS/DPS avalanche problem types were identified by forecasters at the treeline elevation band an average of 6 periods per winter season with an average duration of 17 days (Table 4.9). Overall, the treeline elevation band had a total of 468 days with PS/DPS avalanche problems present, which is equivalent to an average of 78 days per season (Table 4.9). Related to these PS/DPS avalanche problems, forecasters identified 41 PWLs over the entire study period for an average 7 PWLs per season (Table 4.10). These PWLs were typically associated with a *Surface* avalanche problem (e.g. SS, WS) for an average of 11 days before becoming a *Present* PS/DPS avalanche problem, which typically persisted for an average of 22 days (Table 4.10).

The method for finding and tracking possible layers employed in this study identified and tracked a total of 70 separate interfaces (including all PWLs identified by forecasters) that had the potential to become a PS/DPS. On average, 12 interfaces were tracked per season (Table 4.10).

Table 4.9 Season Summaries – PS/DPS Avalanche Problem Types – Treeline Elevation

Season	PS/DPS Av. Prob. occurrences	Avg. Duration (days)	Minimum Length (days)	Maximum Length (days)	Total days with PS/DPS
2012-13	8	9.0	1	36	72
2013-14	8	12.1	2	22	97
2014-15	5	22.8	2	65	114
2015-16	5	14.8	6	28	74
2016-17	6	6.2	1	19	37
2017-18	2	37.0	10	64	74
Average	5.7	17.0	1	65	78
Totals	34	NA	NA	NA	468

Table 4.10 Season Summaries – Tracked Interfaces and Persistent Weak Layers of concern from assessments

Season	# of Tracked Interfaces	# of PWLs	Avg. Days as Surface Problem	Avg. Days Present
2012-13	10	5	10.0	20.8
2013-14	11	9	13.7	32.6
2014-15	15	8	11.4	27.1
2015-16	9	4	11.5	16.5
2016-17	14	8	8.8	22.6
2017-18	11	7	11.4	9.9
Average	11.7	6.8	11.1	21.6
Totals	70	41	NA	NA

A visual examination of the weather and SNOWPACK profile timeseries plots showed that tracked PS/DPS avalanche problems typically followed the occurrences of SS avalanche problems that had buried a substantial weak layer (yellow dots, Figure 4.26) that formed prior to the last storm cycle when conditions were ideal for the formation of persistent grain types (e.g. SH, near-surface FC).

To explore the relationships between the stages of the tracked interfaces and the modelled weather and snowpack observations, I first plotted boxplots (Figure 4.27) and used Kruskal-Wallis and pairwise Wilcoxon rank-sum tests to assess the significance of the observed differences. In addition, I calculated effect sizes r to measure the magnitude of the observed differences. This approach revealed the following differences:

- Median slab thickness increased significantly between each of the stages (*Surface* median = 49.4 cm; *Present* median = 56.4 cm; *Absent* median = 96.0 cm). However, the effect size calculations revealed that the difference between *Surface* and *Present* is only small, whereas the difference between *Present* and *Absent* is medium.
 - Kruskal-Wallis Test: p-value < 0.05
 - Pairwise Wilcoxon Tests:
 - *Surface* vs. *Present* (p-value < 0.01, r = -0.07)
 - *Present* vs. *Absent* (p-value < 0.01, r = -0.30)
- Median slab density increased significantly between each of the stages (*Surface* median = 201.0 kg/m³; *Present* median = 215.2 kg/m³; *Absent* median = 270.5 kg/m³). Again, the effect size calculations revealed that the difference between *Surface* and *Present* is small and the difference between *Present* and *Absent* is medium.
 - Kruskal-Wallis Test: p-value < 0.05
 - Pairwise Wilcoxon Tests:
 - *Surface* vs. *Present* (p-value < 0.01, r = -0.07)
 - *Present* vs. *Absent* (p-value < 0.01, r = -0.28)
- Median slab hardness also increased significantly between each stage (*Surface* median = 1.6; *Present* median = 1.8; *Absent* median = 2.3) with similar results for the differences.
 - Kruskal-Wallis Test: p-value < 0.05
 - Pairwise Wilcoxon Tests:
 - *Surface* vs. *Present* (p-value < 0.01, r = -0.08)
 - *Present* vs. *Absent* (p-value < 0.01, r = -0.25)
- Median weak layer age increased significantly (*Surface* median = 27 days; *Present* median = 27 days; *Absent* median = 64 days). Since the median values for *Surface* and *Present* are identical, the effects size

calculation was only done for the difference between *Present* and *Absent* and revealed a medium difference.

- Kruskal-Wallis Test: p-value < 0.05
- Pairwise Wilcoxon Test:
 - *Present* vs. *Absent* (p-value < 0.01, r = -0.42)
- Median weak layer density only increased significantly between *Present* and *Absent* stages (*Surface* median = 269.0 kg/m³; *Present* median = 277.0 kg/m³; *Absent* median = 344.0 kg/m³) with a medium difference.
 - Kruskal-Wallis Test: p-value < 0.05
 - Pairwise Wilcoxon Test:
 - *Present* vs. *Absent* (p-value < 0.01, r = -0.29)
- Median weak layer hardness also only increased significantly between the *Present* and *Absent* stages (*Surface* median = 2.0; *Present* median = 2.0; *Absent* median = 3.0) with a medium difference.
 - Kruskal-Wallis Test: p-value < 0.05
 - Pairwise Wilcoxon Test:
 - *Present* vs. *Absent* (p-value < 0.01, r = -0.25)

The progression of *Surface* avalanche problems to *Present* PS/DPS avalanche problems to *Absent* is apparent when plotting slab thickness against weak layer age (Figure 4.28).

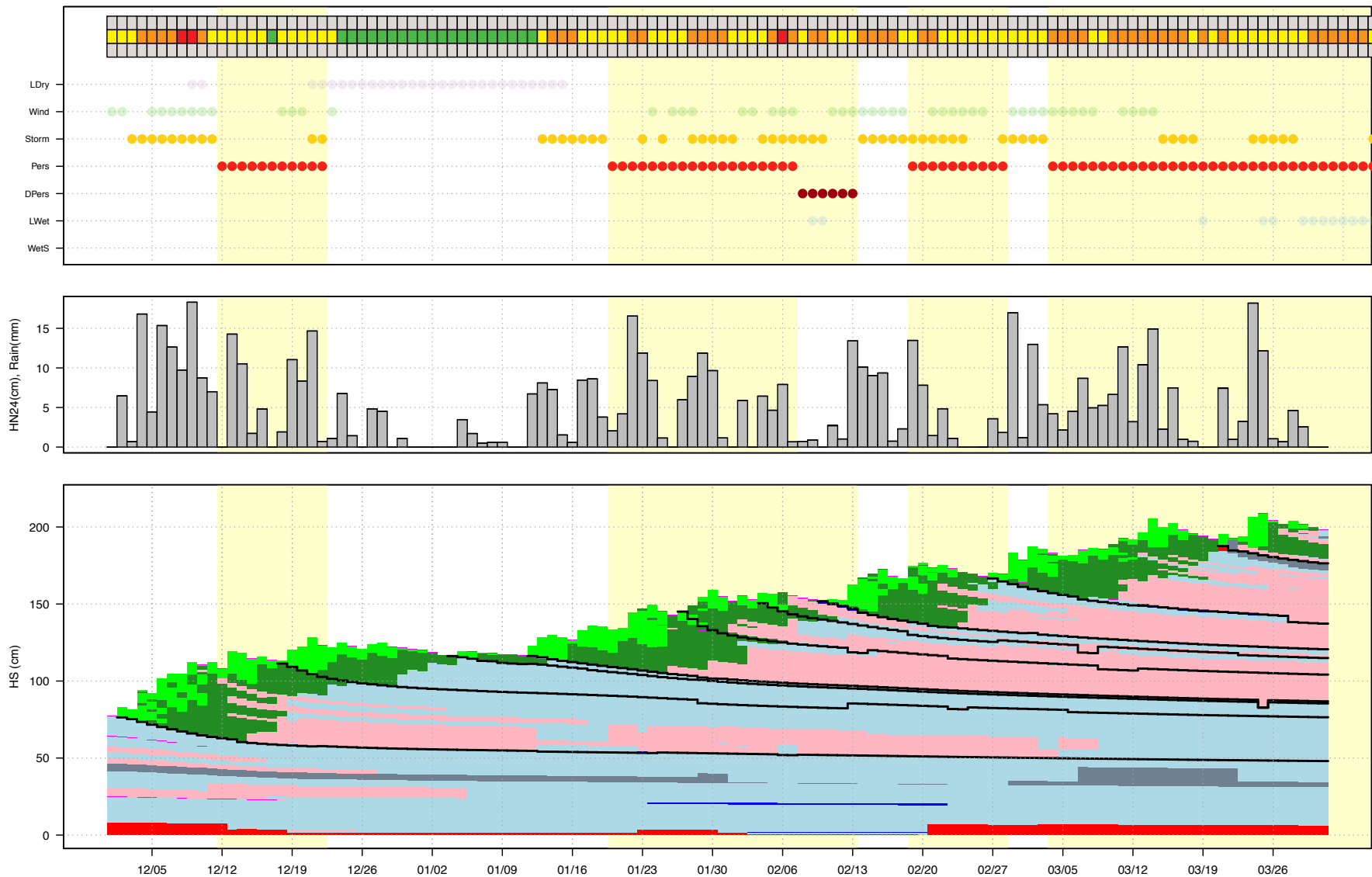


Figure 4.26 Timeseries (2016 Season – Treeline) of PS/DPS avalanche problems, precipitation (HN24 = grey bars, and rainfall = black bars) and snowpack evolution (black lines = tracked layers). Yellow bands represent the presence of a PS/DPS avalanche problem on any given day.

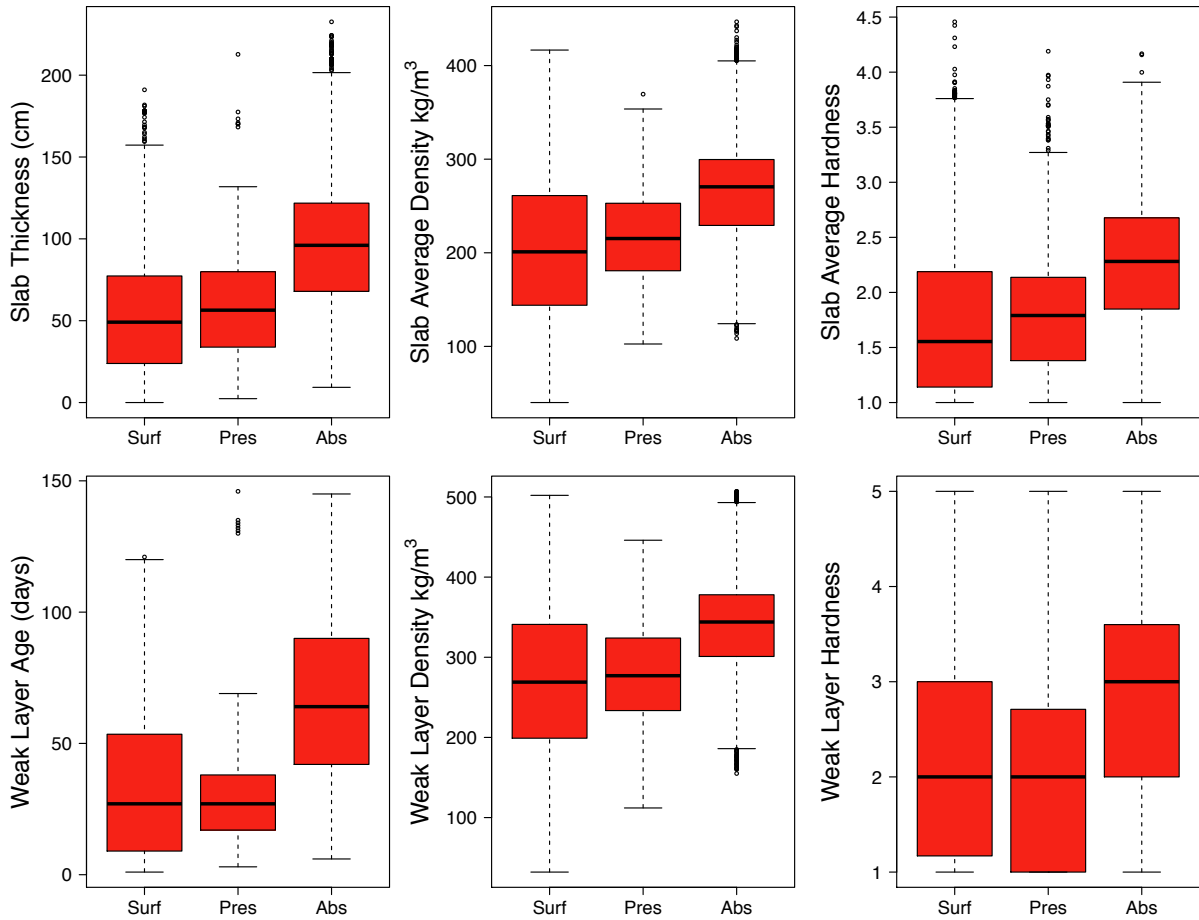


Figure 4.27 Distribution of slab thickness, average density and average hardness and weak layer age, density and hardness when PS/DPS avalanche problems were surface problems, present and absent (2013 - 2018 Seasons).

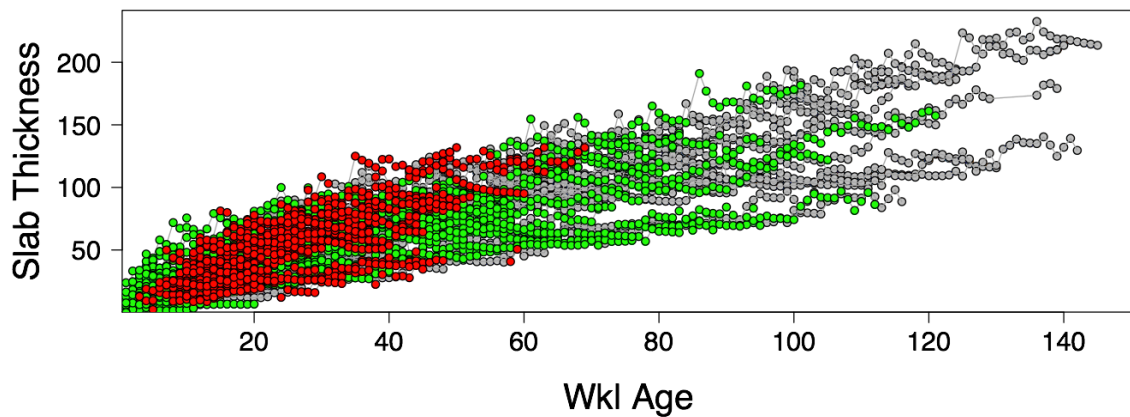


Figure 4.28 Tracked weak layer evolution for all tracked interfaces showing weak layer age versus slab thickness (Red = Surface problem; Green = Present PS/DPS problem; Grey = Absent PS/DPS problem)

Representing PS/DPS avalanche problem relationships with a CIT model

To simplify the PS/DPS avalanche problem CIT analysis, two separate analyses were completed: one for “Turning On” or the switch between *Surface* and *Present* PS/DPS avalanche problems and; one for “Turning Off” or the switch from *Present* to *Absent* PS/DPS avalanche problems. Interestingly, the “Turning Off” model did not produce any significant decision rules, which will be rationalized more in the discussion section.

Across the entire dataset of the 70 tracked interfaces, there was a 31% probability of a tracked interface becoming a PS/DPS avalanche problem. The analysis for “Turning On” PS/DPS avalanche problems computed 14 decision rules that split the dataset into 15 distinct terminal nodes (Figure 4.29). The first and most significant split in the CIT analysis was weak layer age which showed that there was only a 10% probability of a tracked interface becoming a PS/DPS avalanche problem when the interface was less than or equal to 10 days old (Nodes 3, 5 & 6). The most likely conditions for young weak layer of ages 6 to 10 days to become a PS/DPS avalanche problem was with a weak layer grain types of FC, FCxr or DH (Node 6, 40% probability).

If a tracked interface was older than 10 days, there was a 44% probability that it would become associated with a PS/DPS avalanche problem. As the age of the weak layer exceeded the 10-day threshold, the next significant decision rule that emerged was the hardness of the overlying slab. Based on the Hand Hardness scale (1 = very soft (fist), 2 = soft (4 fingers), 3 = medium (1 finger), 4 = hard (pencil point), 5 = very hard (knife), (McClung & Schaerer, 2006)), softer slabs (≤ 2) only had a 26% probability of becoming a PS/DPS avalanche problem, suggesting conditions were not favourable for slab formation above the layer (Nodes 13 & 14). The remaining nodes on the soft slab branch (hardness ≤ 2) highlighted additional variables that relate to forecasters turning on of PS/DPS avalanche problems: when maximum slab temperatures were cold (≤ -5.4 °C), there was less chance of a PS/DPS avalanche problem (Nodes 10 & 11, 6% probability). The final split in this branch was related to a crust being present underneath the tracked interface. If a crust was present, the probability of a PS/DPS avalanche problem being present was substantially higher (50% probability in Node 10 versus 3% in Node 11). However, only 8 cases were included in Node 10 in total. When the maximum slab temperatures were above -5.4 °C, the probability of a PS/DPS

avalanche problem increased to 40% and was driven by the thickness of the weak layer ($\leq 3.73\text{mm}$, 51% probability; $> 3.73\text{ mm}$, 18% probability).

For weak layers older than 10 days with harder slabs (hardness > 2), the probability of forecasters becoming concerned with a PS/DPS avalanche problem increased to 61% and the next significant decision rule related to the grain size of the weak layer itself (Node 15). With large grains in the weak layer ($> 1.47\text{ mm}$), a PS/DPS avalanche problem became almost certain (Node 29, 96% probability). The remaining splits when the weak layer grain size was smaller ($\leq 1.47\text{ mm}$) outlines other weak layer and slab properties that help define when forecasters were possibly concerned with PS/DPS avalanche problems. First, the main split was related to weak layer hardness where hardness greater than 2 decreased the probability of a PS/DPS avalanche problem to 39% followed by the grain type of the weak layer (Nodes 27 & 28). When the weak layer hardness was less than or equal to 2, layer was more susceptible to failure and the probability of a PS/DPS avalanche problem increased to 69%. The relatively small terminal nodes of the following decision rules describe various scenarios where PS/DPS avalanche problems were likely but only on special occasions:

- when the average slab hardness was soft to very soft it was quite likely that a PS/DPS avalanche problem would exist (Nodes 19 & 20, 81% probability), especially earlier in the season;
- when slab were harder and weak layers were at least 1.33 mm thick PS/DPS avalanche problems were almost certain (Nodes 24 & 25, 89% probability) especially as the weak layer got older;
- when the weak layer was extremely thin ($\leq 1.33\text{ mm}$) there was no chance of a PS/DPS avalanche problem (Node 22, 0% probability).

As with the surface avalanche problem analysis, the fact that some of the terminal nodes only include small numbers of observations might indicate that they represent special cases that are not necessarily generalizable.

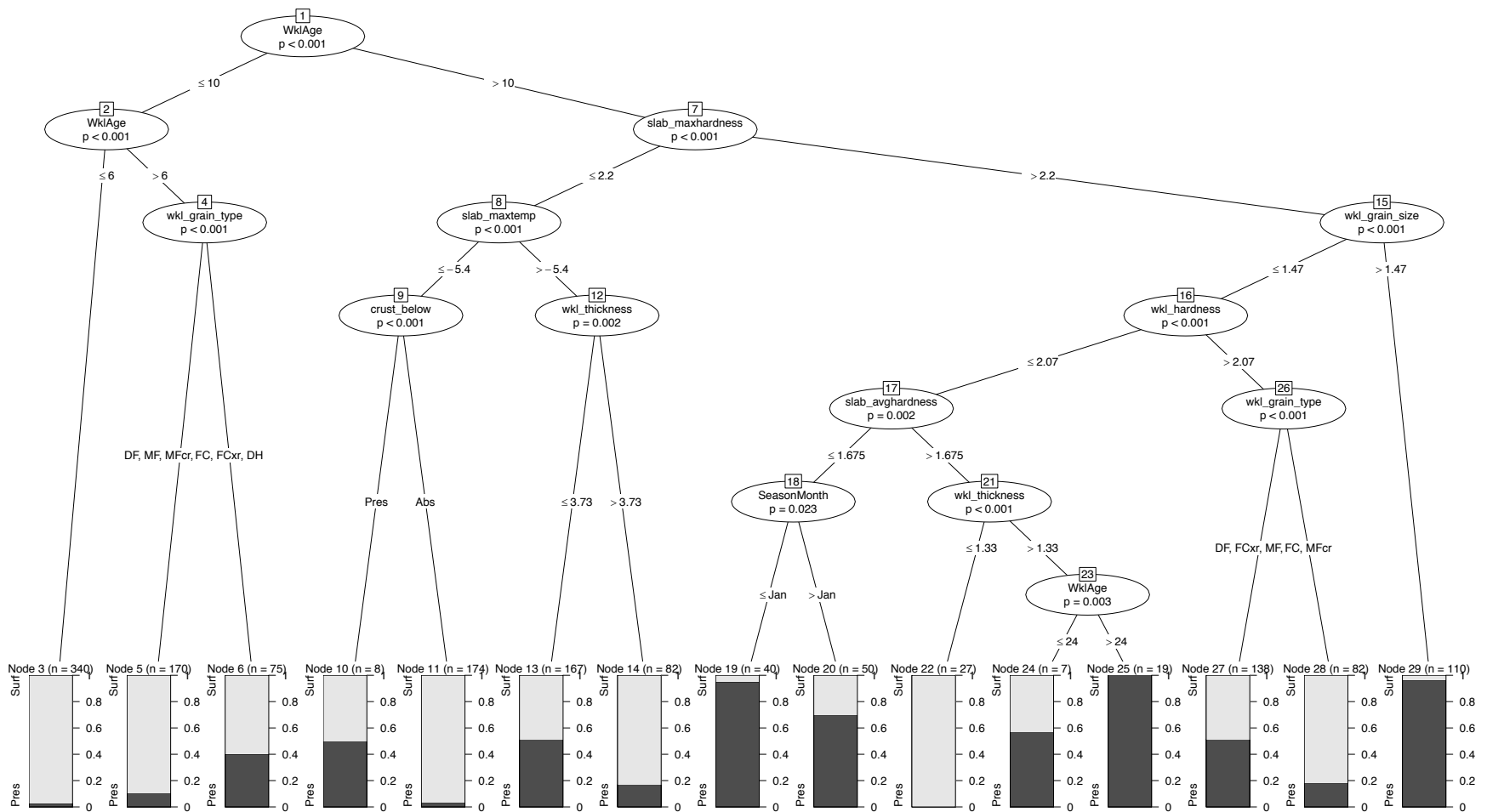


Figure 4.29 Conditional Inference Tree for turning PS/DPS Avalanche Problem on

Chapter 5. Discussion

The purpose of my research was to explore the relationships between modelled weather and snowpack data and human avalanche problems assessments. In the following sections, I combine the findings of the initial data exploration and the CIT analyses into a comprehensive picture that addresses my research question. The resulting synthesis is broken into two main parts: a) the main themes that emerge, and b) the limitations of my research.

5.1. Main Themes Developed from the CIT Analyses

I identified three main themes that emerged from my analyses. In the following sections, I will delve into the how each result relates to the existing knowledge and literature.

5.1.1. Relevant Weather and Snowpack Factors

The results from my analysis of individual surface and persistent slab avalanche problem types confirmed the influences of expected weather and snowpack variables on the presence of forecasted avalanche problems. The CIT models identified many statistically significant splits related to these variables that provide insight into what forecasters might pay attention to when making complex decisions about avalanche hazard.

Surface Avalanche Problem Patterns

What emerged from my surface problem analyses is that the status of different avalanche problems depends on different combinations of weather and snowpack variables. This is not surprising as each avalanche problem type is defined by their own set of variables and locations both spatially and temporally (Haegeli et al., 2010). Many of the main decision rules to emerge can be directly linked to previous studies and rules that forecasters use in the field to assess avalanche conditions.

As expected, any weather and snowpack variables that emerged in the WS and SS avalanche problem CIT analysis had to do with wind and new snow. Explicitly, in the

WS avalanche problem analysis, the 72 h wind run split at 320 m/s·h (average of 16 km/h for 3 days) is on the low end of the thresholds described in the literature where snow transport is the greatest between 25-40 km/h (Föhn, 1980). Since the actual wind speeds are likely higher than predicted by the NWP model (Horton, Schirmer, & Jamieson, 2015), the wind speed thresholds may not be good decision rules, but it is encouraging that they are represented in the CIT model as a variable that relates to forecaster decisions. Another possible influence on the presence or absence of wind variables in all the CIT models (with the exception of WS), is that the discontinuity of the wind information due to the upgrade to the HRDPS between the 2014 and 2015 seasons was not corrected. As the physics and modelling capabilities improve, these splitting rules may get closer to the thresholds currently used by practitioners. As for new snow quantities, the analysis of SS avalanche problems contained many high-level decision rules that emerged at the top of the CIT model. It is predictable that new snow is the driving factor for SS avalanche problem assessments as previous studies have shown that avalanche hazard increases with increasing new snow amounts (Floyer & McClung, 2003; Perla, 1970). Although the decision rule splits seen in the CIT (e.g. HN24: Node 2, 7 cm; Node 27, 2.5 cm; HN72: Node 23, 4 cm, see Figure 4.13) analysis are well below the indicated 30 cm threshold stated by Perla (1970), they are much more similar to the thresholds that emerged from the study done by Haladuick (2014) and the presence of the main snowfall variables (HN24 and HN72) at the top of the decision tree also verifies their importance to forecasters when identifying SS avalanche problems.

The expected weather and snowpack variables that play important roles in the identification of LDRY avalanche problems were in fact the variables that emerged in the CIT model. The first decision rule split based on time of the season was expected since loose, dry snow is more probable earlier in the season before air and snow surface temperatures increase. Since loose, dry snow is constrained to certain weather and snowpack conditions (cold and calm days), it is also reassuring to see air and snow surface temperatures and ski-penetration depth highlighted as decision rules. Ski-penetration depth, as modelled by SNOWPACK, is also considered a proxy for the availability of loose snow. What is also promising is that storm snow density is the major (and only) decision rule that emerged for LDRY avalanche problems persisting. The storm snow density split occurs at a reasonable value of 130 kg/m³ (Simon Horton,

personal communication, 2019) and indicates that as the storm snow settles and the snow begins bonding, there is less chance of a LDRY avalanche problem persisting.

Although the size of the datasets of CORN and LWET avalanche problems was too small for an in-depth analysis, the CIT models showed promise. Cornice avalanche problems, considered a late season phenomenon, occur mainly in the alpine along ridge crests and usually persist once they have formed (Haegeli et al., 2010; Statham, Haegeli, et al., 2018). This is verified in the analysis for CORN avalanche problems with the majority of the assessments occurring after the beginning of March in the alpine and are more likely to persist once forecasters have become concerned about them. Loose wet avalanche problems are also predominantly a late season phenomenon but occur more frequently at lower elevations as warmer spring conditions begin melting the upper levels of the snowpack (Haegeli et al., 2010). This again is confirmed by the analysis for LWET avalanche problems with the majority of assessments occurring after late March when temperatures have increased.

While the modelled predictive threshold values are underestimated and may not be directly meaningful, it is promising to see the relevant variables appear in the models as it is an indication that the weather and snowpack models are capable of identifying relevant factors that influence forecaster decisions. Compounding errors from HRDPS underestimation of precipitation amounts and the resulting snowfall calculations done by SNOWPACK are not accurate representations of what forecasters would expect to see in the field before becoming concerned enough to make a crucial decision about assessing a certain avalanche problem (McClung & Schaerer, 2006). My model validation also points to this underestimation and confirms the effect of precipitation bias on model simulations reported in previous research (Bellaire et al., 2011). Part of the issue also lies in the fact that many of the real field observations are done in well sheltered areas and are not easily extrapolated across the entire region being forecasted since terrain, elevation, and other environmental factors play a large role in the amount of precipitation that accumulates. The HRDPS wind model upgrade in 2015 improved the underestimation of modelled wind speed values, and although it was only accounted for in my analysis of WS avalanche problem types, the accuracy of the improved wind model is partially responsible for the fact that wind variables (wind speed and wind run) did not show up as decision rule splits as often as expected. I believe that this is not only the result of underestimation by the NWP model but also the direct result of the

reliability of using the wind variable from the NWP model as wind is statistically calculated at 10 m elevations on a 2.5 km grid spacing, but in reality, it is highly affected by small scale terrain features that cannot be resolved on a coarse grid. For example, Horton et al. (2015) found poor agreement in the distribution of wind speeds from different HRDPS wind speed variables with measurements from stations in GNP. Although modelled wind speeds are not representative of the actual wind speeds seen at the surface where it can interact with the deposited snow, they are still correlated, hence wind run calculations can still give meaningful information.

Persistent Slab Avalanche Problem Patterns

The analysis of the persistent slab avalanche problems revealed similar patterns seen in the surface avalanche problems but was dominated by snowpack structure variables. The analysis for “turning-on” PS/DPS avalanche problems proved to be insightful in regard to the variables that emerged and was supported by existing literature about persistent slab avalanche problems.

The most important split in the CIT model was the age of the weak layer. Since younger layers do not develop into a persistent problem until they become sufficiently buried and/or the overlying snow has developed into a slab (Haegeli et al., 2010; Statham, Haegeli, et al., 2018), this result is unsurprising. The other important fact to consider is that slabs of snow that overlie young weak layers are usually initially identified as a surface avalanche problem such as a SS or WS avalanche problem. Only if a weak layer persists and the overlying slab begins to densify and harden over time, the problem will transition into a PS/DPS avalanche problem (Klassen, 2014).

After weak layer age, the rest of the significant splits were, not surprisingly, largely driven by snowpack structure with a relatively even distribution of slab and weak layer properties. The main slab properties to emerge were hardness and temperature. In my analysis, slab hardness was used interchangeably with the highly correlated slab density (I removed the density variables). If the weak layer is triggerable, a harder slab will generally result in an increase in fracture propagation and result in a larger, more destructive avalanche (Schweizer, Reuter, van Herwijnen, & Gaume, 2016). Another meaningful predictor that emerged from the CIT analysis is average slab temperature. Since temperature also impacts the stiffness of the slab, warmer temperatures could reduce the stiffness increasing the potential to initiate a fracture in the weak layer, but

the increase in temperature could also decrease the ability for a fracture to propagate over larger distances. A meaningful alternative temperature variable for future consideration could be the temperature gradient from snow surface temperature down to the weak layer temperature. Although temperature gradients impact snow properties over longer time scales, decreased temperature gradients can promote bonding and increased strength, whereas increased temperature gradients, which are associated with colder air temperatures, slows down the bonding process (Zeidler & Jamieson, 2006b). In other words, the temperature gradient drives the type of metamorphism in the snowpack whereas the temperature itself relates to the speed of the metamorphism process. Both hardness and temperature are readily measured in the field, but surprisingly, slab thickness which is one of the main field observations that forecasters focus on during their assessment of PS/DPS avalanche problems did not show up in the CIT model. One possible reason for this is that thickness is highly correlated with weak layer age (thickness increases over time) and is already represented in the primary decision rule splits. Slab thickness is also important to the strength of snowpack and the relative size of associated avalanches. While thinner slabs can be easier to trigger (Zeidler & Jamieson, 2006a), a thicker slab will also result in a larger avalanche once a crack propagation is initiated (Schweizer et al., 2016) which increases the concern that forecasters have surrounding PS/DPS avalanche problem assessments.

Finally, the weak layer properties that emerge from the CIT analysis were hardness, thickness, grain type and grain size. The same weak layer properties have been identified as being important by forecasters in decision support tools such as those by Conlan and Jamieson (2017). Persistent weak layers are often identified as layers composed of SH, DH and FC with relatively large crystal size (Haegeli et al., 2010; Statham, Haegeli, et al., 2018) and the presence of grain type and size in the CIT analysis confirms the importance of these variables. An increase in the hardness of a weak layers results in an increase in the strength of that weak layer (Zeidler & Jamieson, 2006a). Although measuring hardness in the field is partly subjective and difficult to estimate for thin layers (Zeidler & Jamieson, 2006a), the introduction of new field technology could eventually assist with gaining more accurate measurements (McClung, 2018).

Overall, the decision rules that emerged from the CIT model, were reasonable and provided a meaningful connection between the variables used to assess avalanche

problems and the important variables predicted by the models. Although the results have the potential to be used as the foundation for the development of future decision aids, the modelled thresholds are not directly relatable to field observations and the current modelled decision rules only provide insight into what forecasters may pay attention to when assessing avalanche problems in the past. For instance, the modelled probability of a PS/DPS avalanche problem is almost certain when a slab of 1-finger hardness overlies a 10-day old weak layer that has grains larger than 1.5 mm, which is a promising result from this pilot study that can easily be interpreted by operational forecasters.

5.1.2. Insight into Forecaster Practices

The second important theme to emerge from my study is the possible insight into forecaster practice related to the CMAH. Since avalanche forecasting requires substantial judgement (LaChappelle, 1980; McClung, 2002), it is inherently susceptible to human biases and errors. While the CMAH introduced a general framework and language for avalanche hazard assessments (Statham, Haegeli, et al., 2018), it still leaves considerable room for interpretation, which can lead to undesirable inconsistencies (see, e.g. Clark, 2019; Statham, Holeczi, et al., 2018), and means that forecasters can arrive at different conclusions based on identical information (Lazar et al., 2016). Building on this research, the present analyses offer a complementary perspective on how the CMAH is used in operations.

In all my analyses the status of the analyzed avalanche problem from the previous day was consistently the primary decision rule. This result is intuitive and was expected as the previous day's status is the foundation of forecaster assessment of the next day: *Was there a significant change in the weather or snowpack conditions that would change the probability of a certain avalanche problem type occurring?* Depending on the answer, the subsequent splits provide insight into the weather and snowpack conditions that led forecasters to change their assessment. This type of result is a reflection of the practice of Bayesian updating and time dependencies (LaChappelle, 1980; McClung, 2002).

The outlier avalanche problem in all of the CIT models was the WS avalanche problems where the majority of the decision rule splits were not driven by weather or

snowpack variables but rather the status of a concurrent SS avalanche problem. This can be directly linked to the implementation of the CMAH and the evolution of forecaster practice since. Specifically, during the last few seasons in GNP, forecasters appear to have separated WS and SS avalanche problems, not allowing them to be identified simultaneously for reasons explained by Klassen (2014). Predictably then, the status of concurrent WS avalanche problems also plays a big role in the identification of SS avalanche problems. Although it plays less of a role in this analysis, the status of WS avalanche problems occurs as four separate splits further down the decision tree, where its importance is more in refining certain situations where SS avalanche problems occur. This suggests that when conditions align for SS avalanche problems, they take precedence over WS avalanche problems. If discussed at the operational level, insights such as this can help to improve forecaster practice and create a more streamlined approach to avalanche hazard assessment.

5.1.3. The Challenge of “Turning off” Avalanche Problems

The “turning-on” branch of avalanche problems are relatively well defined in all the CIT models through the presence of many decision rule splits that laid out specific scenarios where each avalanche problem was more likely to be identified. What also became clear was that the scenarios for “turning-off” an avalanche problem were harder to explain. Specifically, the CIT analysis for “turning-off” a PS/DPS avalanche problem generated no significant splits. Although this result may not seem meaningful initially, it sheds light on a challenging component of forecasting avalanche problems and is consistent with the less defined “turning-off” branches seen in the surface avalanche problems. The “turning-off” branches of all the surface avalanche problems had considerably fewer nodes and significant splits compared to the “turning-on” branches, even though certain variables that emerged were indeed meaningful (i.e. HN24 and HN72 (SS), HST density (LDRY)). This indicates that while there is some consistency in identifying an avalanche problem initially, when it comes to “turning-off” an avalanche problem, it becomes less clear when and why this should occur. In other words, the available dataset includes much more variability, which prevents the identification of meaningful rules.

Although further exploration and analyses are necessary to examine the “turning-off” of avalanche problems in more depth, incorporating other observations such as

recent avalanche activity could contribute to improving the quality of the analysis in the future. While avalanche activity data available was available for the study area, it was not incorporated into the analysis since a) this study was aimed at understanding the relationships between modelled observations and the forecasted avalanche problems and b) because there is usually no avalanche activity records in data-sparse regions where this modelling approach for avalanche problems might be applied in the future. Another possible approach could be to use likelihood and size as target variables instead of the simple presence or absence of an avalanche problem as these avalanche problem characteristics might be more closely related to the modelled weather and snowpack variables. However, inconsistencies in the assessments of likelihood and size due to human judgement might prevent this analysis approach from providing any more meaningful insights in the future.

5.2. Limitations

Although my study offers meaningful insights into the relationships between modelled weather and snowpack data and forecasted avalanche problems, it is not without its limitations. Firstly, although there were many days with avalanche problems present, the dataset contains very few cases where avalanche problems were “turned-on” or “turned-off”. Hence, a longer dataset would help strengthen the analyses and result in a better understanding of the underlying weather and snowpack conditions needed to “turn-on” or “turn-off” a given avalanche problem. In an ideal scenario, the dataset would contain many more seasons of data than the six seasons available for my research. This limitation is also obvious in the fact that there were only two observations for wet slab avalanches and so they were omitted from the analysis. Although the CIT models that were analyzed should have only been run for avalanche problems with substantially large datasets (Hothorn et al., 2006), some of the lesser occurring avalanche problems (LWET, CORN) showed promising results and were not omitted. As the dataset grows in future years, future analyses will not be subjected to the same limitation.

Another limitation was that the weather and snowpack data was gathered from models run at a single virtual location and then linked to avalanche assessments that were representative of an entire region without taking advantage of the simulations at the other grid points within GNP. While the approach employed in the present study was justified due to the high correlation between the simulated weather and snowpack

observations at the grid points, it nevertheless represents a substantial simplification. Although the simulated observations are representative of a 2.5 km by 2.5 km square and potentially have a larger extent than actual field observations used by forecasters to create their avalanche assessments, these subjectively chosen grid points may not be an accurate representation of the entire region's snow conditions. Haegeli and McClung (2004) referred to this issue as a scale mismatch. To better characterize regional conditions, it will be imperative for future analyses to incorporate more grid points in future analyses to capture a wider variety of terrain influences.

An added limitation in this study is that the study area is only representative of a '*transitional*' snow climate. Since a '*transitional*' snow climate is inherently variable from season to season, it may be difficult to gather meaningful decision rules and thresholds that are representative of the other snow climates (*maritime* and *continental*). As this research field expands in the future it will be important to address this limitation to understand how decision rules and thresholds are possibly affected by weather and snowpack characteristics across all snow climates and regions.

The final limitation in my study was the update of the HRDPS model in the middle of the study period (e.g. the wind variables) (Milbrandt et al., 2016). While improvements in the NWP model are desirable, it created a substantial discontinuity that dramatically reduced the dataset of valid wind speed records for the present analysis. This means that weather data gathered for each season could potentially be generated under different assumptions and underlying physics, and although each consecutive season's weather forecast is possibly more accurate it also affects the accuracy of each season's simulated snowpack structure. This makes the dataset somewhat inconsistent year over year and therefore makes it problematic to compare them to each other and build consistent statistical models. This limitation will continue to appear in future research since models are constantly improved as scientific research evolves.

Chapter 6. Conclusions

In this study, I explored the relationships between modelled weather and snowpack data and human avalanche problems assessments. First, I created a comprehensive dataset of six winter seasons in Glacier National Park, combining public avalanche bulletins with simulated weather and snowpack data. I then thoroughly examined the dataset using many exploratory analysis techniques to gain an initial understanding of how the variables interacted. Surface avalanche problems (WS, SS, LDRY, LWET and CORN) and persistent slab problems (PS and DPS) were analyzed separately due to the differences in the factors contributing to their formation and the distinct data structures. Finally, I used conditional inference trees (CIT; Hothorn et al., 2006) to explore how the presence and absence of avalanche problem types relates to the simulated weather and snowpack variables in a multivariate fashion. Three main result themes emerged from my analyses: 1) Each avalanche problem type has its own set of relevant weather and snowpack variables that contribute to when it is forecasted, 2) Certain results give insight into forecaster practice and offer an interesting perspective on how the CMAH is used in avalanche forecasting operations in Canada, and 3) “Turning avalanche problems off” seems much more challenging for forecasters than turning them on.

The results of my analysis provide a meaningful initial step towards deriving avalanche problem types from simulated weather and snowpack observations and can hopefully be used as the foundation for creating decision aid tools aimed at helping forecasters assess avalanche hazard in the data-sparse regions in the future. Even though the CIT models extracted many of the expected snow and weather variables, the identified threshold values for the splits in the CITs had a tendency to be lower than the values published in the scientific literature or the rules of thumb used by practitioners. I attribute this discrepancy to two main reasons. First, weather and snowpack variables can vary extensively throughout the mountains, and the weather and snowpack values used in the analyses were modelled from a large-scale weather prediction model on a 2.5 km grid that does not necessarily provide a true representation of the local conditions on the ground. The simplification of only using a flat-field simulation from a single grid point from each elevation band for my analysis might further aggravate the issue as the simulated observations might not be representative of the region. The second main

reason for the limitations of the derived CIT models is likely related to the subjectivity of the judgment involved in avalanche forecasting (LaChappelle, 1980; McClung, 2002) and inconsistencies in the application of the CMAH (Clark, 2019; Lazar et al., 2016; Statham, Holeczi, et al., 2018). While the CMAH provides a conceptual framework for assessing and communicating avalanche hazard, the vague definitions of some of the scales included in the model (Thumlert, Statham, & Jamieson, 2019) likely prevent a more consistent application of the framework.

Based on the results that emerged from my analyses, I see the following opportunities for future research on integrating avalanche problems into snowpack simulations. One possible next step could be to focus on the characteristics of avalanche problems (i.e. location, likelihood, and size) instead of their presence or absence, as these characteristics may relate to modelled observations more directly. Another possibility could be to explicitly integrate the spatial variability of the predictions across the forecast area into the model instead of just focussing on one point in space per elevation band. Although there are many NWP grid points within GNP ($n = 225$) distributed across all three elevation bands, my study used only one grid point per elevation band with a 'flat-field' simulation to begin understanding the relationships at a manageable level. This is a major simplification and does not represent the entire picture of the true conditions within forecast regions. Integrating distributions of observations into the model rather than single values would be one way to implement such an approach. In addition to simulating at different grid points, this approach could also include simulations on virtual slopes to also capture the spatial variability due to variation in aspects. Research is currently being conducted in SARP to develop algorithms that can cluster sets of snow profiles and aggregate them into representative snow profiles to describe regional conditions more effectively (Herla et al., In Preparation; Horton et al., 2019). Basing avalanche problem identification on aggregated representative profiles could be another approach to better represent regional patterns. Both of these approaches would help to address the scale mismatch between observations and assessments.

Another possible approach for improving the link between the simulated weather and snowpack observations and the presence or absence of avalanche problem types would be to include other possible predictor variables. SNOWPACK produces a wide range of possible output variables, but the present study primarily focused on variables

that were intuitive and mirror existing forecaster practices to provide practical insight and allow the comparison with existing rules of thumb (e.g. rules for HST, HN48 and HN72 layers). This variable selection process excluded many of the more sophisticated patterns that could be extracted from output data of SNOWPACK simulations. Possible derived variables to consider include precipitation rates, loading rates, or the combined effects of precipitation intensity, quantity and wind variables; differences in temperatures (e.g. 24 h temperature trend or temperature gradients); ratios of hardness or grainsize between weak layers and overlying slab; mechanical properties and stability indices.

Although all of the outlined directions are interesting possibilities for future research, they do not get around the issue that avalanche assessments are inherently subjective judgements that are susceptible to forecaster variability and biases. Developing a decision aid based on historic assessment data will therefore always be at risk of simply perpetuating existing forecaster biases and inconsistencies. This research offers a new perspective on forecaster habits that can potentially be used to develop approaches to improve forecaster consistency. A possible alternative solution to this challenge would be to use the results presented in this study as a starting point for a discussion with expert forecasters about existing forecast practices and how define best practices. Instead of the data-driven development of avalanche problem models pursued in the present study, this would lead to an expert-driven development of prescriptive avalanche problem models similar to the research being done Karsten Müller and colleagues who aim to develop an 'avalanche problem solver,' (Müller et al., 2018) that will automatically predict daily avalanche problems and danger levels based on weather and snowpack conditions for all regions in Norway. Since the two approaches are complementary with their distinct strengths, I believe that the best results will come from a combination of data- and expert-driven research and development.

References

- Armstrong, R. L., & Armstrong, B. R. (1987). Snow and avalanche climates of the western United States: A comparison of maritime, intermountain and continental conditions *IAHS Publ*, 162, 281-294.
- AvalancheCanada. (2019). Retrieved from <https://www.avalanche.ca/>
- Bartelt, P., & Lehning, M. (2002). A Physical SNOWPACK Model for the Swiss Avalanche Warning Part I: Numerical Model. *Cold Regions Science and Technology*, 35, 123-145.
- Bellaire, S., & Jamieson, B. (2013). Forecasting the formation of critical snow layers using a coupled snow cover and weather model. *Cold Regions Science and Technology*, 94, 37-44. doi:10.1016/j.coldregions.2013.06.007
- Bellaire, S., & Jamieson, B. (2013b). *On Estimating Avalanche Danger from Simulated Snow Profiles*. Paper presented at the International Snow Science Workshop, Grenoble, France.
- Bellaire, S., Jamieson, B., & Fierz, C. (2011). Forcing the snow-cover model SNOWPACK with forecasted weather data. *The Cryosphere*, 5(4), 1115-1125. doi:10.5194/tc-5-1115-2011
- Blattenberger, G., & Fowles, R. (2017). Treed Avalanche Forecasting: Mitigating Avalanche Danger Utilizing Bayesian Additive Regression Trees. *Journal of Forecasting*, 36(2), 165-180. doi:10.1002/for.2421
- Brabec, B., & Meister, R. (2001). A Nearest-Neighbor Model for Regional Avalanche Forecasting. *Annals of Glaciology*, 32, 130-134.
- Breiman, L., Friedman, J. H., Olshen, R. A., & Stone, C. J. (1984). *Classification and Regression Trees*. Belmont, CA: Wadsworth.
- Brun, E., Martin, E. H., Simon, V., Gendre, C., & Coleou, C. (1989). An Energy and Mass Model of Snow Cover Suitable for Operational Avalanche Forecasting. *Journal of Glaciology*, 35(121), 333-342.
- CAA. (2014). *Observation Guidelines and Recording Standards for Weather, Snowpack and Avalanches*. Revelstoke, BC, CA: Canadian Avalanche Association.
- CAA. (2016). *Technical Aspects of Snow Avalanche Risk Management: Resources and Guidelines for Avalanche Practicioners in Canada*. Revelstoke, BC, CA: Canadian Avalanche Association.
- Caron, J.-F., Milewski, T., Buehner, M., Fillion, L., Reszka, M., Macpherson, S., & St-James, J. (2015). Implementation of Deterministic Weather Forecasting Systems Based on Ensemble-Variational Data Assimilation at Environment Canada. Part II: The Regional System. *Monthly Weather Review*, 143(7), 2560-2580. doi:10.1175/mwr-d-14-00353.1

- Clark, T. (2019). *Exploring the Link Between the Conceptual Model of Avalanche Hazard and the North American Public Avalanche Danger Scale*. (MRM), Simon Fraser University, (721)
- Coiffier, J. (2011). Half a Century of Numerical Weather Prediction. In *Fundamentals of Numerical Weather Prediction* (pp. 1-14). Cambridge: Cambridge University Press.
- Conlan, M., & Jamieson, B. (2017). A decision support tool for dry persistent deep slab avalanches for the transitional snow climate of western Canada. *Cold Regions Science and Technology*, 144, 16-27. doi:10.1016/j.coldregions.2017.06.013
- Conlan, M., Tracz, D., & Jamieson, B. (2014). Measurements and weather observations at persistent deep slab avalanches. *Cold Regions Science and Technology*, 97, 104-112. doi:10.1016/j.coldregions.2013.06.011
- Côté, J., Gravel, S., Méthot, A., Patoine, A., Roch, M., & Staniforth, A. (1998). The Operational CMC-MRB Global Environmental Multiscale (GEM) Model. Part I: Design Considerations and Formulation. *Monthly Weather Review*, 126, 1373-1395. doi:doi:[https://doi.org/10.1175/1520-0493\(1998\)126<1373:TOCMGE>2.0.CO;2](https://doi.org/10.1175/1520-0493(1998)126<1373:TOCMGE>2.0.CO;2)
- Côté, K., Madore, J.-B., & Langlois, A. (2017). Uncertainties in the SNOWPACK multilayer snow model for a Canadian avalanche context: sensitivity to climatic forcing data. *Physical Geography*, 38(2), 124-142. doi:10.1080/02723646.2016.1277935
- Durand, Y., Brun, E., Merindol, L., Guyomarc'h, G., Lesaffre, B., & Martin, E. (1993). Meteorological estimation of relevant parameters for snow models. *Annals of Glaciology*, 18, 65-71.
- Erfani, A., Mailhot, J., Gravel, S., Desgagné, M., King, P., Sills, D., . . . Jacob, D. (2005). *The High Resolution Limited Area Version of the Global Environmental Multiscale Model and its Potential Operational Applications*. Paper presented at the 11th Conference on Mesoscale Processes, Albuquerque, NM.
- Floyer, J. A., & McClung, D. M. (2003). Numerical avalanche prediction: Bear Pass, British Columbia, Canada. *Cold Regions Science and Technology*, 37(3), 333-342. doi:10.1016/s0165-232x(03)00074-0
- Föhn, P. M. B. (1980). Snow Transport over Mountain Crests. *Journal of Glaciology*, 26(94), 469-480.
- Giraud, G. (1992). *MEPRA: An Expert System for Avalanche Risk Forecasting*. Paper presented at the International Snow Science Workshop, Breckenridge, Colorado, USA.
- Haegeli, P. (2018). Snow Avalanches. In *State of the Mountains Report* (Vol. 1, pp. 19-21): The Alpine Club of Canada.

- Haegeli, P., Atkins, R., & Klassen, K. W. (2010). *Auxiliary material for decision making in avalanche terrain: A field book for winter backcountry users*. Revelstoke, BC: Avalanche Canada.
- Haegeli, P., & McClung, D. M. (2003). Avalanche characteristics of a transitional snow climate—Columbia Mountains, British Columbia, Canada. *Cold Regions Science and Technology*, 37(3), 255-276. doi:10.1016/s0165-232x(03)00069-7
- Haegeli, P., & McClung, D. M. (2004). Hierarchy Theory as a Conceptual Framework for Scale Issues in Avalanche Forecast Modeling. *Annals of Glaciology*, 38, 209-214.
- Haegeli, P., Obad, J., Harrison, B., Murray, B., Engblom, J., & Neufeld, J. (2014). *InfoEx 3.0 - Advancing the data analysis capabilities of Canada's diverse avalanche community*. Paper presented at the International Snow Science Workshop, Banff, AB.
- Haladuick, S. (2014). *Relating field observations and snowpack tests to snow avalanche danger*. (Master of Science), University of Calgary,
- Hendrikx, J., Murphy, M., & Onslow, T. (2014). Classification trees as a tool for operational avalanche forecasting on the Seward Highway, Alaska. *Cold Regions Science and Technology*, 97, 113-120. doi:10.1016/j.coldregions.2013.08.009
- Herla, F., Horton, S., & Haegeli, P. (In Preparation). Aligning snow profiles with dynamic time warping. *Geoscientific Model Development*.
- Horton, S. (2015). *Modelling Hazardous Surface Hoar Layers in the Mountain Snowpack over Space and Time*. (PhD), University of Calgary, Calgary, AB.
- Horton, S., & Jamieson, B. (2016). Modelling hazardous surface hoar layers across western Canada with a coupled weather and snow cover model. *Cold Regions Science and Technology*, 128, 22-31. doi:10.1016/j.coldregions.2016.05.002
- Horton, S., Novak, S., & Haegeli, P. (2019). Exploring Regional Snowpack Patterns with Gridded Models. *Natural Hazards and Earth System Science Discussion*.
- Horton, S., Schirmer, M., & Jamieson, B. (2015). Meteorological elevation and slope effects on surface hoar formation. *The Cryosphere*(9), 1523-1533. doi:10.5194/tc-9-1523-2015
- Hothorn, T., Hornik, K., & Zeileis, A. (2006). Unbiased Recursive Partitioning: A Conditional Inference Framework. *Journal of Computational and Graphical Statistics*, 15(3), 651-674. doi:10.1198/106186006x133933
- Jamieson, B., Haegeli, P., & Gauthier, D. (2010). *Avalanche Accidents in Canada* (Vol. 5 - 1996-2007). Revelstoke, BC: Canadian Avalanche Association.
- Jamieson, B., Haegeli, P., & Schweizer, J. (2009). Field observations for estimating the local avalanche danger in the Columbia Mountains of Canada. *Cold Regions Science and Technology*, 58(1-2), 84-91. doi:10.1016/j.coldregions.2009.03.005

- Klassen, K. W. (2010). *Experience is not enough: Persistent weak layers in Western Canada 2007-2010*. Paper presented at the International Snow Science Workshop, Lake Tahoe.
- Klassen, K. W. (2014). What's the Problem? A Primer on Defining Avalanche Character. *The Avalanche Journal*(Winter), 10-12.
- LaChappelle, E. R. (1965). *Avalanche forecasting: a modern synthesis*.
- LaChappelle, E. R. (1980). The fundamental processes of conventional avalanche forecasting. *Journal of Glaciology*, 26(94), 75-84.
doi:10.3189/S0022143000010601
- Lazar, B., Trautman, S., Cooperstein, M., Greene, E., & Birkeland, K. W. (2016). *North American Avalanche Danger Scale: Do Backcountry Forecasters Apply it Consistently?* Paper presented at the International Snow Science Workshop, Breckenridge, CO, USA.
- Lehning, M., Bartelt, P., Brown, B., & Fierz, C. (2002). A Physical SNOWPACK Model for the Swiss Avalanche Warning Part III: Meteorological Forcing, Thin Layer Formation and Evaluation. *Cold Regions Science and Technology*, 35, 169-184.
- Lehning, M., Bartelt, P., Brown, B., Fierz, C., & Satyawali, P. (2002). A Physical SNOWPACK Model for the Swiss Avalanche Warning Part II: Snow Microstructure. *Cold Regions Science and Technology*, 35, 147-167.
- Lehning, M., Bartelt, P., Brown, B., Russi, T., Stöckli, U., & Zimmerli, M. (1999). Snowpack Model Calculations for Avalanche Warning Based Upon a New Network of Weather and Snow Stations. *Cold Regions Science and Technology*, 30, 145-157.
- Logan, S., & Greene, E. (2014). *The Distribution of Fatalities by Avalanche Problem in Colorado, USA, 1998-99 to 2012-13*. Paper presented at the International Snow Science Workshop, Banff, AB.
- Mailhot, J., Bélair, S., Lefaivre, L., Bilodeau, B., Desgagné, M., Girard, C., . . . Qaddouri, A. (2010). The 15-km version of the Canadian regional forecast system. *Atmosphere-Ocean*, 44(2), 133-149. doi:10.3137/ao.440202
- McClung, D. M. (2002). The Elements of Applied Avalanche Forecasting Part I: The Human Issues. *Natural Hazards*, 25, 111-129.
- McClung, D. M. (2018). Blade hardness gauge as an aid in avalanche forecasting. *Canadian Avalanche Association Spring Meetings*. Penticton, BC.
- McClung, D. M., & Schaerer, P. (2006). *The Avalanche Handbook* (3rd Edition ed.): The Mountaineers Books.
- McClung, D. M., & Tweedy, J. (1994). Numerical avalanche prediction: Kootenay Pass, British Columbia, Canada. *Journal of Glaciology*, 40(135).

- Milbrandt, J. A., Bélair, S., Faucher, M., Vallée, M., Carrera, M. L., & Glazer, A. (2016). The Pan-Canadian High Resolution (2.5 km) Deterministic Prediction System. *Weather and Forecasting*, 31(6), 1791-1816. doi:10.1175/waf-d-16-0035.1
- Morin, S., Fierz, C., Horton, S., Bavay, M., Coléou, C., Dumont, M., . . . Vionnet, V. (2019). Application of Physical Snowpack Models in Support of Operational Avalanche Hazard Forecasting: A Status Report on Current Implementations and Prospects for the Future. *Cold Regions Science and Technology*.
- Müller, K., Engeset, R. V., Landro, M., Humstad, T., Granan, E. B., & Thorset, H. (2018). *Avalanche Problem Solver (APS) - A Decision Support System for Forecasters (Part 1)*. Paper presented at the International Snow Science Workshop, Innsbruck, Austria.
- Obled, C., & Good, W. (1980). Recent Developments of Avalanche Forecasting By Discriminant Analysis Techniques: Methodological Review and Some Applications to the Parsenn Area. *Journal of Glaciology*, 23(92), 315-346.
- ParksCanada (2018). [Operational information].
- ParksCanada. (2019). Glacier National Park. Retrieved from <https://www.pc.gc.ca/en/pn-np/bc/glacier>
- Perla, R. (1970). On Contributory Factors in Avalanche Hazard Evaluation. *Canadian Geotechnical Journal*, 7, 414-419.
- Pozdnoukhov, A., Matasci, G., Kanevski, M., & Purves, R. S. (2011). Spatio-temporal avalanche forecasting with Support Vector Machines. *Natural Hazards and Earth System Science*, 11(2), 367-382. doi:10.5194/nhess-11-367-2011
- Schirmer, M., & Jamieson, B. (2015). Verification of analysed and forecasted winter precipitation in complex terrain. *The Cryosphere*, 9(2), 587-601. doi:10.5194/tc-9-587-2015
- Schirmer, M., Lehning, M., & Schweizer, J. (2009). Statistical Forecasting of Regional Avalanche Danger Using Simulated Snow-cover. *Journal of Glaciology*, 55(193), 761-768.
- Schweizer, J., Bellaire, S., Fierz, C., Lehning, M., & Pielmeier, C. (2006). Evaluating and improving the stability predictions of the snow cover model SNOWPACK. *Cold Regions Science and Technology*, 46(1), 52-59. doi:10.1016/j.coldregions.2006.05.007
- Schweizer, J., & Föhn, P. M. B. (1996). Avalanche Forecasting: An Expert System Approach. *Journal of Glaciology*, 42(141), 318-332.
- Schweizer, J., Jamieson, B., & Skjonsberg, D. (1998). *Avalanche Forecasting for transportation corridor and backcountry in Glacier National Park (BC, Canada)*. Paper presented at the 25 Years of Snow Avalanche Research, Voss, Norway.

- Schweizer, J., Reuter, B., van Herwijnen, A., & Gaume, J. (2016). *Avalanche Release 101*. Paper presented at the International Snow Science Workshop, Breckenridge, CO.
- Shandro, B., Haegeli, P., Statham, G., & Floyer, J. A. (2016). *Spatial and Temporal Distribution of Avalanche Problem Types in Western Canada: An Analysis of the Winters 2010–2016*. Paper presented at the International Snow Science Workshop, Breckenridge, CO, USA.
- Sinickas, A., Jamieson, B., & Maes, M. A. (2016). Snow avalanches in western Canada: investigating change in occurrence rates and implications for risk assessment and mitigation. *Structure and Infrastructure Engineering*, 12(4), 490-498. doi:10.1080/15732479.2015.1020495
- Statham, G. (2008). *Avalanche Hazard, Danger and Risk: A Practical Explanation*. Paper presented at the International Snow Science Workshop, Whistler, BC, Canada.
- Statham, G., Campbell, S., & Klassen, K. W. (2012). *The AvalX Public Avalanche Forecasting System*. Paper presented at the International Snow Science Workshop, Anchorage, AK, USA.
- Statham, G., Haegeli, P., Birkeland, K. W., Greene, E., Israelson, C., Tremper, B., . . . Kelly, J. (2010a). *A Conceptual Model of Avalanche Hazard*. Paper presented at the International Snow Science Workshop, Lake Tahoe, CA.
- Statham, G., Haegeli, P., Birkeland, K. W., Greene, E., Israelson, C., Tremper, B., . . . Kelly, J. (2010b). *The North American Public Avalanche Danger Scale*. Paper presented at the International Snow Science Workshop, Squaw Valley, CA, USA.
- Statham, G., Haegeli, P., Greene, E., Birkeland, K. W., Israelson, C., Tremper, B., . . . Kelly, J. (2018). A Conceptual Model of Avalanche Hazard. *Natural Hazards*, 90(2), 663-691. doi:10.1007/s11069-017-3070-5
- Statham, G., Holeczi, S., & Shandro, B. (2018). *Consistency and Accuracy of Public Avalanche Forecasts in Western Canada*. Paper presented at the International Snow Science Workshop, Innsbruck, AU.
- Stull, R. (2016). *Practical Meteorology: An Algebra-based Survey of Atmospheric Science*. University of British Columbia: BC Campus Open Textbook Project.
- Team, R. C. (2019). *R: A language and environment for statistical computing*. Vienna, Austria: R Foundation for Statistical Computing.
- Techel, F., Mitterer, C., Ceaglio, E., Coléou, C., Morin, S., Rastelli, F., & Purves, R. S. (2018). Spatial consistency and bias in avalanche forecasts – a case study in the European Alps. *Natural Hazards and Earth System Sciences*, 18(10), 2697-2716. doi:10.5194/nhess-18-2697-2018
- Thumlert, S., Statham, G., & Jamieson, B. (2019). The Likelihood Scale in Avalanche Forecasting. *The Avalanche Journal*(Fall), 24-28.

Zeidler, A., & Jamieson, B. (2006a). Refinements of empirical models to forecast the shear strength of persistent weak snow layers PART A: Layers of faceted crystals. *Cold Regions Science and Technology*, 44(3), 194-205.
doi:10.1016/j.coldregions.2005.11.005

Zeidler, A., & Jamieson, B. (2006b). Refinements of empirical models to forecast the shear strength of persistent weak snow layers Part B: Layers of surface hoar crystals. *Cold Regions Science and Technology*, 44(3), 184-193.
doi:10.1016/j.coldregions.2005.11.004